

UNSW AUSTRALIA

SCHOOL OF MECHANICAL AND MANUFACTURING  
ENGINEERING

---

# Mission Design and Specification for a Space Based Aircraft Monitoring System

---

BACHELOR OF MECHATRONICS ENGINEERING, HONOURS THESIS

*Author:*

Thien NGUYEN

*Supervisors:*

Dr. Naomi TSAFNAT

Dr. Ediz CETIN

*Student Number:*

z3288816

Dr. Barnaby OSBORNE

Friday 23<sup>rd</sup> May, 2014

---

## Publications to Date

Following the work undertaken during this thesis, the following publications have been accepted for peer review

1. "Tracking Aircraft via a Low-Earth-Orbit CubeSat Constellation"

**2013 AIAA Region VII-AU Student Conference**

UNSW, Kensington, Australia, 27-29th November 2013

Full text available in Appendix A

2. "Space Based ADS-B via a Low-Earth Orbit CubeSat Constellation"

**65th International Astronautical Congress**

**21st IAA Symposium on Small Satellite Missions**

Toronto, Canada, 29th September - 3rd October 2014

Abstract and acceptance letter reproduced in Appendix B

---

## **Declaration**

I hereby declare that this submission is my own work and to the best of my knowledge it contains no materials previously published or written by another person, or substantial proportions of material which have been accepted for the award of any other degree or diploma at UNSW or any other educational institution, except where due acknowledgement is made in the thesis. Any contribution made to the research by others, with whom I have worked at UNSW or elsewhere, is explicitly acknowledged in the thesis. I also declare that the intellectual content of this thesis is the product of my own work, except to the extent that assistance from others in the project's design and conception or in style, presentation and linguistic expression is acknowledged.

---

Thien Nguyen

3288816

Friday 23<sup>rd</sup> May, 2014

---

## Abstract

Automatic Dependent Surveillance-Broadcast (ADS-B) is currently being adopted by aviation authorities around the world as the standard method for tracking aircraft during flight. ADS-B coverage is available on most of the landmass in Europe, North America, Australia and South East Asia. However, gaps in coverage exist over regions where installing ADS-B receiver stations is not economically viable or feasible, such as over oceans and poles. To close these gaps, ADS-B signals can be received and retransmitted from satellites in Low Earth Orbit (LEO). There is an increased commercial interest in implementing ADS-B re-transmitting satellite constellations. The Iridium NEXT and second Globalstar constellations of LEO satellites that are currently under development will provide a space based ADS-B service. Using a constellation of CubeSats provides a more economical solution, with lower production, launch and satellite replacement costs. The key challenge in the design of such system entails balancing coverage area and revisit times against cost and CubeSat technological limitations.

In this thesis we provide analysis of these trade-offs and provide an insight into requirements of such a system. We have modelled popular flights over the North Pole and Pacific and Atlantic Oceans (where ADS-B coverage is not available) in Systems Tool Kit (STK) with standard commercial ADS-B transmitters. These flight paths were analysed to determine the coverage requirements of a space based ADS-B system. Aviation safety requirements from various global authorities were researched to determine the system update rates necessary to provide a safety critical service. These requirements lay the groundwork for the systems development necessary to launch and operate an ADS-B constellation.

# Contents

Publications to Date . . . . .	i
Declaration . . . . .	ii
Abstract . . . . .	iii
<b>List of Figures</b>	vii
<b>List of Tables</b>	xii
Nomenclature . . . . .	xiii
<b>1 Introduction</b>	1
1.1 Problem Statement . . . . .	2
1.2 Thesis Structure . . . . .	2
<b>2 Background Theory and Literature Review</b>	3
2.1 ADS-B . . . . .	4

## *CONTENTS*

---

2.2	CubeSats . . . . .	9
2.3	Satellite Constellations . . . . .	11
2.4	Literature Review . . . . .	15
<b>3</b>	<b>Experimental Method and Design</b>	<b>25</b>
3.1	Mission Overview . . . . .	26
3.2	Experimental Parameters . . . . .	29
3.3	Analysis Tools . . . . .	37
3.4	Model Input Data and Assumptions . . . . .	39
<b>4</b>	<b>Results and Analysis</b>	<b>43</b>
4.1	Raw Results . . . . .	44
4.2	Data Processing . . . . .	46
4.3	Trends and Analysis . . . . .	48
4.4	Access Periodicity . . . . .	65
4.5	Weighted Decision Matrix . . . . .	67
4.6	Special Case Study - MH370 . . . . .	72
<b>5</b>	<b>Conclusions and Future Work</b>	<b>75</b>

## *CONTENTS*

---

5.1	Conclusions . . . . .	76
5.2	Future Work . . . . .	79
	References	81
	Appendices	88
A	2013 AIAA Region VII-AU Student Conference	
	Full Text of Accepted Paper	88
B	65th International Astronautical Congress	
	Abstract and Acceptance Letter	99
C	Experimental Parameters	103
D	Student's t Distribution	104

# List of Figures

2.1	ADS-B and radar coverage in Australia . . . . .	6
2.2	ADS-B coverage in the US as of 30/06/2013 . . . . .	7
2.3	Global areas without ADS-B coverage . . . . .	8
2.4	The GOMSpace QB50 Platform - an example of a 2U CubeSat . . . . .	9
2.5	CubeSat sizes, ranging from the single 1U to the triple 3U . . . . .	10
2.6	Iridium Satellite constellation showing a) a view over Australia and South East Asia and b) the view from above the south pole. Data taken from STK . . . . .	12
2.7	Iridium Satellite constellation path over a 2D projection of the surface of the Earth. Data taken from STK . . . . .	13
2.8	The 8 Globalstar Orbital planes as shown from a) above Australia and South East Asia and b) above the south pole. Data from STK . . . . .	14
2.9	The Ground Track of the 48 Globalstar Satellites. Data from STK . . . . .	14
2.10	Overview of the ALAS system . . . . .	16

## *LIST OF FIGURES*

---

2.11	ADS-B Duplex coverage provided by the second generation Globalstar constellation	16
2.12	Aireon System Concept . . . . .	18
2.13	SAPID receiver Antenna design . . . . .	20
2.14	Aircraft detected by Proba V over Europe . . . . .	21
2.15	3D render of the GOM-X1 satellite, showing the expanded helical receiver antenna	22
2.16	Preliminary plot of planes detected by GOM-X1 . . . . .	23
3.1	Popular flight routes . . . . .	28
3.2	Trans-Oceanic Flight paths, as modelled in STK . . . . .	31
3.3	Generalisations of trans-Oceanic Flight paths used for analysis . . . . .	32
3.4	Ground track of the 12 satellite reference configuration in STK . . . . .	34
3.5	3D model of the 12 satellite reference configuration in STK . . . . .	35
4.1	Output of allfitdist when applied to the access periods of the LAX-Narita flight using the reference constellation described in Section 3.2.3.1 . . . . .	47
4.2	Ground track of the tested Molniya orbit . . . . .	48
4.3	Ground track of the tested geosynchronous orbit . . . . .	49
4.4	Coverage gap (as a fraction of total analysis time) as affected by altitude vari- ations. Lower is better . . . . .	52

## *LIST OF FIGURES*

---

4.5 Maximum coverage gap as affected by altitude variations. Lower is better . . . . .	52
4.6 Minimum received isotropic power as affected by altitude variations. Higher is better. . . . .	53
4.7 Coverage gap (as a fraction of total analysis time) as affected by altitude variations with a 3 satellite constellation. Lower is better . . . . .	53
4.8 Maximum coverage gap as affected by altitude variations retested with a 3 satellite constellation. Lower is better. . . . .	54
4.9 Ground track of satellites inclined at 60 degrees, shown with the test flight paths	55
4.10 Ground tracks of constellations inclined between 30 degrees and 90 degrees . . . . .	57
4.11 Coverage gap (as a fraction of total analysis time) as affected by inclination variations. Lower is better . . . . .	58
4.12 Maximum coverage gap as affected by altitude variations. Lower is better. . . . .	59
4.13 Minimum received isotropic power as affected by inclination variations. Higher is better. . . . .	59
4.14 Flight in dead zone between satellite planes, inclined at 70 degrees. View from North Pole . . . . .	61
4.15 Coverage gap (as a fraction of total analysis time) as affected by number of satellites per plane. Lower is better . . . . .	63
4.16 Maximum coverage gap as affected by number of satellites per plane. Lower is better. . . . .	63

## *LIST OF FIGURES*

---

4.17 Minimum received isotropic power as affected by number of satellites per plane. Higher is better. . . . .	64
4.18 Fitted distributions of the periodicity of Access times for the LAX-Heathrow flight from the reference constellation. . . . .	65
4.19 Fitted distributions of the periodicity of Access times for the LAX-Heathrow flight from the reference constellation. . . . .	66
4.20 The second harmonic deviation from a straight line path, showing required sam- ple points . . . . .	70
4.21 Distribution of scores from decision matrix . . . . .	71
4.22 Probability map of possible crash locations of the MH370 . . . . .	72
4.23 Simulated MH370 flight path with 18 satellite constellation . . . . .	73
5.1 18 satellite configuration rendered in STK showing a) the view above North America and b) the view above the Arctic . . . . .	77
5.2 Ground track of the 18 satellite configuration, rendered in STK . . . . .	78

# List of Tables

3.1	'Reference' constellation configuration . . . . .	34
3.2	Varying input parameters used for data and analysis . . . . .	35
3.3	Raw data generated by STK . . . . .	37
3.4	Link Parameters used in STK . . . . .	39
3.5	Cruising speeds of typical commercial aircraft . . . . .	41
3.6	STK Parameters used for each flight model . . . . .	41
3.7	Airport global co-ordinates . . . . .	42
4.1	Sample access data for satellite 1 of the reference case . . . . .	44
4.2	Sample of link budget data from a simulation of a link between a flight and a satellite . . . . .	45
4.3	Calculated access times from Matlab . . . . .	46
4.4	Altitude variations used using the 12 satellite reference case . . . . .	50

*LIST OF TABLES*

---

4.5	Orbital parameters for 3 satellite test . . . . .	51
4.6	Inclination variations used . . . . .	56
4.7	Number of satellite variations used . . . . .	62
4.8	Parameters used to evaluate constellation effectiveness . . . . .	68
4.9	The three highest scoring constellations after applying the weighted decision matrix	71
4.10	Results from MH370 simulation using 18 satellites . . . . .	74
5.1	18 satellite configuration with the best score . . . . .	77
C.1	Orbital parameters of all experimental cases studied . . . . .	103

# Nomenclature

<b>Symbol</b>	<b>Units</b>	<b>Description</b>
ADS-B		Automatic Dependent Surveillance Broadcast
ALAS		ADS-B Link Augmentation System
ANSP		Air Navigation Service Providers
ATC		Air Traffic Control
ATCRBS		Air Traffic Control Radar Beacon System
ATM		Air Traffic Management
BER		Bit Error Rate
C Band		IEEE defined electro-magnetic transmission band, between 500 and 1000MHz
C/N	dB	Carrier (or signal) to Noise Ratio
C/No	dB*Hz	Carrier to Noise Density Ratio
CASA		Civil Aviation Safety Authority
COTS		Commerical Off The Shelf
DLR		German Aerospace Centre
Eb/No	dB	Energy per Bit to Noise Density
EIRP	dBW	Effective Isotropic Radiated Power
ESA		European Space Agency

## *NOMENCLATURE*

---

<b>Symbol</b>	<b>Units</b>	<b>Description</b>
EU		European Union
Frequency	MHz, GHz	Megahertz
g/T	dB/K	Antenna gain-to-noise-temperature
GNSS		Global Navigation Satellite System
L Band		IEEE defined electro-magnetic transmission band, between 1 and 2GHz
LAX		Los Angeles International Airport
LEO		Low Earth Orbit
LHR		London Heathrow Airport
MEO		Medium Earth Orbit
NRT		Narita Airport
Power	W	Watts
RAAN		Right Angle of Ascending Node
RTCA		Radio Technical Comission for Aeronautics
S Band		IEEE defined electro-magnetic transmission band, between 2 and 4GHz
SABIP		Space Based ADS-B In-Orbit Demonstration Payload
SDR		Software Defined Radio
STK		Systems Tool Kit
UAT		Universal Access Transceiver Standard

# Chapter 1

## Introduction

Automatic Dependent Surveillance Broadcast (ADS-B) is quickly being adopted as the standard method for Air Traffic Control (ATC) Management in Europe, Australia and the United States. The currently available methods that provide ADS-B coverage to Air Navigation Service Providers (ANSPs) and ATC towers rely on terrestrial antennae which operate on line-of-sight. As a result aircraft cannot be tracked via ADS-B over oceanic and polar regions where installing ADS-B compatible ground stations is not practical. The recent development of the lost Malaysian Airlines flight MH370 on March 8th, 2014 highlights the detriment of not having constant, global, real-time coverage of commercial aircraft. These coverage gaps can be closed with the implementation of a space-based ADS-B receiver system.

This thesis explores the possibility of implementing a space-based ADS-B system on a constellation of Low-Earth-Orbit (LEO) CubeSats. Implementing such a system on using CubeSats rather than commercial satellites could be done at lower cost and lower risk. There is ongoing research in the implementation of ADS-B systems from LEO, focussing on developing and evaluating the performance of single receiver units from small satellites. The success and

interest of these small satellite ADS-B experiments gave motivation for further development of a CubeSat constellation. This thesis presents a parametric study into the performance of different constellation designs when used to track transoceanic flights. The evaluated ADS-B coverage will be compared against changing the orbital elements of different constellations in order to determine the ‘best possible’ design option.

## **1.1 Problem Statement**

A satellite-based ADS-B system will need to provide coverage to flights that are out of range of terrestrial ADS-B receivers. Geographically, this means that the proposed constellation needs to provide line-of-sight access to planes flying transoceanic or polar flight paths. The constellation also needs to provide enough coverage time to properly detect all flights in the area of interest and generate regular ‘updates’ for ANSPs to properly track any flight at any given time. The constellation will need to have a communications architecture that performs reliably enough receive and decode ADS-B signals from LEO. The subsequent satellite technology requirements produced from the constellation should accommodate the technological limitations of the CubeSat design form.

## **1.2 Thesis Structure**

This work presented in this thesis is divided into four chapters. Background theory and a review of ongoing research into space based ADS-B systems is presented in Chapter 2. The design of the experiments used to simulate the performance of potential ADS-B satellite constellations is presented in Chapter 3. Analysis of these results and the performance of each constellation is presented in Chapter 4, with a special case study for the MH370 flight given in Section 4.6. Finally a set of conclusions and recommendations for further study is given in Chapter 5.

# Chapter 2

## Background Theory and Literature Review

A number of fundamental concepts regarding the nature of ADS-B signals and CubeSat constellation design were researched so that the needs of a space based ADS-B system could be properly defined. Current regulatory requirements for terrestrial ADS-B receivers were examined in order to define the requirements for a space based analogue. Satellite constellations with similar coverage requirements were examined in order to develop a design framework.

Academic and commercial groups have already shown interest in the concept of a space-based ADS-B network. There was a particular research focus on implementing ADS-B on a small satellite and CubeSat scale at lower cost and lower risk, with more than one technology demonstrator currently in orbit. Their research has proven that the small satellite based technology is possible. However there has been little research into the design of a satellite constellation specifically tailored for the needs of aircraft using ADS-B, motivating the further study into ADS-B constellation design.

## **2.1 ADS-B**

ADS-B is an aircraft tracking system based on digital aircraft-to-ground and aircraft-to-aircraft transmissions. It is intended to support the existing Air Traffic Control Radar Beacon System (ATCRBS) which uses radar to track aircraft. ADS-B is now being adopted as a primary ATC management system in the United States of America [1], the European Union and Australia [2].

### **2.1.1 Data Structure**

ADS-B systems expand upon the function provided by Secondary Surveillance Radar (SSR) by requiring that extra data be periodically broadcast by all aircraft, without interrogation. The expanded data set includes Global Navigation Satellite System (GNSS) positioning and emergency telemetry. The ADS-B standard requires an update rate of once every second [3].

Current ADS-B systems use the GNSS data acquired by on-board avionics for position determination [4]. This data is transmitted to ground ATC stations and shared between aircraft in order to allow for accurate tracking of aircraft position for both ATC stations and other aircraft in the immediate vicinity.

ADS-B is also capable of relaying other aircraft telemetry data. As a minimum, the Australian Civil Aviation Safety Authority (CASA) specify the following to be included in an ADS-B data-set [5, Clause 8.2.3]:

- **Position** - determined via on-board avionics, including GNSS systems
- **Position Integrity Information** - indicating the level of trust with the positioning data
- **Pressure Altitude** - the altitude of an aircraft as determined by on-board altimeter
- **Aircraft Identification**

- **Version Number** - the version number and compliancy of the on-board avionics equipment.

In addition, the Australian ATC system has specified an additional 'highly desirable' data set [5, Clause 8.2.4]:

- **SPI Indication** - Special Position Identification, intended to supplement position data in the initial packet
- **Emergency Flag**
- **Emergency Priority Status Information**
- **Velocity Information**
- **GNSS Height**
- **Vertical Rate**
- **Aircraft category**

### 2.1.2 Transmission and Modulation

ADS-B data is intended to be transmitted over either the Universal Access Transceiver Standard (UAT), or the 1090MHz Mode S Extended Squitter, previously used by SSR. Specifications for ADS-B over UAT is given in [6] and over Mode S in [3]. ADS-B is broadcast on a random-access basis with particular aircraft identified by information in their data packets [7].

### 2.1.3 Coverage

Tracking via ADS-B requires aircraft to be within the line-of-sight of a ground station [2]. ADS-B coverage areas vary with altitude and the existence of obstructing features in the terrain

surrounding a ground station. Australia is one of the earliest adopters of ADS-B technology, with coverage over 100 percent of Australia's landmass as shown in Figure 2.1 [2].

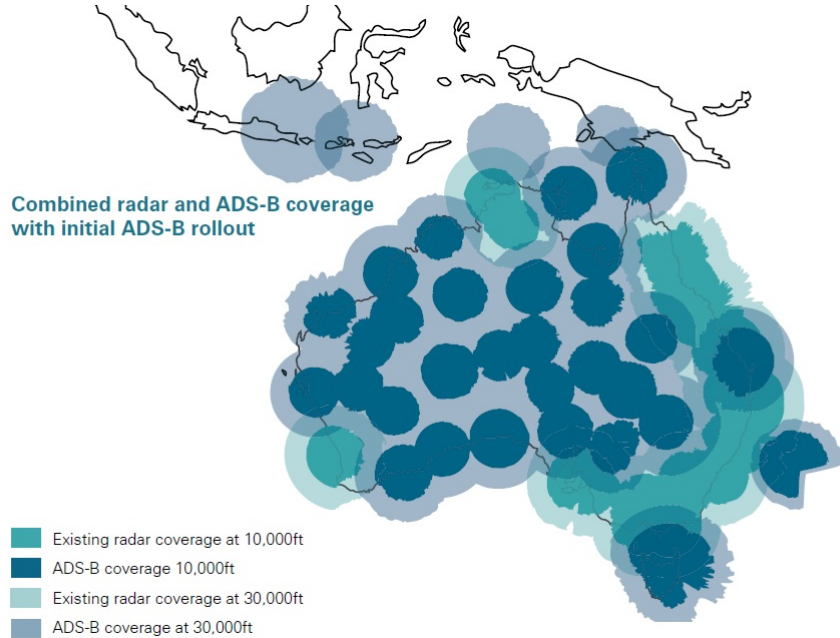


Figure 2.1: ADS-B and radar coverage in Australia, reproduced from [2]

Out of the range of these ground stations, aircraft tracking via ADS-B is not possible. Although comprehensive coverage is currently being implemented in Australia [2], the Asia-Pacific region [4] and much of North America [1], there still exists areas, particularly over oceanic and polar regions where the service is not available. Figure 2.2 shows the state of ADS-B coverage in US as of June 30th, 2013.

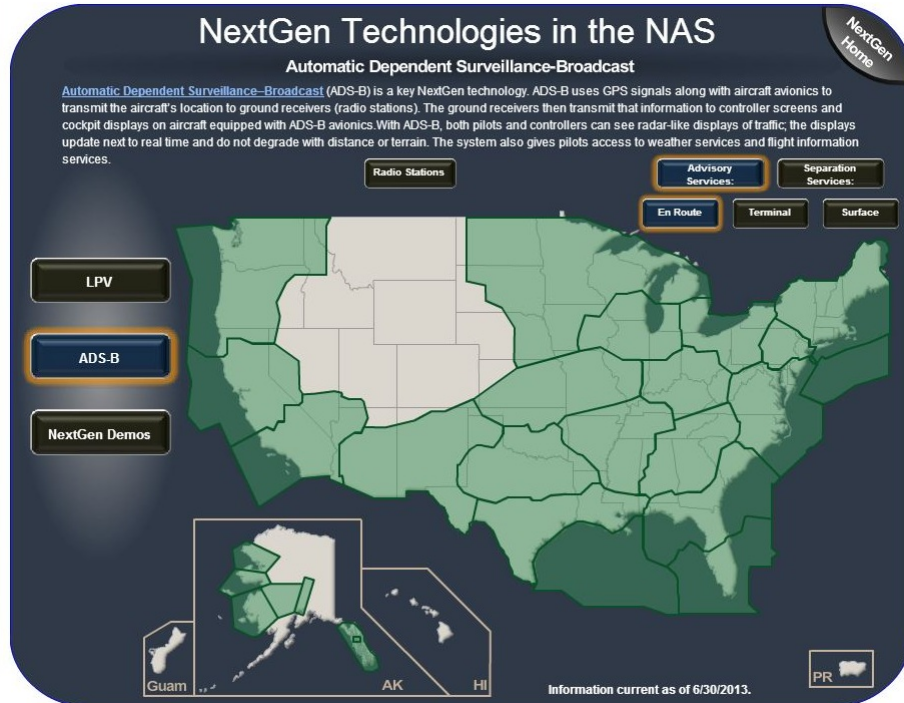


Figure 2.2: ADS-B coverage in the US as of 30/06/2013, reproduced from [8]

Some solutions exist for ADS-B coverage in remote and marine areas. Areas where ADS-B is not adequately covered is illustrated in Figure 2.3, as estimated by [9]. Ground stations installed on oil platforms currently provide coverage over the Gulf of Mexico [1]. Both Globalstar and Iridium NEXT propose global coverage via Low Earth Orbit (LEO) satellite constellations to be launched in 2014 [9, 10].

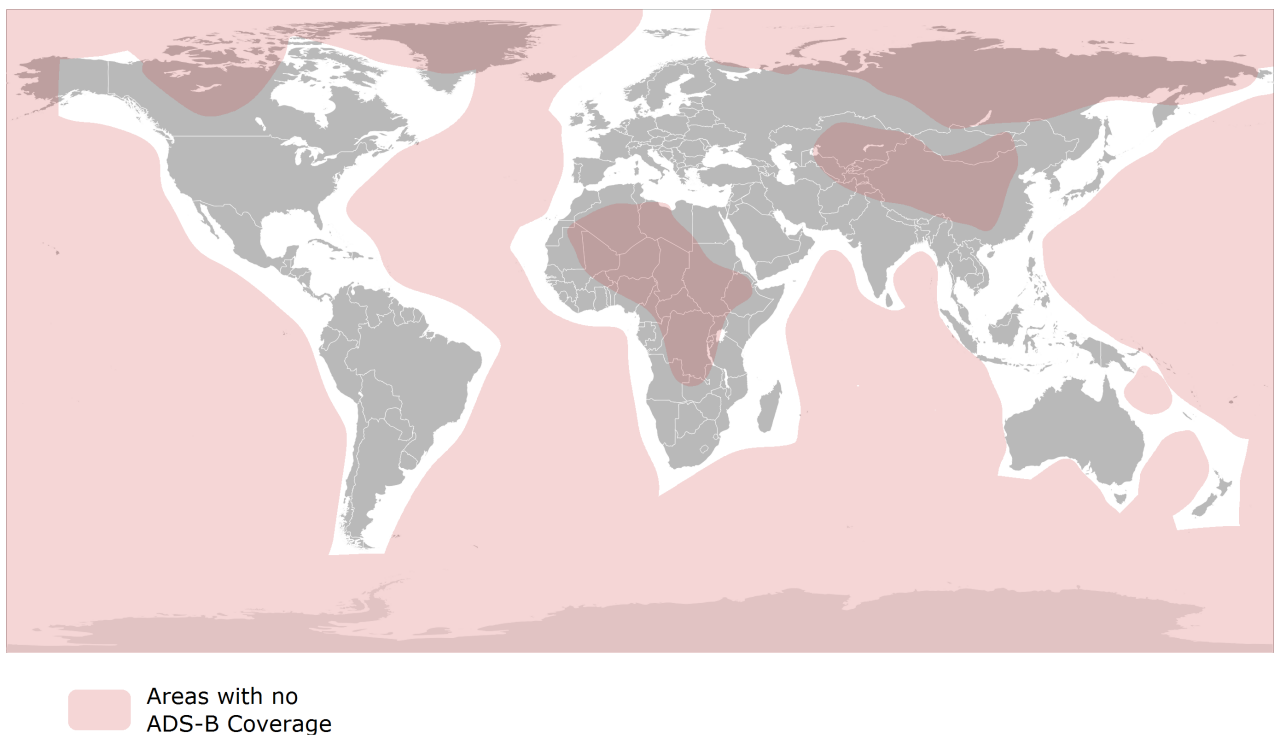


Figure 2.3: Global areas without ADS-B coverage, as estimated by [9]

## 2.2 CubeSats

CubeSats are a family of pico-satellites whose mechanical and launch-interface subsystems conform to an open-source standard [11]. The standard specifies a series of low-cost satellites that allow for the development space technology to be more accessible. These satellites are characterised by the number of ‘units’ they contain. Each ‘unit’ defines a roughly  $100 \times 100 \times 100$ mm cube-shaped physical envelope and a 1kg maximum weight. Satellites with multiple ‘units’ have a greater mass and payload volume budget. An example of a 2-unit (2U) CubeSat is shown in Figure 2.4.

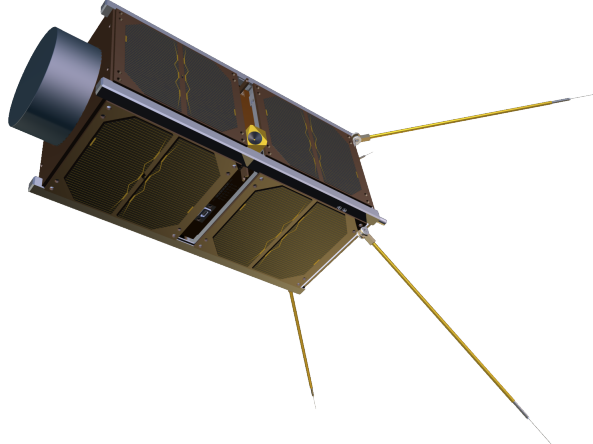


Figure 2.4: The GOMSpace QB50 Platform - an example of a 2U CubeSat, reproduced from [12]

The size and standardisation of CubeSat design have made them accessible to non-military and non-commercial space interest groups, including academic and hobbyist groups. The launch interface design is such that multiple CubeSats can be launched on the same vehicle at reduced cost [13]. The proliferation of open-source CubeSat designs has allowed the academic and hobbyist community to collaborate and refine CubeSat design concepts. The resulting reduction in design and launch makes developing space-bound payloads more accessible with less risk and lower cost than large scale satellite missions. The use of CubeSats could be more economically

effective than the use of commercial satellites

### 2.2.1 Specifications

Generic CubeSat specifications are given by the California Polytechnic State University (Cal Poly) [11]. These specifications identify a basic mechanical envelope, materials to be used and a standard launch interface.

Generally, a CubeSat consists of a stacked cube-configuration with 4 rails, each running along the edges of the satellite parallel to the Z axis. Launch and separation switches are located on the bottom face of each of these rails. The design of generic CubeSats is shown in Figure 2.5.

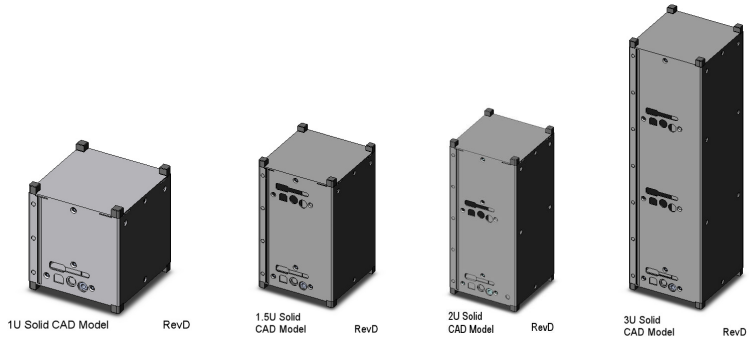


Figure 2.5: CubeSat sizes, ranging from the single 1U to the triple 3U. Reproduced from [14]

### 2.2.2 Typical Applications

CubeSats are heavily used by the academic community due to their cost-effectiveness and the low risk associated with mission and platform development. Subsequently the majority of CubeSat missions are associated with academic study and prototype demonstration. Satellites such as the University of Toronto's CanX-1 [15] and the University of Tokyo's XI-V [16] were built to prove the respective university's capability for space technology development. The GOM X-1 ADS-B CubeSat is discussed later in Section 2.4.5.

## 2.3 Satellite Constellations

Satellite constellations define a number of satellites in a particular configuration. Constellations are often used when the coverage, downlink opportunities or system update rate provided by a single or two satellites is not sufficient. The GNSS constellations, for example the Global Position System (GPS) or Global Navigation Satellite System (GLONASS) constellations, provide global GNSS coverage from a number of satellites in different medium earth orbits (MEO). Satellite communications provided from LEO constellations, such as the Iridium and Globalstar constellations, can be used as exemplars from which a LEO ADS-B constellation could be designed.

In order to define a constellation of circular orbits, the following orbital elements need to be defined for each satellite [17]

- **Altitude** - the altitude defines the height of the satellite above the average radius of the Earth<sup>1</sup>
- **Inclination** - the angle the orbit makes with the equator
- **Right Angle of Ascending Node (RAAN)** - the location of the intersection between the ground track of the satellite with the equator
- **True Anomaly** - the arc angle traced out by the satellite along its orbit from apogee.

Further detail on each of these orbital elements is given in [17].

---

<sup>1</sup>The standard Keplerian element of semi-major axis is then given by  $a = \text{Altitude} + 6378.1 \text{ km}$

### 2.3.1 Iridium

The Iridium Satellite Constellation is a network of 66 LEO satellites which provide mobile communication services over a global coverage network. The system provides voice and data coverage for subscribers equipped with Iridium hardware, including mobile handsets and data modems. The intention is that the system will work in remote areas of the Earth where reliable mobile and wireless data over conventional means (i.e. 3G and emerging 4G technologies) is not available. The current and first generation of satellites has been in operation since 1999 and surpassed 500,000 subscribers in September of 2011 [18].

The space segment of the system consists of 66 satellites in Low Earth Orbit at an altitude of approximately 780km. The satellites are evenly distributed amongst six polar co-rotating planes each spaced 31.6 degrees apart in longitude (RAAN), with the first and sixth planes counter-rotating and spaced 22 degrees apart [19, 20]. The planes have a near circular orbit [21]. Each orbital plane has 11 satellites evenly distributed across the orbit. This configuration is shown in Figures 2.6 and 2.7.

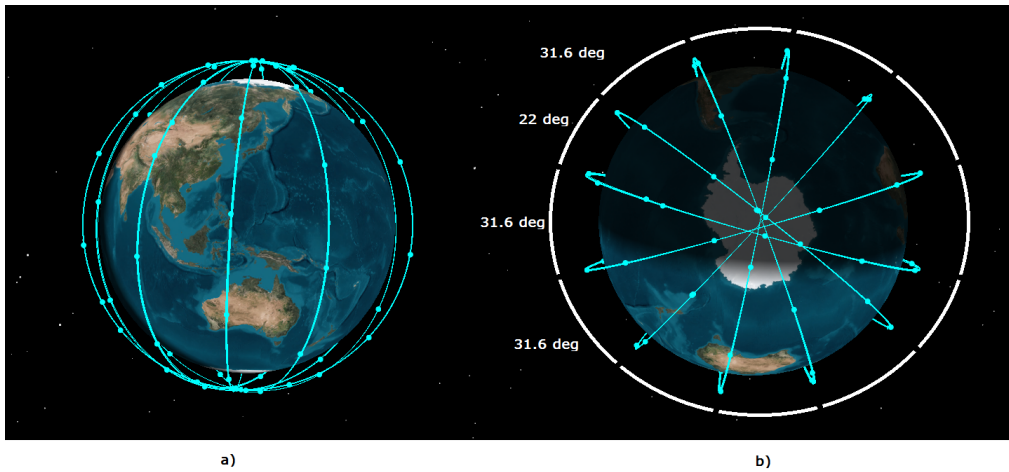


Figure 2.6: Iridium Satellite constellation showing a) a view over Australia and South East Asia and b) the view from above the south pole. Data taken from STK

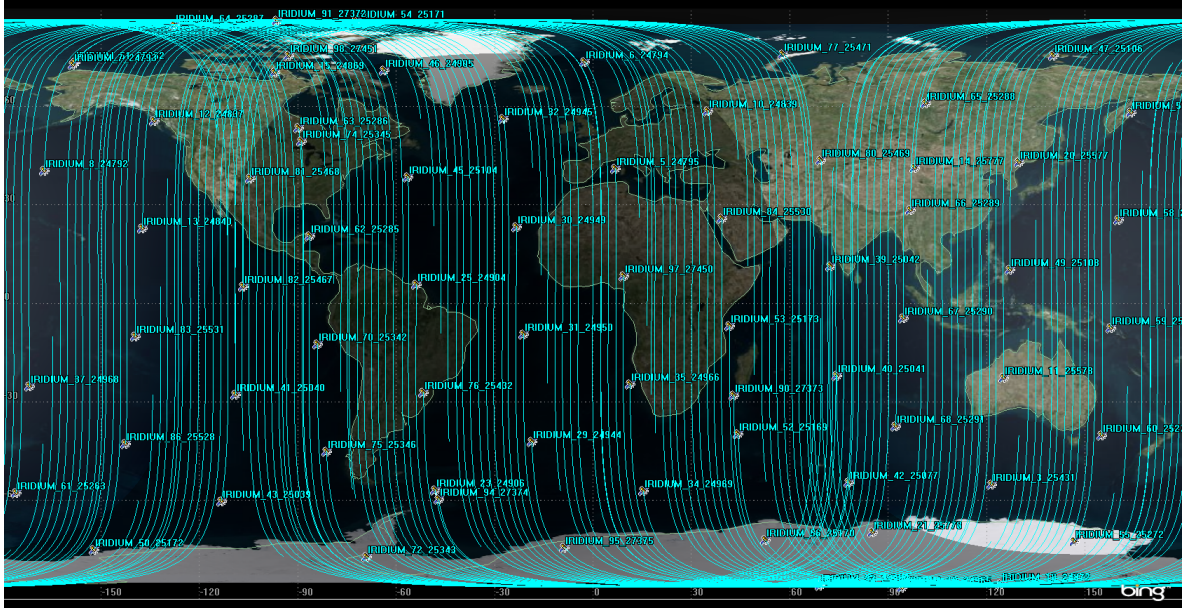


Figure 2.7: Iridium Satellite constellation path over a 2D projection of the surface of the Earth.  
Data taken from STK

### 2.3.2 Globalstar

The Globalstar Constellation consists of 48 LEO satellites that provide mobile communication services that, as far as end-users are concerned, are much the same as those offered by Iridium, as detailed in Chapter 2.3.1. Globalstar Inc. provide voice and data coverage over service areas where traditional public switched telephone network (PSTN) data links are not available. Unlike Iridium, Globalstar does not provide 100 percent global coverage, with swaths only covering areas between 70 degrees north and south latitudes [22].

The space segment of the Globalstar system consists of 48 satellites equally distributed in eight orbital planes. Each orbital plane contains 6 satellites and is inclined at  $52^\circ$  [22, 23]. Data from STK indicates that the orbits have equally spaced right ascensions of ascending node (RAANs) between  $0^\circ$  and  $360^\circ$ , offset  $45^\circ$  from each other. Each satellite is in a roughly circular orbit, with an altitude of 1414 kilometres [23] and a period of approximately 115 minutes. The eight

## CHAPTER 2. BACKGROUND THEORY AND LITERATURE REVIEW

---

orbital planes are illustrated in Figure 2.8, with the ground track of all 48 satellites shown in Figure 2.9.

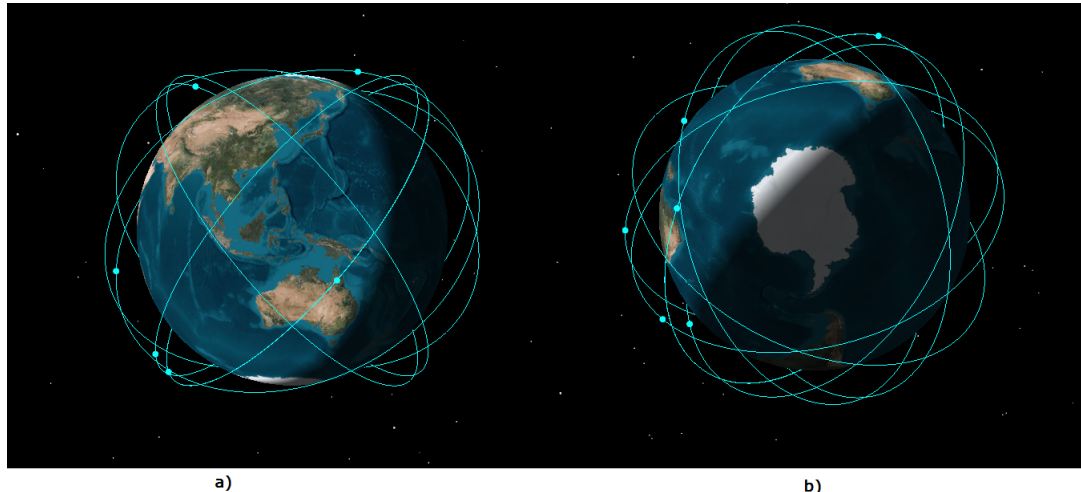


Figure 2.8: The 8 Globalstar Orbital planes as shown from a) above Australia and South East Asia and b) above the south pole. Data from STK

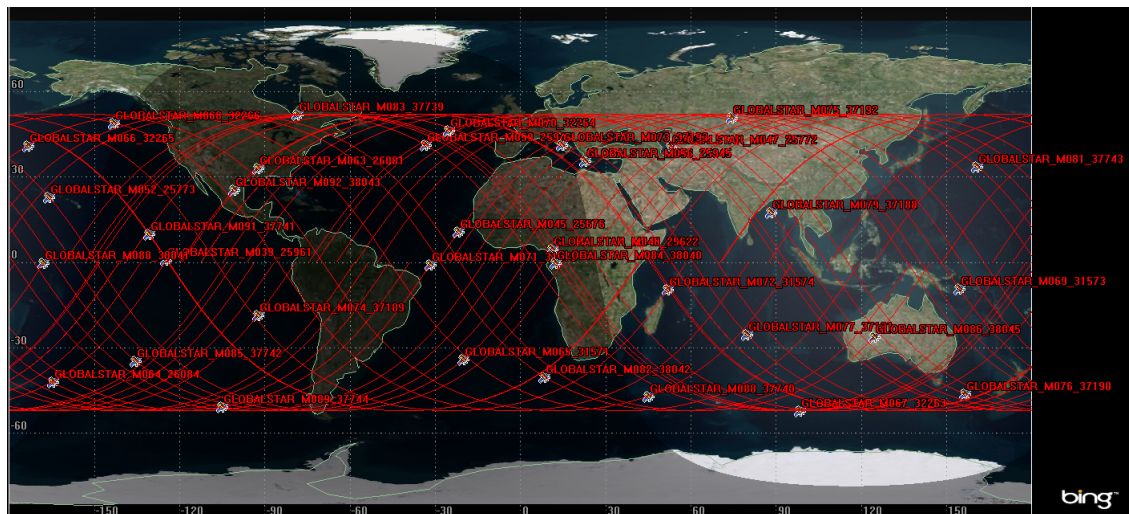


Figure 2.9: The Ground Track of the 48 Globalstar Satellites. Data from STK

## 2.4 Literature Review

A number of academic and commercial groups have shown interest in the concept of developing a space-based ADS-B receiver network. Globalstar and Iridium have committed to delivering constellations with full global coverage, piggybacking on their satellite phone network. Thales, ESA and GomSpace have each developed their own small-satellite ADS-B receivers.

### 2.4.1 ADS-B Link Augmentation System (ALAS)

ADS-B Technologies have developed the ALAS as a space-based ADS-B coverage solution. The ALAS will be flown as hosted payloads on the Globalstar's second generation constellation of satellites. The system is expected to provide global coverage with a one-second update rate [10].

The ALAS is intended to operate by relaying ADS-B data (received via the normal L and S band transmissions) to ground based gateways through the C band. These gateways would then relate that data to Air Traffic Management (ATM) systems as necessary. The system would be full duplex and is designed to transparently augment the existing ADS-B ground coverage network. This operation is illustrated in Figure 2.10. This is intended to be an indirect link that requires on-board aircraft to install additional C-band transponders. In this sense it would not be a true 'drop in' service. Complete ADS-B coverage using this system would incur significant cost to pilots and aircraft manufacturers.

ADS-B Technologies reported that the second generation Globalstar constellation will provide coverage over most continental areas, with minimal coverage over international waters [10]. This is illustrated in Figure 2.11.

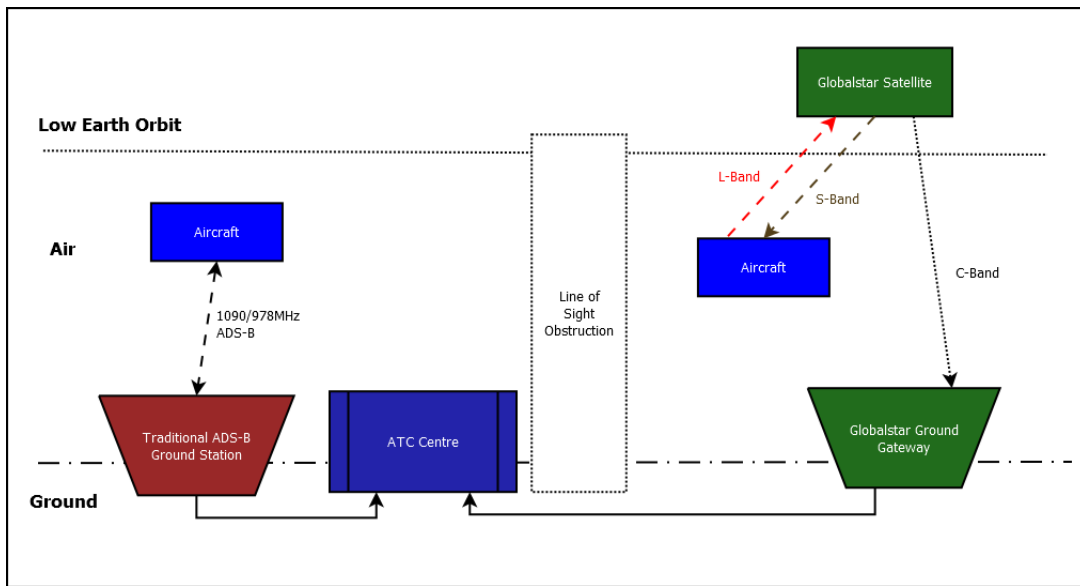


Figure 2.10: Overview of the ALAS system, after [10]

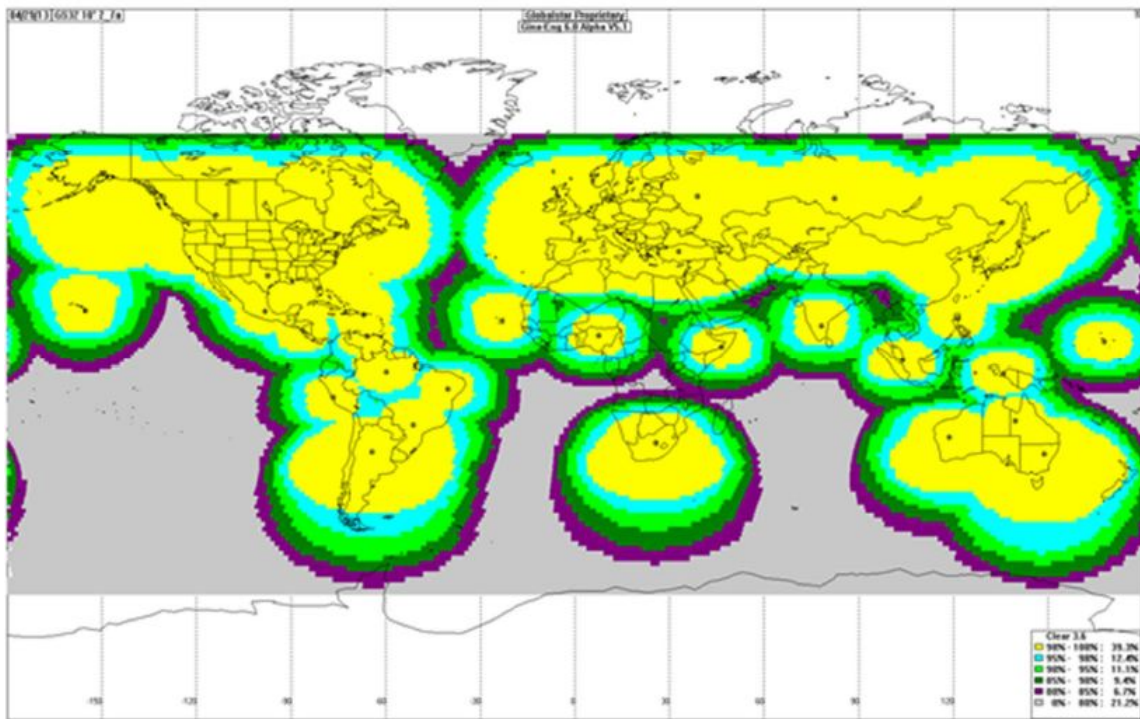


Figure 2.11: ADS-B Duplex coverage provided by the second generation Globalstar constellation, reproduced from [10]

ALAS would have two major shortcomings -

1. The system would require both ANSPs and Aircraft to purchase additional L and S band transceivers to communicate with the space segment. ALAS would not be compatible with standard ADS-B hardware implementation.
2. The second Globalstar constellation would have limited coverage due to its orbit configuration and communication infrastructure. The inclination of the Globalstar orbits would not provide ADS-B coverage over the poles, and would rely on a permanent link with ground stations restricts the predicted coverage to continental areas. This is illustrated in Figure 2.11.

ALAS is expected to be operational in late 2014 [10]. ADS-B Technologies have not yet released any information about buy-in models for ANSPs.

### **2.4.2 Aireon**

As of June 2014, Aireon LLC were developing an space-based, ADS-B reliant ‘global aviation surveillance system’ [9] to be flown on the Iridium NEXT constellation of LEO satellites. The constellation was expected to provide complete global coverage, including over polar regions [24].

This system was presented as flight path solutions for both ANSPs and commercial airlines. Marketing material claimed that intelligent flight path planning will save airlines fuel costs with more optimised routes [24]. No independent analyses or verifications of these claims were found. The service was expected to be available by 2017.

The concept presented for the system suggested that unlike the Globalstar-hosted ALAS, Aireon would use the standard Mode S Extended Squitter carrier signal in order to receive ADS-B

signals [25]. This concept is illustrated in Figure 2.12. This had a distinct advantage in that no additional hardware is required in order to implement the system.

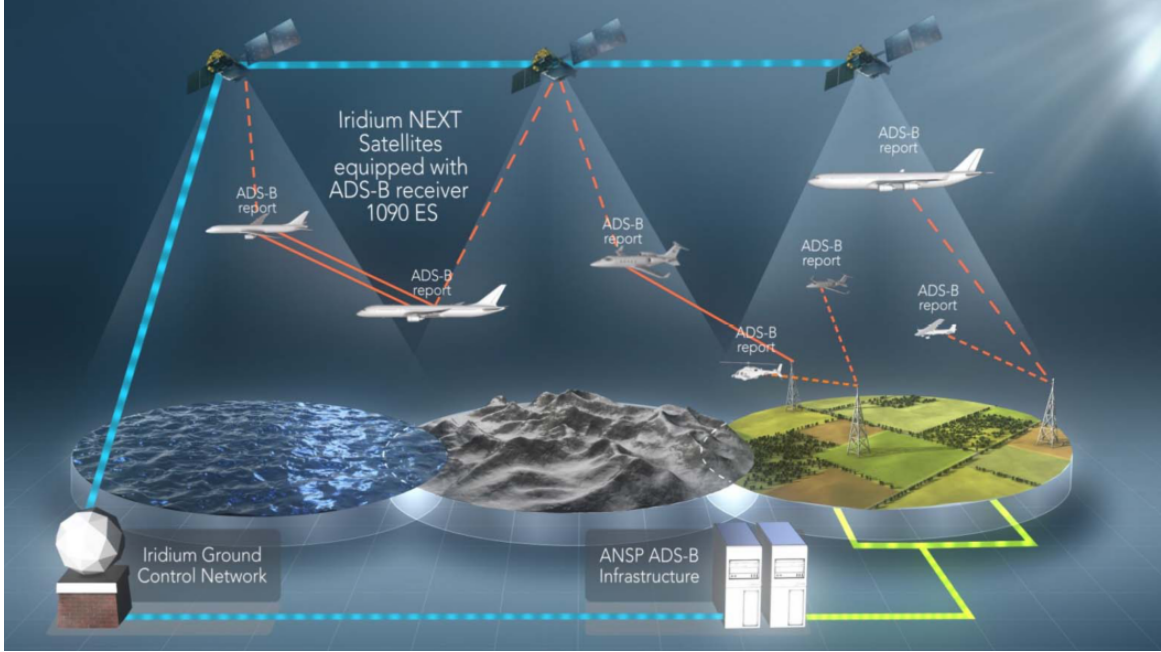


Figure 2.12: Aireon System Concept, reproduced from [25]

Details on the intended orbit and performance standards for the Iridium NEXT constellation had not yet been made publicly available. Descriptions of the Iridium NEXT's intended services suggested that the orbital configuration and control model would be similar to the first Iridium constellation discussed in Section 2.3.1 [9].

Although this provided the complete coverage required by the problem statement, it was expected that the cost-model for the system will be quite high. The launch and operations of the first Iridium constellation was complex and costly enough such that mismanagement of the project's investment and return resulted in Iridium filing for bankruptcy a year after the launch of the final satellite in August 1999 [26]. The total project and operations cost of a smaller CubeSat constellation would be much lower and therefore have significantly less risk. The solution put forward in this thesis could prove to be more economically effective.

### 2.4.3 Spaced Based ADS-B In-Orbit Demonstration Payload (SABIP)

SABIP was presented as space-based ADS-B receiver system designed to operate over the standard Mode S 1090MHz carrier signal currently being developed by Thales Alenia Space Deutschland. The successful implementation of this receiver would enable ADS-B signals to be relayed from LEO without extra infrastructural cost. Specifically, existing Mode S transponders used by aircraft and ANSPs could still be used without significant augmentation to existing equipment. The system was intended to receive and record ADS-B messages, decode those messages and then assemble reports that can be transmitted to ground stations and ANSPs [7].

The research put forward that the chief challenge in designing the receiver was mitigating signal degradation due to high-density traffic. The Mode S frequency is time-shared for both ADS-B transmissions and Traffic Collision Avoidance Systems (TCAS) for all aircraft. The enlarged antenna footprint from LEO meant that both of these signals need to be detected and processed for a high number of aircraft. The footprint of a receiver from LEO would have a radius of approximately 3200 nautical miles whilst a terrestrial Mode S receivers typically have a footprint of 200 nautical miles. This degraded the detection of squitter signals over Mode S transmission [7].

The proposed solution consisted of an ADS-B antenna which has multiple spot beams, each covering a limited area. The models of this antenna are shown in Figure 2.13. The exact number and configuration of spot beams had yet to be determined and required further study of signal degradation due to transmission density [7].

This research identified the key need to deal with signal collisions and maintaining a high probability of aircraft detection. In particular, the issues with detection probability given a high number of aircraft agree with the Mode S receiver requirements described in [27]. This

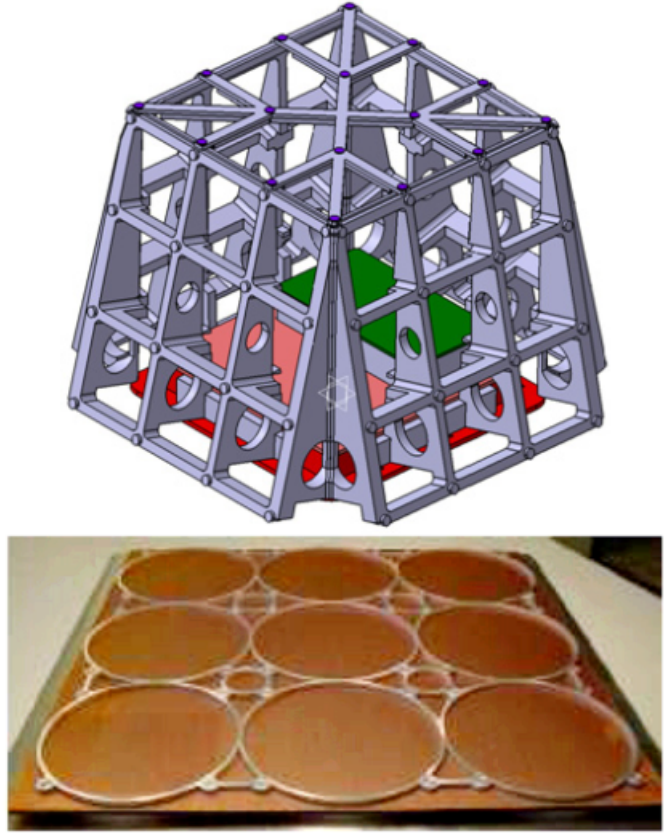


Figure 2.13: SABIP receiver Antenna design, reproduced from [7]

means that re-visit time and scan time for a particular area on Earth will be key parameters in evaluating the effectiveness of any given ADS-B constellation

The technology developed by Thales could also form a foundation for the implementation of a CubeSat-based ADS-B receiver system. Signal collision and resolution problems outlined in the paper would be experienced by any in-orbit ADS-B receiver. Although the exact antenna dimensions prohibit SABIP from being incorporated into a CubeSat form-factor, the same design principles would need to be incorporated into the design of a more suitably sized receiver. Similarly the data storage and analysis framework put forward in [7] could be used for the ground and space segment of the ADS-B system. The research indicated that the technology

required for a spaced-based ADS-B receiver is certainly possible in the CubeSat form factor.

#### 2.4.4 Proba V

In early 2013, the European Space Agency (ESA) launched their fifth experimental Proba satellite, Proba V, with a guest ADS-B Payload. Like SABIP, the ADS-B payload is designed to receive signals via the native Mode S 1090Mhz carrier. The receiver, designed by the German Aerospace Center (DLR) was designed to receive ADS-B from LEO in Proba V’s 820km orbit [28–30]. Proba V is travelling in a Sun-synchronous polar orbit at an altitude of 820km [29].

As of June 2014, the satellite was tracking aircraft over Northern Europe [28]. Tests to determine the sensitivity of the receiver to issues caused by signal density (as put forward by [7]) were ongoing. Figure 2.14 shows the results from the initial proof of concept, with aircraft being detected in Europe [29]. No further results beyond this proof of concept have been published. However this provided further evidence for the viability of receiving ADS-B signals from LEO, particularly from an altitude as high as 820km.

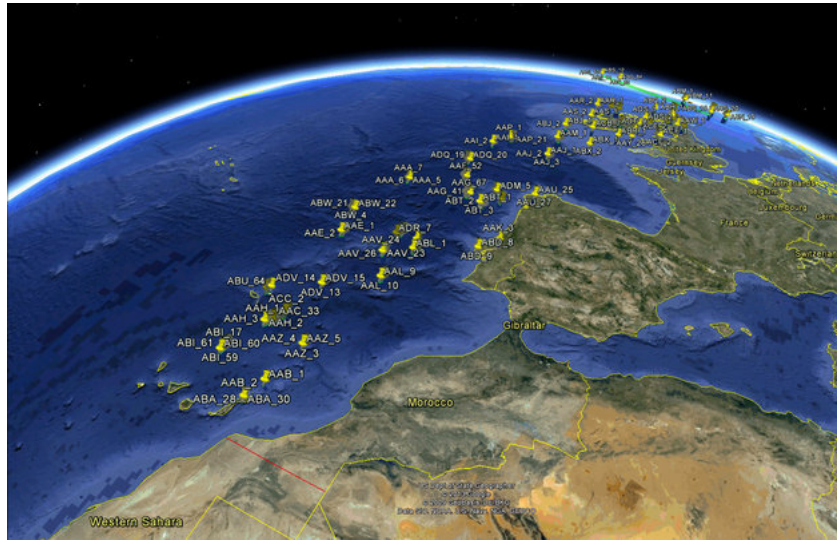


Figure 2.14: Aircraft detected by Proba V over Europe, reproduced from [29]

### 2.4.5 GOM-X1

The GOM-X1 was a 2U CubeSat intended to perform a number of space-based experiments using software defined radio (SDR), the primary being a spaced-based ADS-B receiver. The satellite was developed as a collaborative effort between GomSpace, DSE Airport Solutions (now Insero Software [31]) and Aalborg University. The primary mission of the satellite was to demonstrate that ADS-B reception is capable from a CubeSat platform in LEO. Data received from onboard sensors would be compared with ground-based ADS-B data to verify the correctness of the data acquired from LEO [32, 33].

ADS-B signals were to be received via a custom SDR payload. The SDR is designed to be able to have a reconfigurable decoder structure. The intention of the experiments was to evaluate the effectiveness of different decoder configurations. This data would be used for further refinements to space-based ADS-B CubeSat modules. A helical receiver antenna is used in order to maximise the gain going into the system, pictured in Figure 2.15. GOM-X1 used a standard commercially off-the-shelf (COTS) bus available from GomSpace [33].

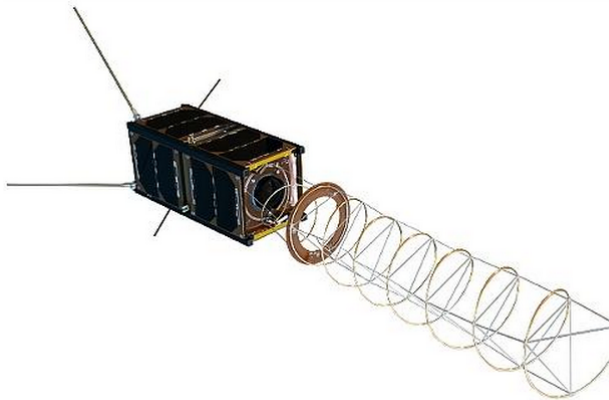


Figure 2.15: 3D render of the GOM-X1 satellite, showing the expanded helical receiver antenna, reproduced from [32]

The satellite was successfully launched in November of 2013 into an circular orbit of 600km altitude and 97.8 degrees of inclination. GOM-X was still ‘fully commissioned’ and operational in June of 2014 [32,34]. GomSpace released a ‘preliminary plot’ of the received aircraft positions, reproduced in Figure 2.16, showing detected aircraft mostly in the northern hemisphere.

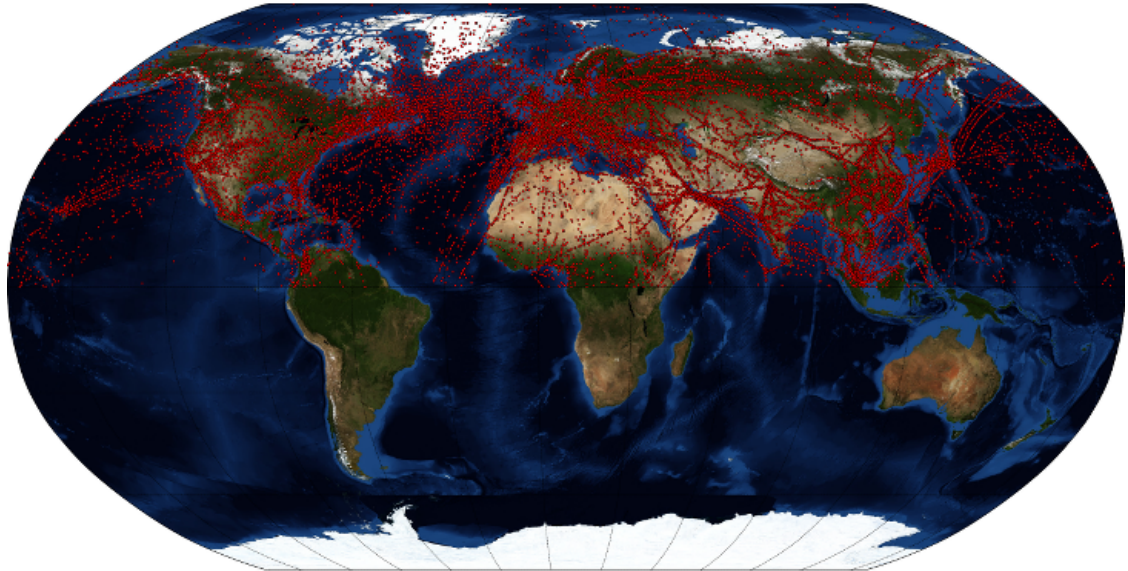


Figure 2.16: Preliminary plot of planes detected by GOM-X1, reproduced from [32]

The early success of the mission provides a good indication of the viability of a CubeSat based ADS-B receiver. However no data is provided on the quantitative performance of the receiver. Of particular interest would be the aircraft detection rate of a given pass or scan of the satellite. Being able to determine the statistical likelihood of aircraft detection from the GOM-X1 would provide a hard systems constraint for the design of a CubeSat constellation. The data presented in this thesis will instead provide a range of constraints on the sensitivity of the required ADS-B receiver from the analysis of proposed constellations.

### **2.4.6 Conclusions**

The survey of current technologies show that there is commercial motivation for the development of ADS-B systems from space. ALAS and Aireon represent significant commercial investment in the development of space-based ADS-B systems. Although the large commercial risk is absorbed significantly by having the payloads ‘piggy-back’ on the Globalstar and Iridium NEXT constellations, the costs of the buy-in model are not yet known.

Proba V, SABIP and GOM-X1 demonstrate that there is significant interest in implementing space-based ADS-B on small satellites. Proba V and SABIP are both designed for use on smaller satellites with the intention of potentially lowering the cost of a space-based ADS-B system. Proba V in particular has already demonstrated success, though that success has not yet been quantified. The success of GOM-X1 proves that the technology is viable on a CubeSat scale.

These examples show that there is ongoing interest and motivation in developing an economic solution for a space-based ADS-B system. The Iridium NEXT and Globalstar constellations provide guaranteed system update and coverage but the design is not necessarily optimised for ADS-B coverage. Given the success of technology demonstrators for small satellites, there is sufficient motivation for development of a low cost ADS-B constellation using CubeSats.

# Chapter 3

## Experimental Method and Design

In general terms we were interested in the ability for a given constellation of LEO satellites to provide ADS-B coverage in the absence of land-based ADS-B receivers. To evaluate this, popular flights over the Atlantic and Pacific Oceans were simulated in STK. The simulation was extended to include communication links to LEO satellites. Different satellite constellations were simulated and the link-budget data for each test case was collected. The efficacy of a constellation was determined by comparing the aggregated access times and link budgets for the ADS-B links between a given trans-oceanic flight and the overhead satellites. The full set of STK simulation files is available at [35]

## **3.1 Mission Overview**

The root requirement of a satellite-based ADS-B system was the provision of ADS-B coverage over regions where terrestrial systems did not currently provide coverage (in particular, oceans and poles). Within this requirement were a number of variable mission parameters that affected the design and economic cost of resulting satellite systems. Varying the parameters and analysing the performance of resulting designs was used for a mission trade-off analysis, presented in Section 4.5.

### **3.1.1 System Users**

A spaced based ADS-B system would have two key user groups

- Air Navigation Service Providers
- Airlines and air transportation service providers

Although Australia, America and Europe were able to implement terrestrial ADS-B stations, rolling out terrestrial stations to cover all interest areas was not necessarily cost effective. This was particularly true in regions such as South East Asia. In such areas, the technology and economic base did not exist to make terrestrial deployment viable [7]. In these situations a satellite-based system could more effectively augment existing ADS-B coverage for use by ANSPs.

Another key user would be airlines and other air transportation services. Greater position and telemetry coverage of aircraft over oceanic and polar regions would facilitate more optimal flight path co-ordination. ADS-B assisted flight routing would allow for narrower longitudinal and latitudinal track separation, allowing for more flights to travel on desired fuel-saving paths. A

flight simulation analysis presented by Iridium LLC suggests that increased density of planes in jet streams can result in fuel savings of up to 450 litres per oceanic flight [25].

### **3.1.2 System Update Rate**

The update rate of a space-based ADS-B system defined timeliness with which aircraft data can be updated and disseminated terrestrially. Having a high-effective update rate was crucial in range of airports with ATC towers having to co-ordinate a large density of aircraft traffic. With ADS-B, terrestrial ATC towers typically achieved at least 1 update per second, depending on airport capacity [27]. For the purposes of live tracking and safety control, an update rate in the order of 1 second to 30 seconds would be required. An update rate in the order of 5 to 10 minutes would enable satisfactory tracking by airlines and air transport services at less cost. A lowest cost system with an update rate of 1-2 hours could be useful for occasional tracking of aircraft making oceanic flights. This, however, would be inadequate for safety applications or any short-range terrestrial flights.

### **3.1.3 Revisit Time**

Due to the random access nature of Mode S Extended Squitter, the number of aircraft surveyed by an ADS-B receiver was limited. Scanning for a shorter period, or scanning an area with more aircraft would result in more ADS-B collisions and a drastically reduced detect rate. ‘Missing’ aircraft in this manner would be unacceptable from a safety perspective. Suggested solutions for high density areas included more sophisticated antenna design with spot beams [7], or variable-periodicity of ADS-B signals [27].

For ADS-B reception via satellite, a populated area could be either scanned for a longer period, or ‘re-scanned’ over multiple revisits. This would moderate the need for a larger or more sophisticated and costly antenna array. A longer scanning period could be achieved slowing

the ground-track of the space segment over key areas. This would particularly be a problem on CubeSats where technology capability was limited. The revisit time would therefore be defined by limitations of the antennae array and on-board processing technology for ADS-B signal reception. More detail on current small-satellite ADS-B receiver research is discussed in Section 2.4.

### 3.1.4 Geographical Coverage

Full global coverage would be achieved by a series of polar or near polar orbits, such as the Iridium Satellite constellation [19,20]. Achieving full coverage would be the most costly solution, requiring the largest number of satellites and ground stations. At the very least, the ADS-B system should at least cover the North Atlantic, North Pacific and Indian Oceans and South East Asia in order to meet the root system requirement. These areas had the highest amount of air traffic not covered by terrestrial ADS-B systems as shown in Figure 3.1. Monitoring these regions with specific orbits can reduce the number of spacecraft required in order to provide the coverage gap required by the system. Coverage of the poles would provide extra benefit, opening up polar flight paths.



Figure 3.1: Popular flight routes, from [36]

## 3.2 Experimental Parameters

During this thesis, simulations were carried out in order to design and evaluate different ADS-B constellation options. Input parameters for each simulation were defined and varied to carry out a parametric study. The output parameters were used in order to quantify system performance and provide a means of quantitative comparison between constellation options.

### 3.2.1 Performance Metrics

ADS-B coverage for each satellite constellation was analysed on a flight-by-flight basis. For a given constellation, the communication link was analysed separately for a sample of trans-oceanic test flights. Each link was characterised by three parameters -

- **Access Times** - the periods of time during which a flight had line-of-sight to at least one overhead satellite and therefore could theoretically establish an ADS-B link. This was available as primary data from STK.
- **Coverage Gap Times** - the periods of time during which a flight has line-of-sight access to no satellites in the constellation. This was calculated by processing raw data from STK.
- **Received Isotropic Power** - the power of the ADS-B signal after it has been propagated from a flight to an overhead satellite. This was available as primary data from STK <sup>1</sup>.

---

<sup>1</sup>Although the STK communication toolkit was capable of RF link characterisation beyond simply received isotropic power, it was found that the ‘simple’ antenna models used were not adequate for that level of analysis. The results, typified by Table 4.2, show a very high bit-error rate and bad signal-to-noise ratio. The values were such that the development of a signal processing module would be near impossible. A more realistic set of signal characteristics could be achieved by more sophisticated antenna and RF models. However the knowledge required to design the model was beyond the scope of this thesis. Instead, we simply used received power as a comparative indicator of RF performance of the system.

## CHAPTER 3. EXPERIMENTAL METHOD AND DESIGN

---

- **Cost of Operation and Launch** - A larger number of satellites or a more complex constellation would present an increased launch and operations cost. The total cost of operation was important when performing the trade-off analysis for different constellation parameters

From this data, four values were computed and used as performance metrics to evaluate the efficacy of a constellation -

1. **Total coverage gap fraction** - the fraction of time a simulated flight spends without being able to transmit ADS-B signals to a satellite. This would be representative of the time the flight would expect to spend out of communication for a given period of time. This was calculated by the formula

$$\text{Gap Fraction} = \frac{\text{total time with no access to a satellite}}{\text{total analysis time}}$$

2. **Maximum gap time** - the maximum amount of time a flight spends without a communication link to a satellite. This represents the worst case scenario for the amount of time a flight would spend out of communication.
3. **Average Gap Time and Average Access Time** - the mean of access times and coverage gap times identified during the analysis period. This would give an indication of the periodicity of the 'access-no access' cycles that a flight would experience.
4. **Minimum Received Isotropic Power** - the minimum power of an ADS-B signal as it is received by a satellite. This can be used to later determine the link budgets and perform the system definition for a given satellite in the constellation.
5. **Total Number of Satellites** - the number of satellites required by a particular constel-

CHAPTER 3. EXPERIMENTAL METHOD AND DESIGN

lation was used as an indication of launch and operations cost. It was assumed that each satellite was identical and therefore the relative cost of launch was well represented by the number of satellites specified <sup>2</sup>.

The relative importance of these performance metrics will be compared in Section 4.5

### 3.2.2 Flight Selection

Data from global flight paths was provided by OpenFlights [36] with all paths reproduced in Figure 3.1. The advantages of space-based ADS-B coverage would mainly come from areas where ground-coverage is not possible. For this reason, flight paths that were primarily over land-masses were not considered for analysis. This eliminated the majority of flights originating in the Europe and ending in any of Africa, Asia and Australia. Analysis then focussed on flights passing over the Atlantic and Pacific Oceans. These flights were mostly between the United States and Europe, Asia and Australia, as shown in Figure 3.2.



Figure 3.2: Trans-Oceanic Flight paths, as modelled in STK

<sup>2</sup>The cost of launch and operations would also be significantly affected by the effects of atmospheric drag, a phenomenon which decreases the ideal operational lifetime of all satellites in LEO. However the variability of the atmosphere and ‘aerodynamic’ satellite design was such that no good model existed to estimate the effect of atmospheric drag. As such this parameter was not accounted for in this thesis.

## CHAPTER 3. EXPERIMENTAL METHOD AND DESIGN

---

Of these flights, three generalisations were defined and one flight from each generalisation was used for modelling -

1. **North America to Asia** - The path between Los Angeles International Airport (LAX) and Narita airport (NRT) in Tokyo Japan
2. **North America to Europe** - The path between LAX and Heathrow (LHR).
3. **North America to Australia** - The path between LAX and Sydney (SYD) International Airport.

These three flight routes are illustrated in Figure 3.3.

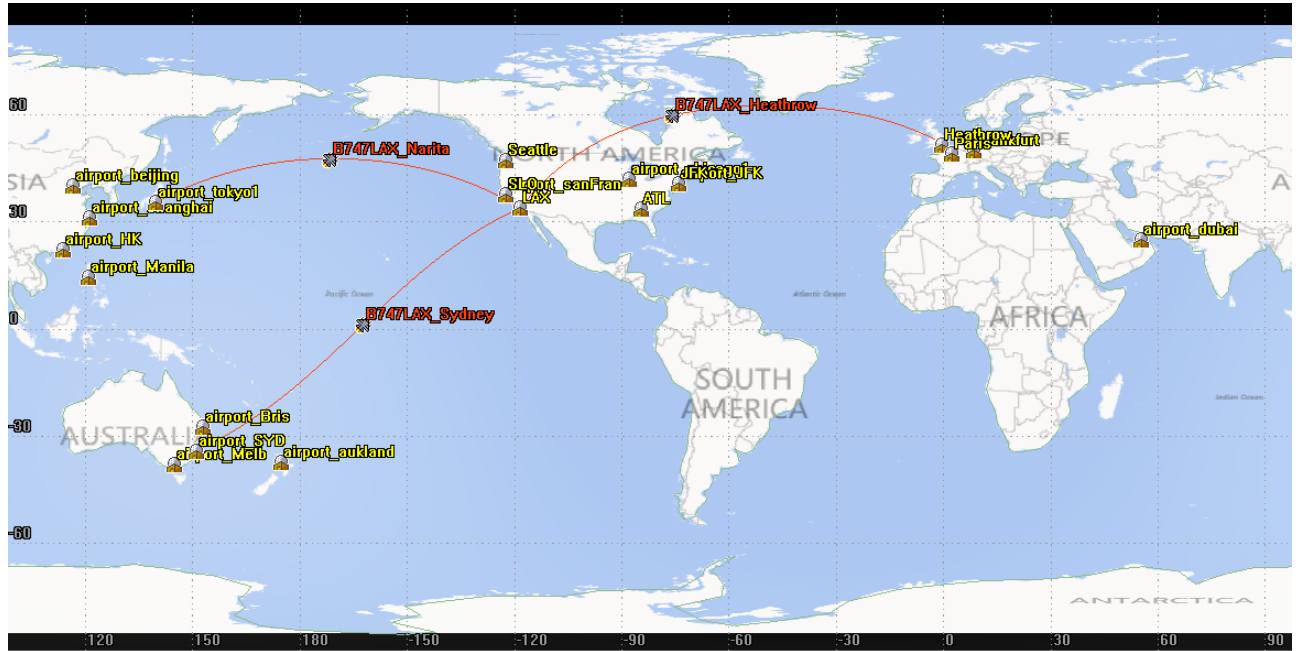


Figure 3.3: Generalisations of trans-Oceanic Flight paths used for analysis

The performance of a given constellation was determined by examining the ADS-B coverage available for each flight by the parameters outlined in Section 3.2.1. The flights were simulated

as going continuously back and forth between their two destination airports. The effect of this periodicity is expanded upon in Section 3.2.5.

### 3.2.3 Input Variables

The performance metrics presented in Section 3.2.1 were evaluated against different constellation configurations. Initial tests, discussed later in Section 4.3.1, ruled out Molniya and geosynchronous orbits as practical solutions. The parametric study was then restricted to Low-Earth Orbits, varying orbital parameters from a ‘reference case’.

#### 3.2.3.1 Reference Case

The reference case was chosen to be a constellation of 12 satellites distributed in three circular orbital planes, each with four equispaced satellites. Each orbital plane was inclined at 60 degrees and were at an altitude of 700km above the Earth (a semi-major axis of 7078.14km). The three planes were separated by 120 degrees of ‘longitude’ or right angle of ascending node (RAAN), starting from 0 degrees for plane one. The four satellites within each plane were separated by true anomalies of 90 degrees. These parameters are summarised in Table 3.1. The ground track of the configuration is shown in Figure 3.4 and the 3D representation is given in Figure 3.5

It was expected that change in inclination, altitude and number of satellites will effect the performance of a given constellation. An increase in altitude would result in an increase in orbital period, but would also increase the receiver footprint of a given satellite with a greater field of view. The change in inclination would vary the maximum and average coverage gap times as the ground traces intersect with the flight paths in different ways. The change in the number of satellites would change the average and maximum ADS-B coverage gaps, but provide a trade-off with the number of satellites requiring production, maintenance and replacement.

Table 3.1: ‘Reference’ constellation configuration

Parameter	Value
Total number of satellites	12
Orbital planes	3
Satellites per plane	4
Separation between planes	120 deg RAAN
Spacing within a plane	90 deg true anomaly
Orbit type	Circular, LEO
Semi-major axis	7078.14km (700km altitude)

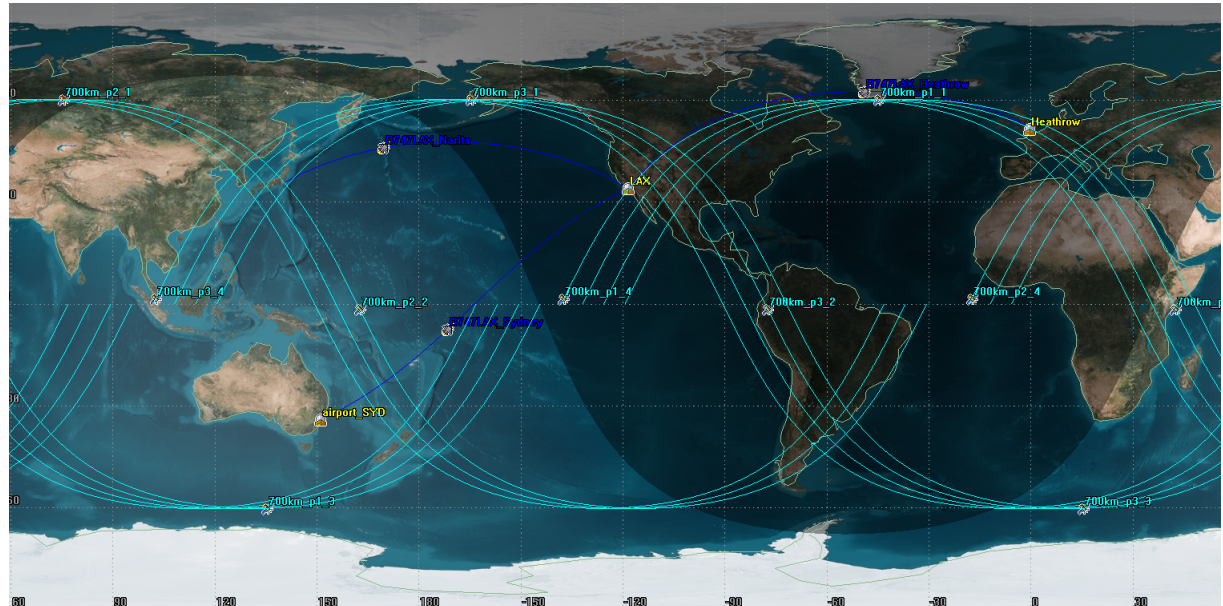


Figure 3.4: Ground track of the 12 satellite reference configuration in STK

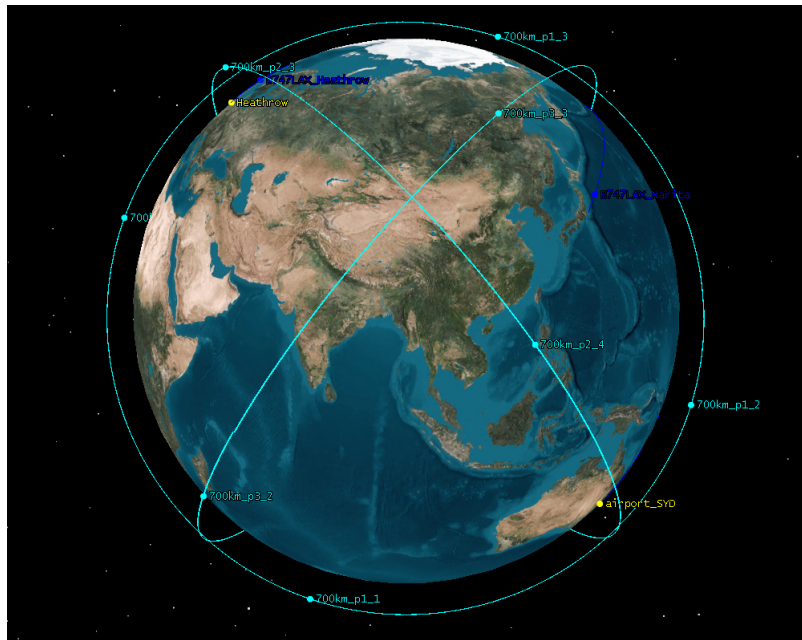


Figure 3.5: 3D model of the 12 satellite reference configuration in STK

### 3.2.4 Test Cases

From the reference case, inclination, altitude and number of satellites per-plane were varied according to the values presented in Table 3.2. The full table of cases evaluated is given in Appendix C.

Table 3.2: Varying input parameters used for data and analysis

Input Parameter	Minimum	Maximum	Step Size
Altitude	400km	800km	50km
Satellites per plane	1	6	1
Inclination	$30^\circ$	$90^\circ$	$10^\circ$

### **3.2.5 Analysis Period**

Synchronisation and periodicity were taken into account in selecting an analysis period. The discrepancy between air speed of planes (in the order of 250m/s) and the orbital velocity of LEO satellites (in the order of 8km/s) resulted in asynchronous behaviour. This was also complicated by the speed of the Earth's rotation underneath the orbital planes. The analysis period was therefore chosen to be long enough to such that -

- The effective ground track for one satellite would form a continuous swath between the latitudes of inclination. The length of period was chosen so that the ground track would repeat over the same global co-ordinates at least once.
- The aggregate results of analysis would accurately take into account all cases where the lack of synchronisation between orbital period and flight time would produce abnormal results. That is, sufficiently many orbital and flight periods are repeated in order to observe an accurate aggregate effect and identify each of the worst-case scenarios.

After initial tests it was found that an analysis period of approximately six days was appropriate. In STK the scenario was analysed between 12:00AM on December 3rd, 2013 to 12:00AM December 9th, 2013,  $\pm$  24 hours to allow for varying flight times.

### 3.3 Analysis Tools

The work carried out used a combination of STK, Matlab and Microsoft Excel in order to simulate, process and display the relevant data. Observations and analysis was carried out based upon the outputs from each of the three steps in the experimental process.

#### 3.3.1 STK

STK version 10.0.2 was used in order to simulate flights, satellite orbits and communication links over the relevant analysis period. The flight paths of interest were chosen according to the process outlined in Section 3.2.2 and the characteristics defined in Section 3.6 were programmed into STK in order to create the plane and flight models. Each satellite constellation was modelled as a collection of standard satellites, with orbital parameters as specified in Section 3.2.4. The STK Communications Toolkit was then used to simulate the ADS-B links between the modelled flights and satellites, outputting data about access times and link budget. The simulation was run continuously for the duration of the analysis period discussed in 3.2.5. The raw data generated by this model is described in Table 3.3.

Table 3.3: Raw data generated by STK

Data	Description
Access Times	The start and stop times of periods where a particular flight can access a particular satellite. This is output as .csv files per test of all accesses for the flight and the satellites in the orbit of interest during the test.
Link Budget	Characteristics of the communication link established during each flight-to-satellite access. Of particular interest is the received isotropic power at the satellite. This is output as .csv files per test of all accesses for the flight and the satellites in the orbit of interest during the test.

### **3.3.2 Matlab**

Matlab was used in order to concatenate and sort the data generated by the STK simulation and output the performance data specified in Section 3.2.1. The access times .csv files were sorted and concatenated in order to extract the ‘gap’ times where a flight has no access to any satellite. Periods of ‘access’ and ‘gap’ were averaged and the minima and maxima were extracted for further analysis and display. Similarly the link budget .csv files were analysed in Matlab to extract the minimum received isotropic power for each flight.

### **3.3.3 Excel**

Finally, the data outputted from Matlab was imported into Microsoft Excel in order to easily display the data for the analysis of trends and the calculation of the system trade-off decision matrix.

## 3.4 Model Input Data and Assumptions

Data used in the simulations was researched from official sources was used in order to generate simulations that would closely represent the expected true-to-life situations.

### 3.4.1 Link Type

A series of simplifying assumptions were made about the characteristics of the ADS-B links being analysed. The parameters used in the STK link model are summarised in Table 3.4.

Table 3.4: Link Parameters used in STK

Parameter	Value	Description	Source
Transmitter Model	‘Simple Transmitter Model’	The transmitter model type used by STK to propagate and analyse link budgets	[37]
Equivalent Isotropically Radiated Power (EIRP)	240W	Power transmitted through an ADS-B antenna assuming zero losses between transponder and antenna	[38–41]
Bit Error Rate (BER)	$10^{-6}$	Minimum bit error rate of a link	[42]
Modulation Type	‘Pulsed Signal’	Type of modulation used in the link	
Bandwidth	8MHz	The bandwidth of an ADS-B Signal	[42]
Frequency	1090MHz	The carrier frequency of ADS-B and Mode S signals	[37]
Receiver Model	‘Simple Receiver Model’	The receiver model type used by STK to analyse links from transmitters	[37]

Transmission power was generalised based upon a survey of commercially available transponders

[38–41] to 240W, transmitted with the assumption that there were insignificant signal losses between the transmitter and antenna. The minimum bit-error rate (BER) was set to  $10^6$  bits per second based on the ADS-B transmission specification released by the RTCA [42]. A ‘pulsed signal’ was used in order to model the radar-like behaviour of ADS-B, as suggested by [37] and no filter was applied to the output. The signal bandwidth was set to 8MHz (+/- 4MHz) as specified by [42].

These parameters were input to a ‘Simple Transmitter Model’ was used in STK, as the suggested model to use during the system engineering process [37]. Modelling a more complex transmitter model and defining antenna and propagation type were considered outside the scope of this thesis.

Each of the satellites in the space segment was given a ‘Simple Receiver Model’. The receiver gain divided by system noise temperature  $G/T$  was left unchanged from the default  $20K$ . Other link parameters would be automatically completed upon analysis of a link with a specified transmitter [37].

### **3.4.2 Flight Characteristics**

Analysis focussed primarily on the performance of ADS-B coverage for a plane during the transoceanic portion of the flight path of interest. Planes within range of an airport would already be serviced by the airport’s ground ADS-B receivers. Flights were therefore modelled as single aircraft travelling at a constant cruise speed and altitude between the source and destination airports, ignoring landing and take-off procedures.

Typical cruise altitudes for commercial airliners range between 30 000 and 40 000 feet. The lower bound of 30 000 feet was chosen in order to maximise the distance travelled by an ADS-B transmission, producing a worst case scenario for signal loss.

### CHAPTER 3. EXPERIMENTAL METHOD AND DESIGN

---

The Boeing 747 was chosen as a ‘typical’ commercial transoceanic aircraft, with a cruising speed of 913 km/h. The 747 was chosen after examining a cross section of the typical cruising speeds of popular ‘long haul’ commercial aircraft, given in Table 3.5.

Table 3.5: Cruising speeds of typical commercial aircraft

Manufacturer	Model	Speed (km/h)	Speed(km/s)	Source
Boeing	747-400	913	0.25361	[43]
Boeing	777-200	1029	0.28584	[44]
Boeing	757-200	980	0.27222	[45]
Airbus	A380	945	0.2625	[46]

A summary of the aircraft parameters used in STK is given in Table 3.6

Table 3.6: STK Parameters used for each flight model

Parameter	Value
Altitude	9.144 km (30,000 feet)
Speed	0.2536 km/sec (913 km/h)

The global co-ordinates for the 4 airports of interest were taken from [36], presented in Table 3.7.

Table 3.7: Airport global co-ordinates, from [36].

Airport Name	City	Code	Longitude	Latitude
Los Angeles International Airport	Los Angeles	LAX	33.9425°N	118.4081 °W
London Heathrow Airport	London	LHR	51.4775°N	0.4614 °W
Narita International Airport	Tokyo	NRT	35.7653°N	149,3856 °E
Sydney Airport	Sydney	SYD	33.9461°S	151,1772 °E

### 3.4.3 Satellite Characteristics

The standard STK satellite model was used to model each satellite in the test constellations. It was assumed that there would be attitude control aligning the antenna element with the nadir and no active station keeping systems. The STK `J4Perturbation` orbit propagator was used in order to account for the oblateness of the Earth.

# Chapter 4

## Results and Analysis

The input parameters detailed in Part 3 were simulated in STK and their performance evaluated using tools in Matlab and Microsoft Excel. Initially a set of exotic constellations were tested and ruled out as being impractical and ineffective. Parameters from the reference case detailed in Section 3.2.3.1 were then varied to see the effect on the performance metrics used to define the effectiveness of a space-based ADS-B system. The full set of raw and processed data is available at [35].

## 4.1 Raw Results

From each simulation in STK, two raw data sets were extracted - a series of access times and the link-budget characterisation for the modelled satellite constellation. The

### 4.1.1 Access Times

Access times were output from STK as tables of access periods. Each access period represented a period of time where the flight in question was able to establish an RF link with a particular overhead satellite. Access time tables were grouped by satellite and by flight analysed. Start and stop times were given in fraction of days from January 1st, 1900. A sample of raw data, taken from the reference case from Section 3.2.3.1 is presented in Table 4.1. This data shows the first five accesses between a flight from LAX to Heathrow and two of the satellites in the constellation. All results were concatenated and sorted into for further analysis in Section 4.2.

Table 4.1: Sample access data for satellite 1 of the reference case

Access	Start Time (UTCG)	Stop Time (UTCG)	Duration (sec)
1	41611.05	41611.06	945.833
2	41611.12	41611.13	955.49
3	41611.19	41611.20	949.135
4	41611.26	41611.27	958.031
5	41611.33	41611.34	930.449

### 4.1.2 Link Budget

Link budget data was sampled by STK every hour. As with the access times, data was grouped per flight per satellite in the constellation. Each sample of data included the transmitted power

## CHAPTER 4. RESULTS AND ANALYSIS

---

(EIRP), received frequency, received isotropic power and other link characteristics. A sample of data outputted from STK from one link is given in Table 4.2. This data was taken from the simulation of the reference case from Section 3.2.3.1 and shows the first 10 samples of the link budget data from a communication link between an LAX-Heathrow flight and one of the satellites in the constellation. This data was also concatenated and sorted for further analysis, as presented in Section 4.2.

Table 4.2: Sample of link budget data from a simulation of a link between a flight and a satellite

Time (UTCG)	EIRP (dBW)	Frequency (GHz)	Rcvd. Iso. Power (dBW)	Flux Density (dBW/m <sup>2</sup> )	g/T (dB/K)	C/No (dB*Hz)	Bandwidth (kHz)	C/N (dB)	Eb/No (dB)	BER
41611.05	23.979	1.09	-139.95	-117.75	-114.97	-26.32	8000.00	-95.36	-86.32	0.50
41611.05	23.979	1.09	-138.93	-116.72	-115.56	-25.88	8000.00	-94.91	-85.88	0.50
41611.05	23.979	1.09	-137.76	-115.56	-114.62	-23.79	8000.00	-92.82	-83.79	0.50
41611.06	23.979	1.09	-136.45	-114.24	-111.52	-19.37	8000.00	-88.40	-79.37	0.50
41611.06	23.979	1.09	-134.96	-112.76	-105.35	-11.71	8000.00	-80.74	-71.71	0.50
41611.06	23.979	1.09	-133.30	-111.10	-95.07	0.23	8000.00	-68.80	-59.77	0.50
41611.06	23.979	1.09	-131.57	-109.36	-80.30	16.73	8000.00	-52.30	-43.27	0.50
41611.06	23.979	1.09	-130.10	-107.89	-64.44	34.06	8000.00	-34.97	-25.94	0.47
41611.06	23.979	1.09	-129.57	-107.36	-57.96	41.07	8000.00	-27.96	-18.93	0.44

## 4.2 Data Processing

The raw per-satellite data from STK was combined to create a data set representative of the performance of the constellation in question. A sample of the output from Matlab is given in Table 4.3, with start and stop times given in fraction of days since January 1st, 1990. This sample was taken from the LAX-Heathrow flight simulation with reference case constellation of satellites.

Rows of access times for all satellites were sorted by access start time. The difference between the access start time of the current row and the access stop time of the previous row was used to calculate the gap time between accesses. In the case of overlapping access times, the difference is negative and discarded (marked in Table 4.3 as ‘N/A’). For these cases, the total access time is calculated as the difference between the end of the last calculated gap and the beginning of the current gap.

Table 4.3: Calculated access times from Matlab

Satellite Number	Access Number	Access Start Time	Access Stop Time	Access Length (s)	Gap Start Time	Gap Stop Time	Gap Length(s)
2	6	41611.38	41611.39	845.73	41611.37	41611.38	664.42
1	6	41611.40	41611.41	N/A	41611.39	41611.40	711.17
8	1	41611.41	41611.41	891.41	N/A	N/A	N/A
4	6	41611.42	41611.43	N/A	41611.41	41611.42	676.12
7	1	41611.42	41611.43	895.24	N/A	N/A	N/A
3	6	41611.44	41611.44	N/A	41611.43	41611.44	681.03
6	1	41611.44	41611.45	848.90	N/A	N/A	N/A
2	7	41611.45	41611.46	N/A	41611.45	41611.45	697.37
5	1	41611.45	41611.46	936.46	N/A	N/A	N/A
1	7	41611.47	41611.48	N/A	41611.46	41611.47	560.17

### 4.2.1 Statistical Modelling

The periodicity and frequency of concatenated access periods (discarding ‘N/A’ values) was indicative of the number of ‘discrete’ sample points available along a flight. A lower average period of access meant a higher access and update rate for a particular flight path. This higher effective sample rate would allow for potential deviations from a flight path to be detected earlier and with greater resolution. The access periods for each flight and each constellation were analysed statistically by finding the statistical model of best fit. This was achieved using the `allfitdist` tool from [47]. An example of the fitted distribution is given in Figure 4.1. From the ‘best fit’ model, the mean and standard deviation of the periods were extracted for consideration in the decision matrix.

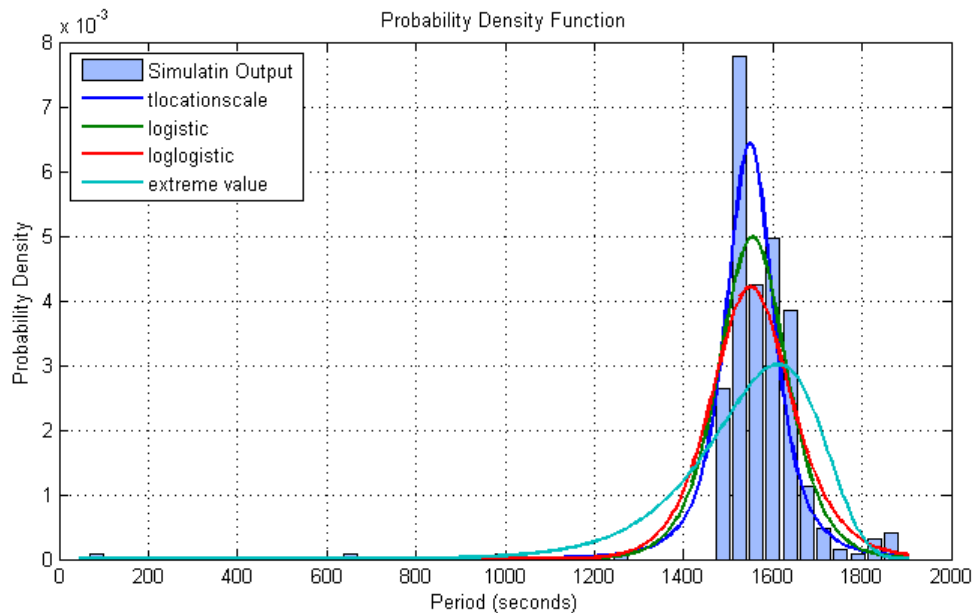


Figure 4.1: Output of `allfitdist` when applied to the access periods of the LAX-Narita flight using the reference constellation described in Section 3.2.3.1

## 4.3 Trends and Analysis

### 4.3.1 Initial Constellation Tests

During preliminary testing, a Molniya and geosynchronous orbit were simulated. The results ruled them out as practical orbit options, restricting the bulk of study to LEO satellite constellations.

#### 4.3.1.1 Molniya Orbit

A highly inclined molniya orbit was tested with orbital configuration such that the apogee<sup>1</sup> of the orbit occurred over the LAX-Heathrow and LAX-Narita flight paths. The ground track of this orbit is shown in Figure 4.2. It was observed that the satellite would ‘hang’ for long periods of time over the apogee potentially allowing for a longer coverage time. Initial tests yielded a minimum received isotropic power of -162.0 dBW. This was more than 100 times weaker than the worst signal of -140.5 dBW from the set of tested LEO constellations.

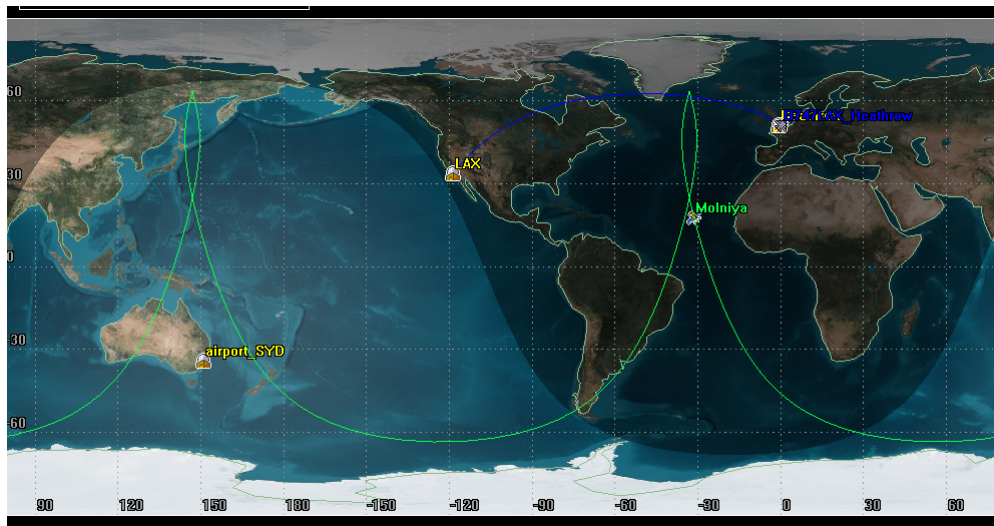


Figure 4.2: Ground track of the tested Molniya orbit

<sup>1</sup>Point at which the satellite is farthest from the Earth. For more detail on Molniya orbits See [17]

## CHAPTER 4. RESULTS AND ANALYSIS

---

The access times for the LAX-Heathrow flight were evaluated by adding the additional constraint of having a minimum received isotropic power of at least -150.5 dBW (10 times weaker than the worst LEO constellation). This produced a coverage gap fraction of 0.992 %, meaning that the flight would spend more than 99% of the time not being able to communicate with an overhead satellite. This result and the poor signal performance resulted in the family of Molniya orbits being ruled out for further analysis.

### 4.3.1.2 Geosynchronous

A geosynchronous orbit<sup>2</sup> was tested with an inclination of 60 degrees and suborbital longitude of -30 degrees in order to place the ground track above the LAX-Heathrow flight. The ground track is given in Figure 4.3. The minimum received RX power ranged between -160.3 dBW in the best case and -161.7 dBW in the worse case. This orbit was then dismissed because of the poor performing worst case signal when compared with LEO constellations.

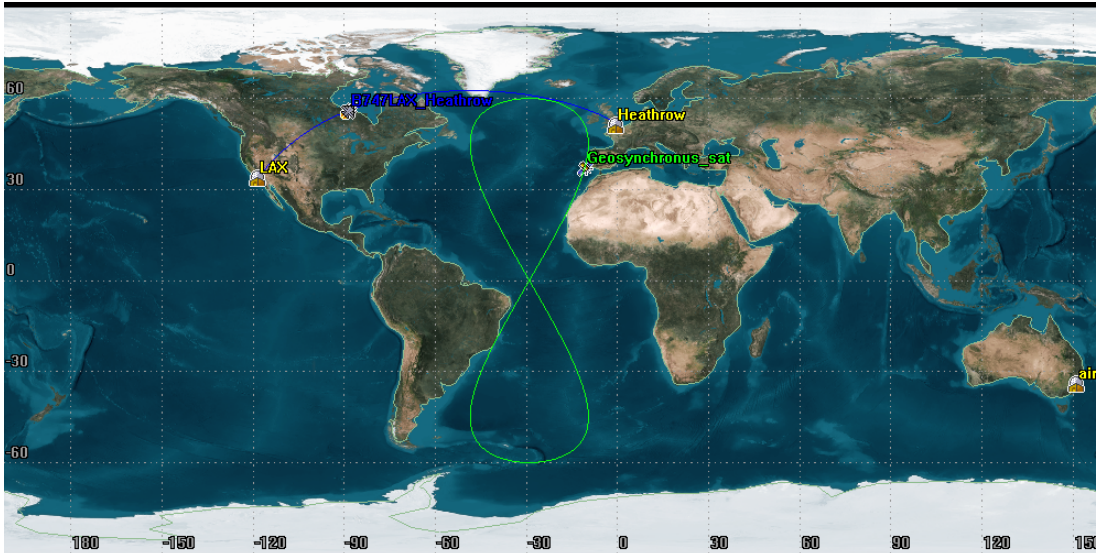


Figure 4.3: Ground track of the tested geosynchronous orbit

---

<sup>2</sup>See [17] for full definition of geosynchronous

### 4.3.2 Altitude Variations

This series of tests involved evaluating the effect of uniformly changing the altitudes of each satellite from the reference case specified in Table 3.1 on the performance metrics outlined in Section 3.2.1. All altitudes tested were restricted to LEO

#### 4.3.2.1 Input Variables

From the reference case specified in Table 3.1, the altitudes of each satellite were varied between 400km and 800km in 50km steps according to Table 4.4.

Table 4.4: Altitude variations used using the 12 satellite reference case

Case Number	Altitude (km)	Semi-Major Axis (km)
1	400	6778.14
2	450	6828.14
3	500	6878.14
4	550	6928.14
5	600	6978.14
6	650	7028.14
7	700	7078.14
8	750	7128.14
9	800	7178.14

All other orbital parameters remained constant as per Table 3.1.

After initial testing, it was hypothesised that the high number of satellites in the reference constellation was causing a high degree of overlap between coverage from different satellites. This phenomenon would pollute the observed trend of the access-coverage behaviour. The set of experiments was therefore repeated using a smaller 3 satellite constellation with orbital

parameters specified in Table 4.5. The range of altitudes tested was the same as specified in Table 4.4.

Table 4.5: Orbital parameters for 3 satellite test

Satellite	RAAN	True Anomaly
1	0	0
2	120	120
3	240	240

#### 4.3.2.2 Trends

The results for altitude variations against the resulting coverage gap fractions, maximum gap period and minimum received signal power are shown in Figures 4.4, 4.5 and 4.6 respectively. The results show that the coverage gap fraction and maximum coverage gap become lower with a higher satellite altitude. However the minimum received isotropic power was reduced with higher altitude. The coverage trends for the repeated three-satellite constellation test are given in Figures 4.7 and 4.8, showing the same trends.

#### 4.3.2.3 Discussion

The results for both coverage gap times and received RF power behaved as expected. Satellites at higher altitudes have a greater line of sight range<sup>3</sup> increasing the probability with which any one flight could be ‘seen’ by a satellite. The difference in orbital period between the extremes of altitude (1 hour and 32.5 minutes at 800km against 1 hour and 42.9 minutes at 400 km) was less than 10% and had minimal effect on the periodicity of access times. The net effect was the observed increase in coverage time and decrease of coverage gaps for any given flight path.

---

<sup>3</sup>The area on Earth within which objects will have a direct line of sight toward a satellite, allowing for a simple RF link to be made.

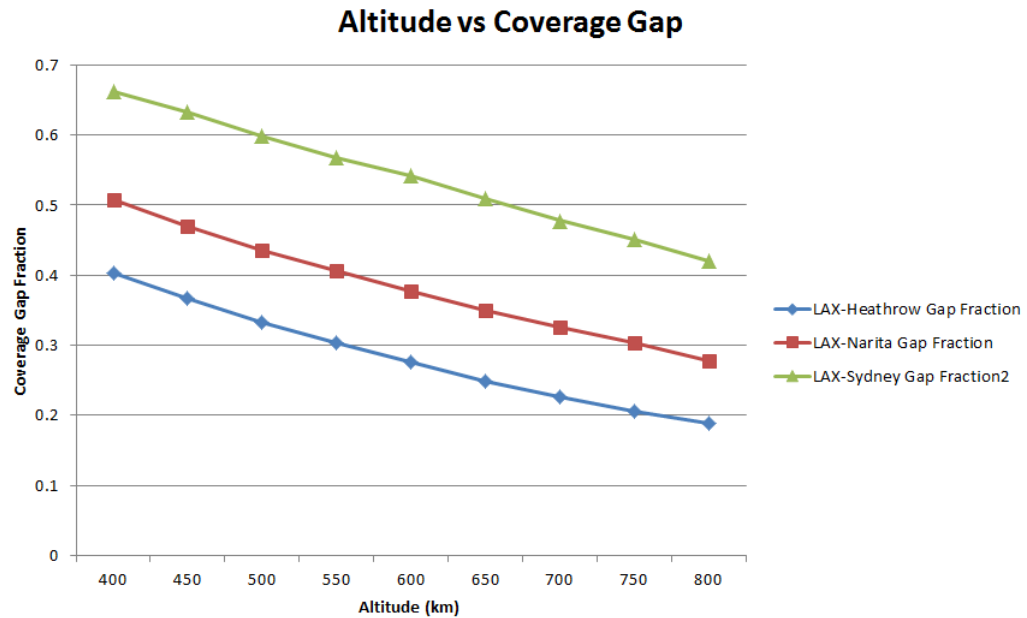


Figure 4.4: Coverage gap (as a fraction of total analysis time) as affected by altitude variations. Lower is better

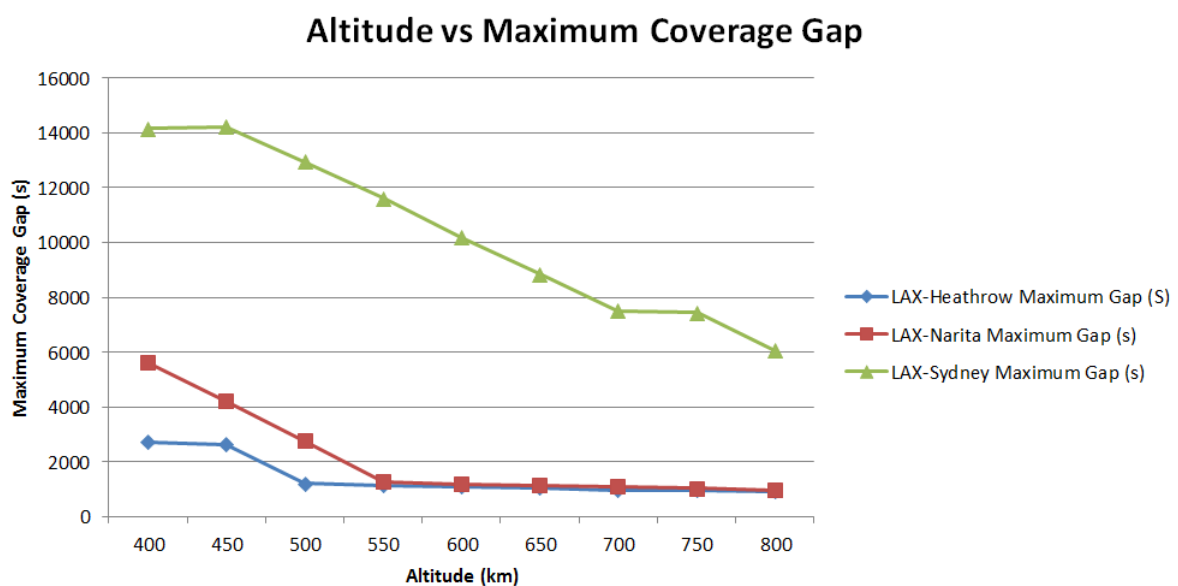


Figure 4.5: Maximum coverage gap as affected by altitude variations. Lower is better

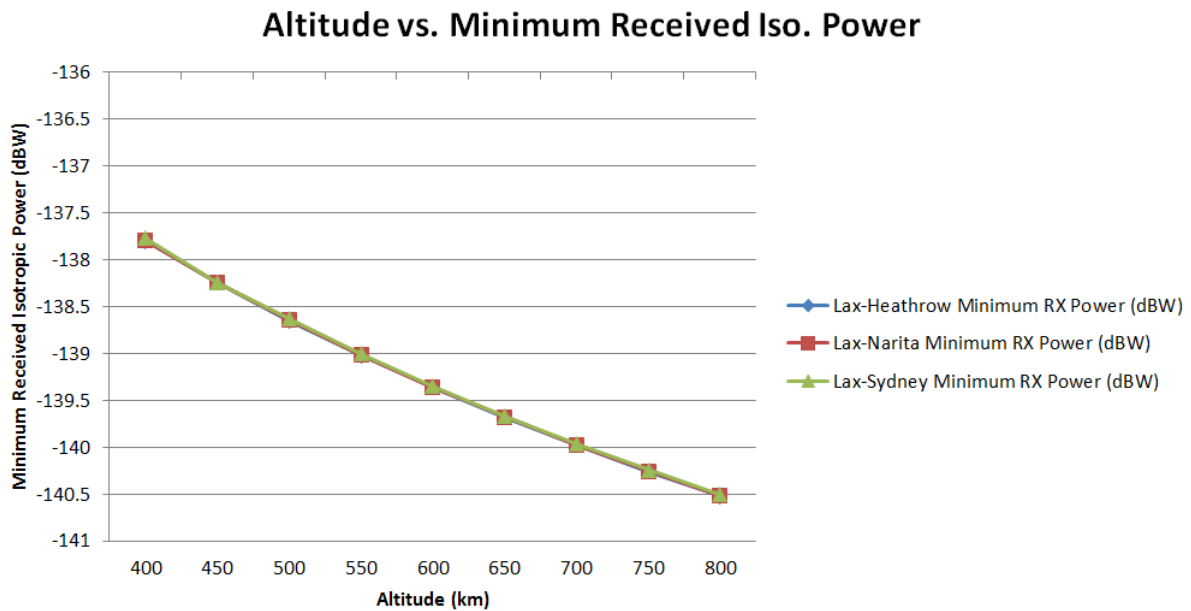


Figure 4.6: Minimum received isotropic power as affected by altitude variations. Higher is better.

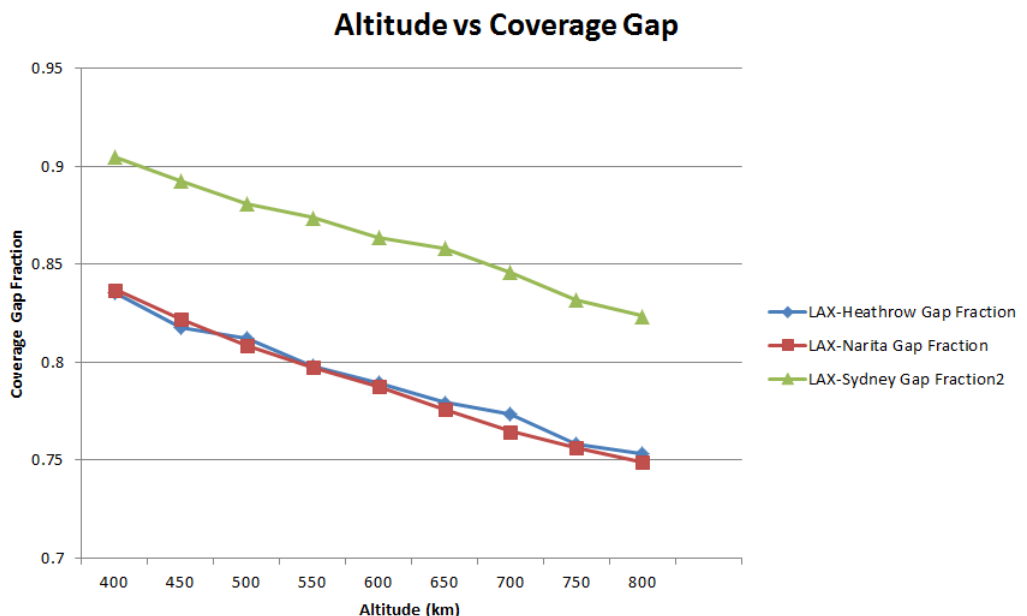


Figure 4.7: Coverage gap (as a fraction of total analysis time) as affected by altitude variations with a 3 satellite constellation. Lower is better

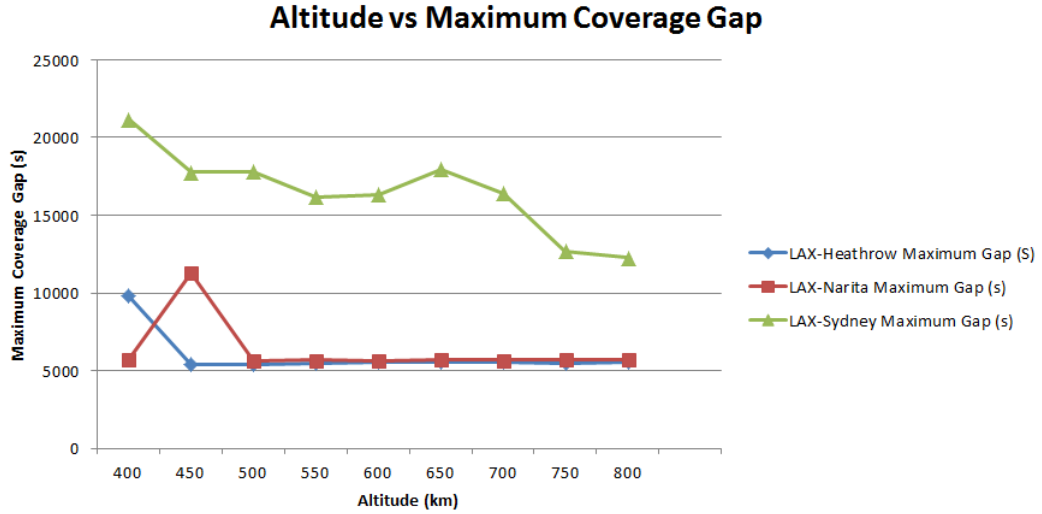


Figure 4.8: Maximum coverage gap as affected by altitude variations retested with a 3 satellite constellation. Lower is better.

The trends observed in the coverage-access times for the three-satellite test shown in Figures 4.7 and 4.8 matched those quite closely with those seen in the reference case with 12 satellites. This indicated that the number of satellites did not affect the trend observed in either case

There was a significant observed difference in coverage gaps for the flights between LAX and Sydney and LAX and Heathrow or Narita. The maximum coverage gaps for LAX-Sydney were worse by one order of magnitude of time, as is shown in Figure 4.5. This is due to the fact that 60 degree inclination of the satellites resulted in ground tracks that were almost coincident with the flight paths between LAX and Narita or Heathrow, as can be seen in Figure 4.9. The geometry of the ground tracks was not optimised for the flight path between LAX and Sydney, resulting in a less desirable maximum coverage gap.

Despite the increased access time at higher altitudes, however, a significant drop in received signal strength is observed between 400km and 800km altitude. There was an expected drop due to the increased distance and subsequent increased free-space path loss of any electromagnetic wave. The minimum received isotropic power is optimised at 400km, with a measurement of

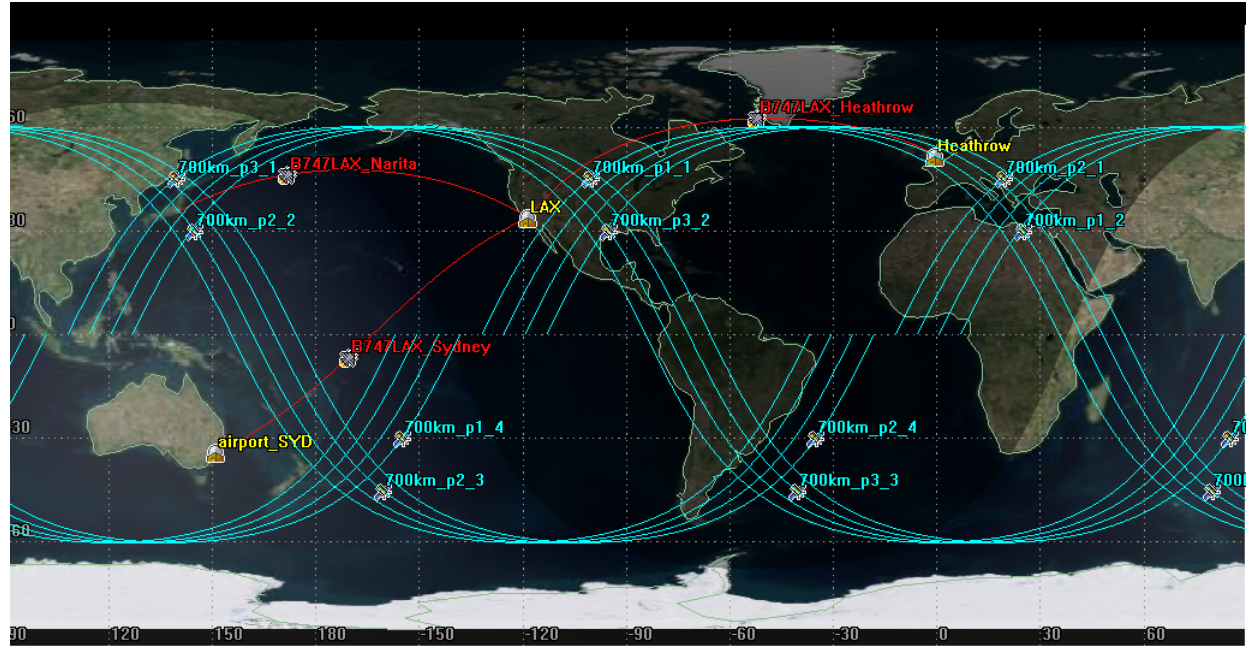


Figure 4.9: Ground track of satellites inclined at 60 degrees, shown with the test flight paths

-137.8 dBW and is the least optimised at 800km with a measurement of -140.5 dBW. This is a difference of 2.7 dB, meaning that from 400km altitude to 800km altitude, the raw signal power has been reduced by a factor of 1.86. This will affect ADS-B detectability as weaker signals will be harder to detect and process. The effect of this on the performance of the system is evaluated later in Section 4.5.

The minimum trigger threshold level for an ADS-B receiver class R3 (Extended) as specified by the RTCA is set at -84 dBm [3] or equivalently -114 dBW. This is already well above that reported possible with the standard STK transmitter-receiver model at 400 km altitude.

### **4.3.3 Inclination Variations**

This series of tests involved evaluating the effect of uniformly changing the inclination of each satellite from the reference case specified in Table 3.1 on the performance metrics outlined in Section 3.2.1.

#### **4.3.3.1 Input Variables**

From the reference case specified in Table 3.1, the inclinations of each satellite were varied between 30 degrees and 90 degrees in 10 degree steps according to Table 4.6.

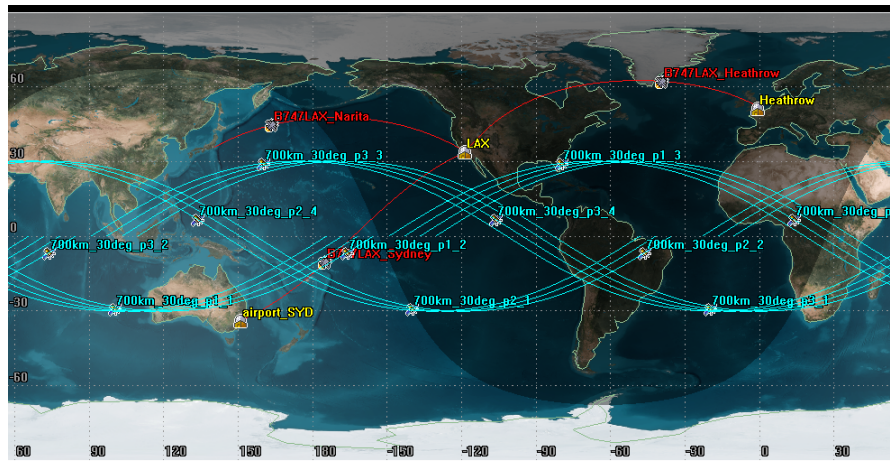
Table 4.6: Inclination variations used

Case Number	Inclination (degrees)
1	30
2	40
3	60
4	70
5	80
6	90

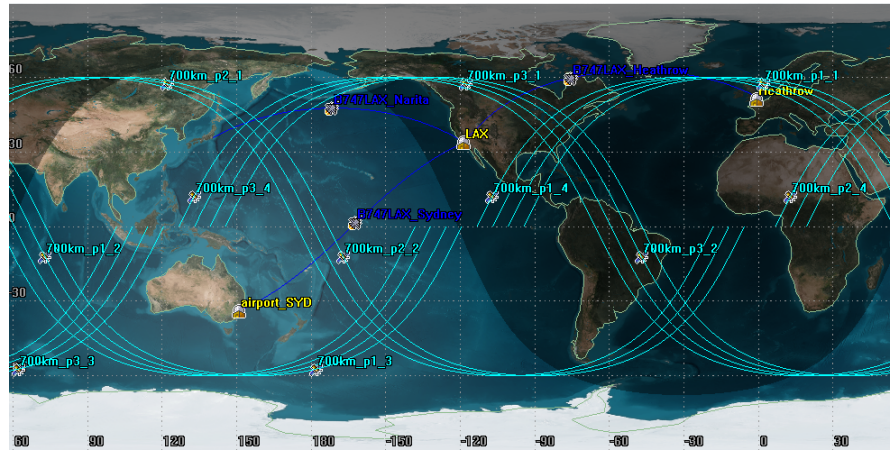
All other orbital parameters remained constant as per Table 3.1. The ground tracks of the constellation inclined at 30 degrees, 60 degrees and 90 degrees is shown in Figures 4.10a, 4.10b and 4.10c respectively.

## CHAPTER 4. RESULTS AND ANALYSIS

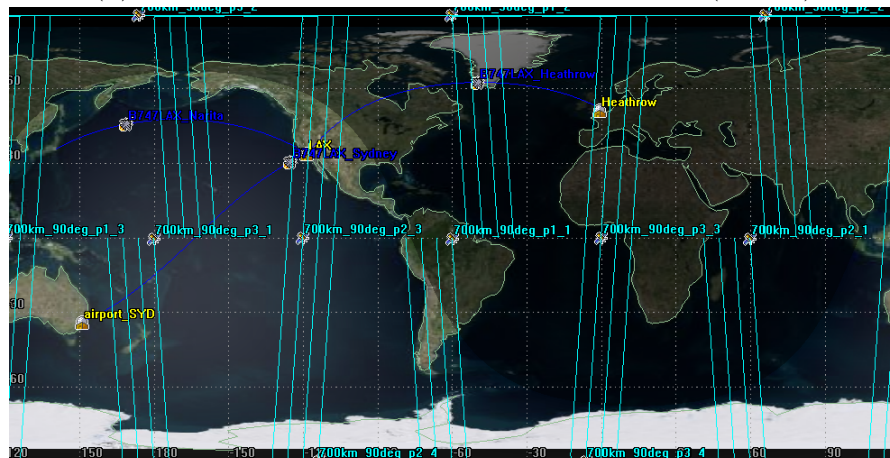
---



(a) Ground track of satellites inclined at 30 deg (Case 1)



(b) Ground track of satellites inclined at 60 deg (Case 3)



(c) Ground track of satellites inclined at 90 deg (Case 6)

Figure 4.10: Ground tracks of constellations inclined between 30 degrees and 90 degrees

### 4.3.3.2 Trends

The results for inclination variations against the resulting coverage gap fractions, maximum gap period and minimum received signal power are shown in Figures 4.11, 4.12 and 4.13 respectively. Each parameter behaved differently for each flight.

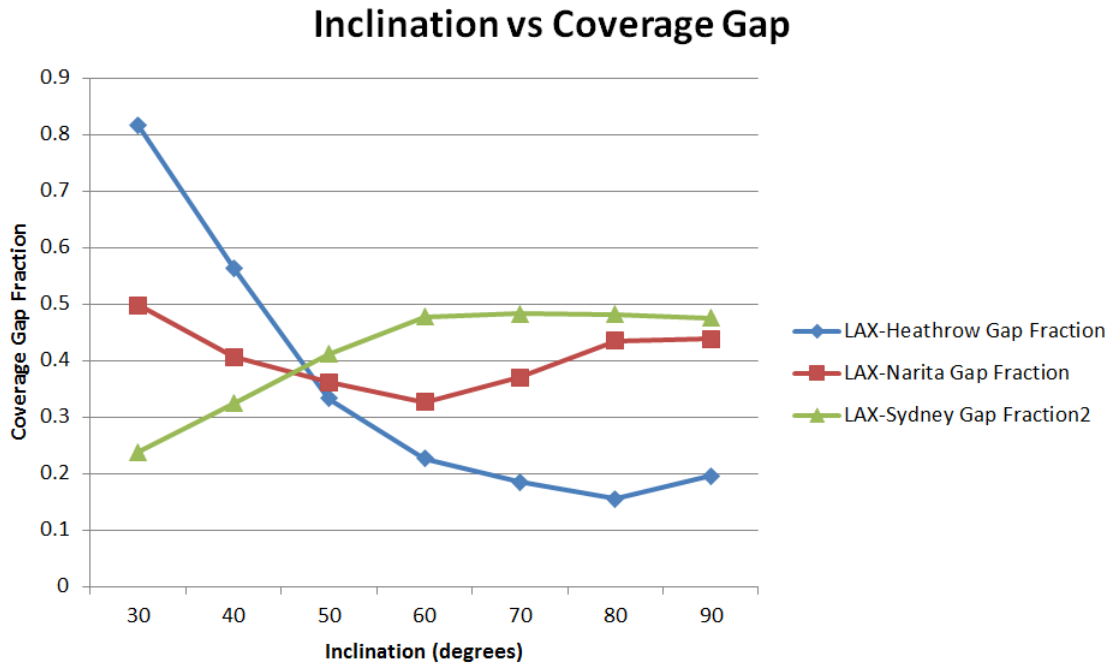


Figure 4.11: Coverage gap (as a fraction of total analysis time) as affected by inclination variations. Lower is better

### 4.3.3.3 Discussion

At lower inclinations, the ground tracks of the satellite have a significant degree of coincidence with the flight path between LAX and Sydney, as seen in Figure 4.10a. This results in the LAX-Sydney flight path having an optimised maximum coverage time and coverage fraction at 30 degrees inclination as can be seen on Figures 4.11 and 4.12. Increasing inclinations resulted in a higher coverage gap ratio, before settling at 60 degrees and remaining constant through to 90 degrees.

### Inclination vs Maximum Coverage Gap

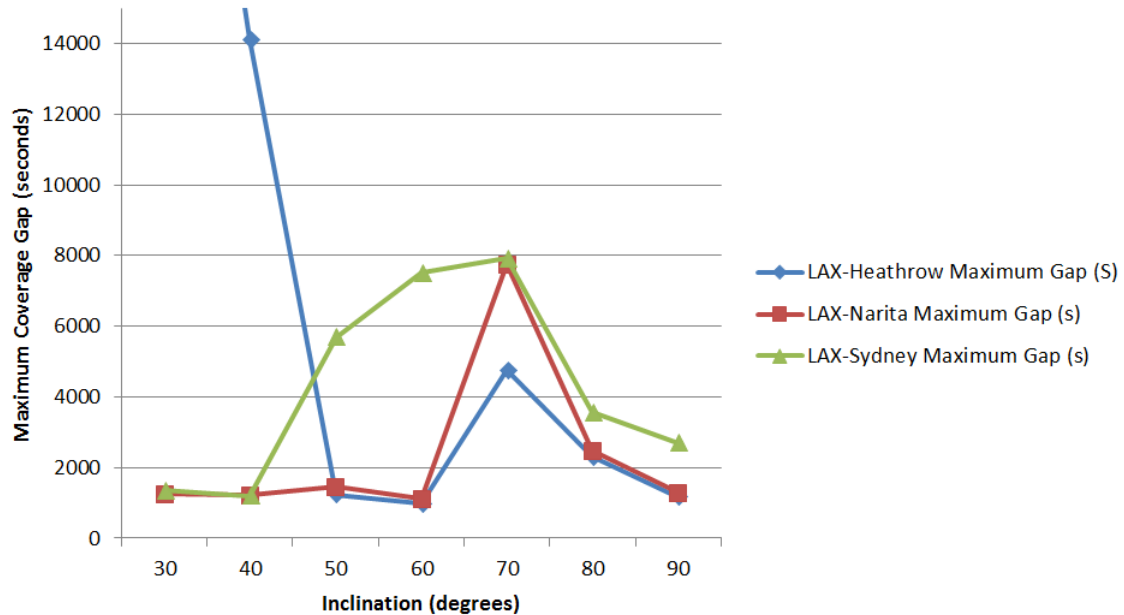


Figure 4.12: Maximum coverage gap as affected by altitude variations. Lower is better.

### Inclination vs Received Power

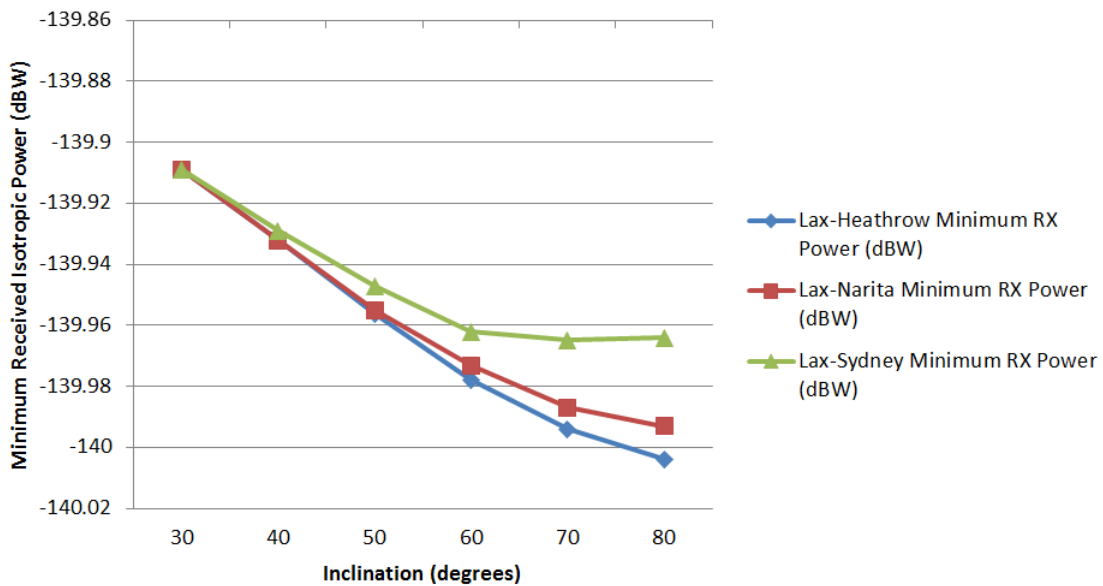


Figure 4.13: Minimum received isotropic power as affected by inclination variations. Higher is better.

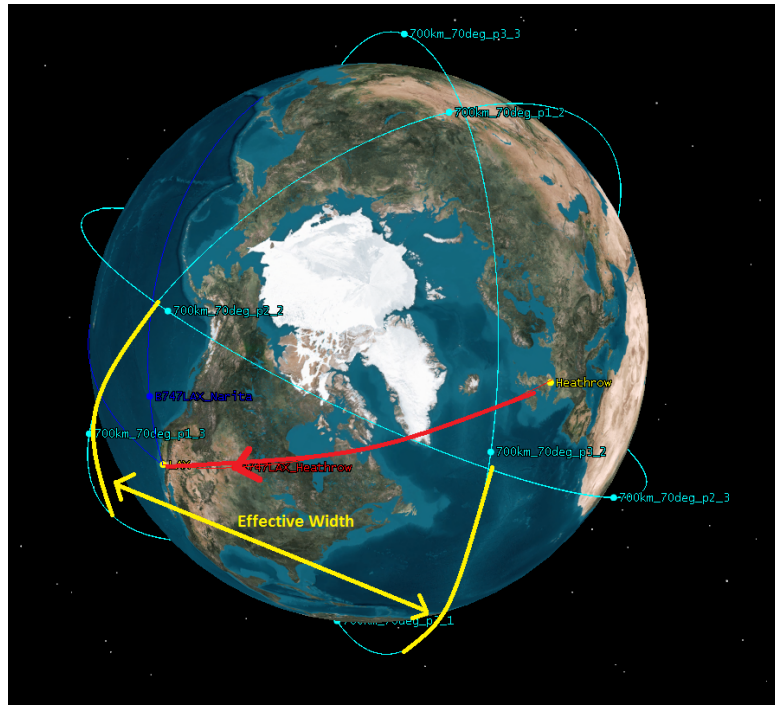
## *CHAPTER 4. RESULTS AND ANALYSIS*

---

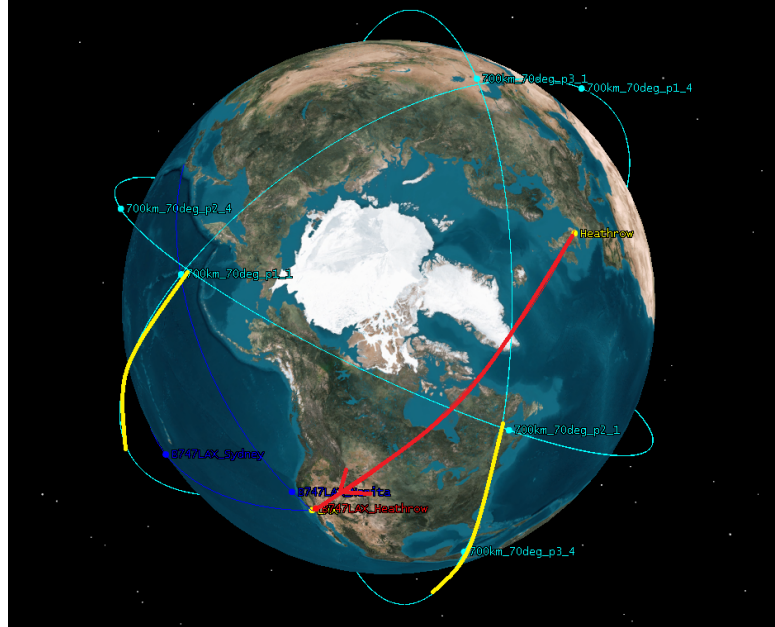
The relatively high inclination of the LAX-Heathrow flight path resulted in poor coverage performance with the constellation at low inclinations. At low inclinations there were few opportunities for line of sight to be established between the LAX-Heathrow flight, with access periods only occurring when satellites reached high latitudes at the same time as the flight was at a low latitude. The resulting maximum gap (not shown in Figure 4.12 for scale purposes) approximately 8 hours and 18 minutes - more than half the duration of the flight. The aggregate result also yielded a poor coverage gap fraction performance below 50 degrees, as seen in Figure 4.11. The effect sharply decreased with higher inclinations, with coverage gaps lowering to an acceptable level after 50 degrees.

All flight paths observed a spike in maximum coverage gap time with satellites inclined at 70 degrees, as seen in Figure 4.12. This occurred due to the geometry of the constellation and the effect of the Earth's rotation under the constellation. Figure 4.14a shows that the effective width between the two orbital planes of the satellite is quite high, creating an effective radio dead zone in which the pictured plane cannot access a satellite. Although the plane continues to travel out of the dead zone, the rotation of the Earth underneath the constellation moves the position of the plane back into the dead zone, as demonstrated in Figure 4.14b. At inclinations of 80 degrees and 90 degrees this effect is mediated by the changing geometry and intersections between satellite ground tracks and flight paths, resulting in more acceptable coverage gaps.

There is relatively little change in the minimum received isotropic powers, with values ranging between -139.9 dBW and -140.02 dBW as seen in Figure 4.13. The observed trend occurs due to the satellite having a higher chance of being directly overhead with higher inclinations, resulting in a shorted free-path propagation distance for the ADS-B signal. However this effect was quite small, only resulting in a net change of 0.12 dB across the experimented range.



(a) Flight initially in dead zone of no ADS-B access between planes



(b) Rotation of Earth eastward keeps the flight in the dead zone for an extended period of time

Figure 4.14: Flight in dead zone between satellite planes, inclined at 70 degrees. View from North Pole

### 4.3.4 Satellite Number Variations

This series of tests involved evaluating the effect of changing the number of satellites in the constellation on the performance metrics outlined in Section 3.2.1. The same three-plane orbital configuration was kept from Table 3.1, whilst the number of satellites per-plane were changed.

#### 4.3.4.1 Input Variables

From the reference case specified in Table 3.1, the number of satellites per each of the 3 planes were varied between 1 and 6 according to Table 4.7.

Table 4.7: Number of satellite variations used

Case Number	Satellites per plane	Total Satellites
17	1	3
18	2	6
19	3	9
20	4	12
21	5	15
22	6	18

All other orbital parameters remained constant as per Table 3.1.

#### 4.3.4.2 Trends

The results for satellite number variations against the resulting coverage gap fractions, maximum gap period and minimum received signal power are shown in Figures 4.15, 4.16 and 4.17 respectively. Generally it was seen that increasing the number of satellites per plane decreased the coverage gaps, whilst the minimum received RF power remained the same

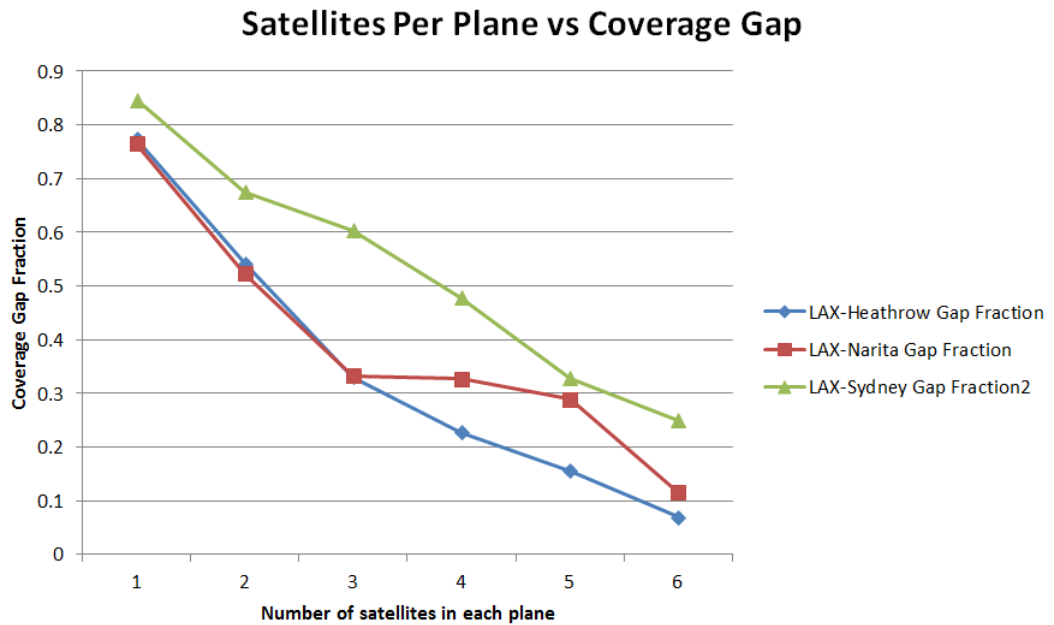


Figure 4.15: Coverage gap (as a fraction of total analysis time) as affected by number of satellites per plane. Lower is better

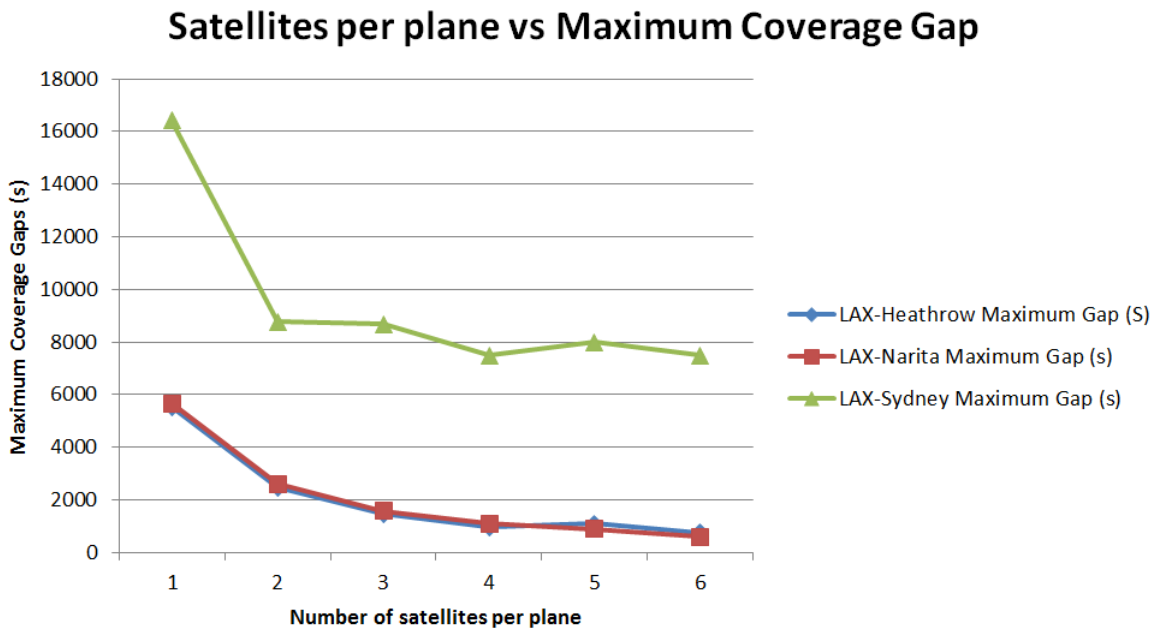


Figure 4.16: Maximum coverage gap as affected by number of satellites per plane. Lower is better.

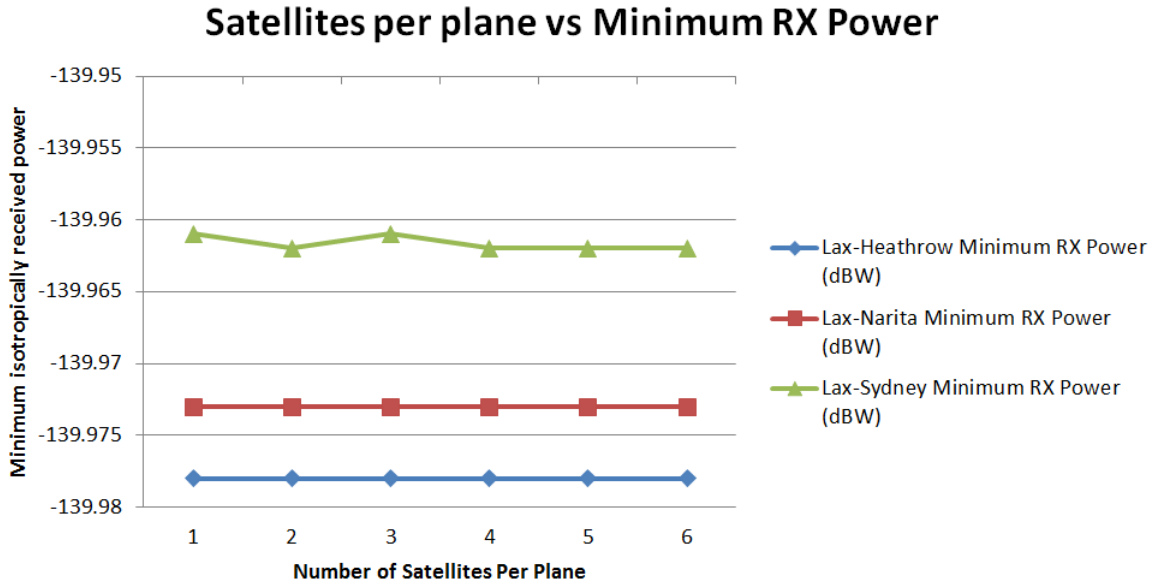


Figure 4.17: Minimum received isotropic power as affected by number of satellites per plane. Higher is better.

#### 4.3.4.3 Discussion

As expected, increasing the number of satellites increased the coverage times available for each flight. Figures 4.15 and 4.16 show that a higher number of satellites results in less coverage gaps. A higher number of satellites per plane increased the probability with which a given flight was able to see at least one satellite, and also increased the revisit time for a given area on the Earth. The number of satellites in the constellation did not affect the minimum received RF power, as seen in the flatness of Figure 4.17.

Despite the net beneficial effect on the ADS-B system, the number of satellites needs to be weighed against the cost and maintenance. Increasing the number of satellites did increase the effectiveness of the space based ADS-B coverage constellation. However a higher number of satellites will require an increased launch and maintenance cost, especially when considering the need to distribute the satellites evenly and potential replacement at end of life.

## 4.4 Access Periodicity

The distributions of coverage periods for all constellations tested were strongly modal, with the majority having one dominant mode. Figure 4.18, from the reference constellation observing the LAX-Heathrow flight, shows a typical distribution. The periods shown all fall within a tight band around the mean, with some outliers and modes to the left and right of the mean. After applying `allfitdist` [47], it was found that the Student's t distribution with a location and scale transformation applied, as shown in Figure 4.18. An analysis of the Student's t distribution is given in Appendix D.

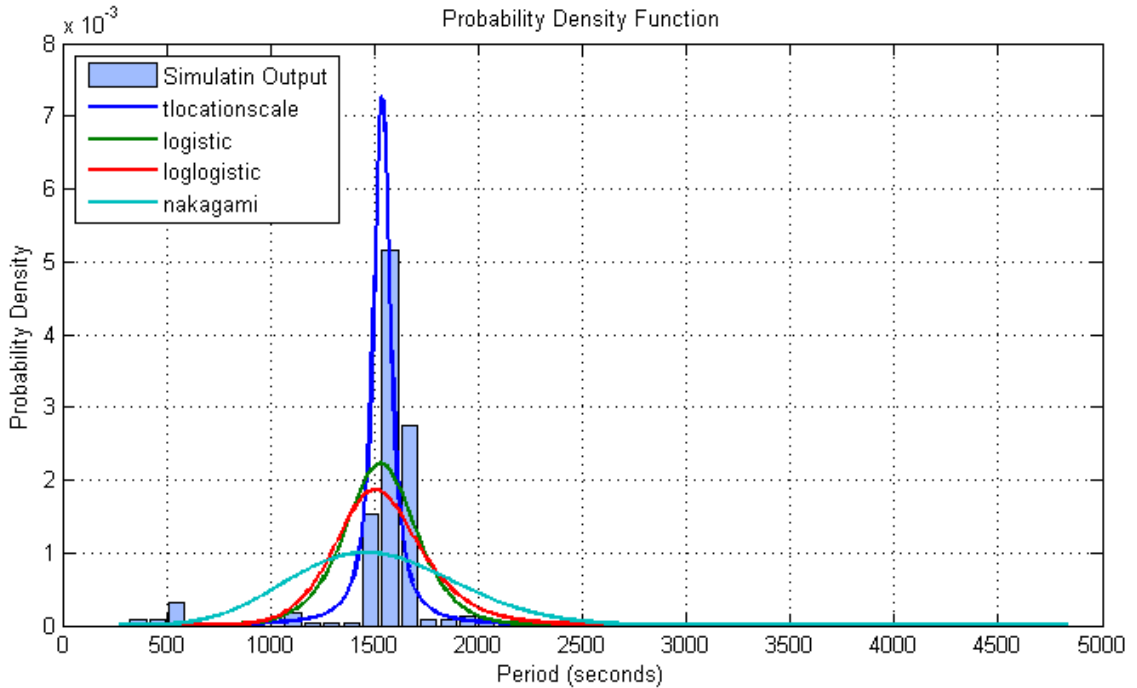


Figure 4.18: Fitted distributions of the periodicity of Access times for the LAX-Heathrow flight from the reference constellation.

For constellations with more than 12 satellites, the extracted parameters from `allfitdist` yielded values for the degrees of freedom,  $\nu$ , for which the variance is undefined. Empirically, this was observed as the case if the band of most probable periods was too narrow for analysis

## CHAPTER 4. RESULTS AND ANALYSIS

---

using the Student's t distribution as the model. In these cases, the narrow variance was considered desirable and so for the purposes of comparative analysis, the 'variance' score in the weighted decision matrix was given the highest score, 10.

It was found that for constellations with a lower number of satellites, there was less of a dominant node and more of an even spread of distributions. Figure 4.19 shows the histogram for a six-satellite constellation, showing a larger spread of results. In these cases, `allfitdist` yielded different distributions of best fit, as shown in Figure 4.19. Although these fits are not exact, the extracted variance value was considered a good indicator of comparative variance in periodicity. The standard deviations from these distributions were extracted computationally

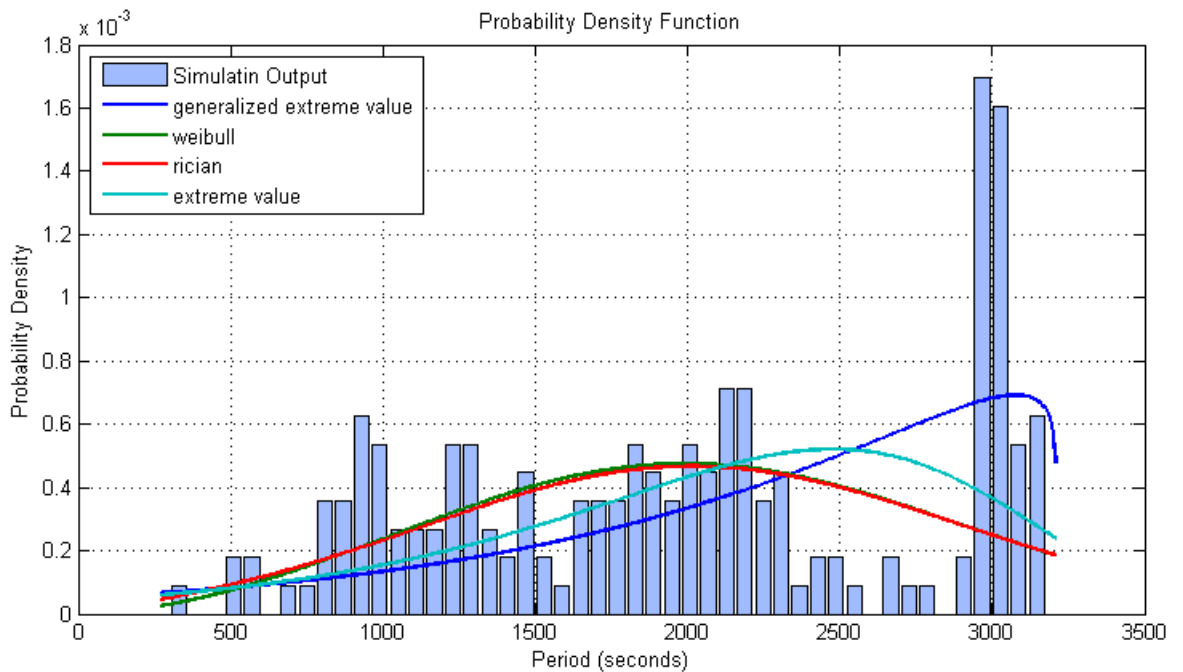


Figure 4.19: Fitted distributions of the periodicity of Access times for the LAX-Heathrow flight from the reference constellation.

## 4.5 Weighted Decision Matrix

The results from Chapter 4 were collated for numerical comparative analysis using a weighted decision matrix. The results of each performance parameter were linearised to provide scores between 1-10. Weights were applied to each score according to the importance of the parameter to the effectiveness of a space-based ADS-B system. An aggregate score for a constellation was summed from each of the weighted scores and this was used to numerically compare different the different constellations tested.

### 4.5.1 Parameter Weight Matrix

Each of the four performance metrics described in Section 3.2.1 were considered differently for each of the tested flight paths detailed in Section 3.2.2. In addition to these, total number of satellites was also considered for evaluation of overall cost of the system. The parameters used in the weighted decision matrix are given in Table 4.8

The weights were applied as shown in Table 4.8 subjectively, representing one particular design philosophy. Each flight path was weighted equally in favour evaluating each constellation without geographical bias<sup>4</sup>. Fraction of coverage gap was determined to be the strongest factor as a higher score would ease the system requirements of a number of key factors, including signal collision avoidance and raw samples available. This was followed by minimum received RX power, which would be a defining system requirement for a space based ADS-B sensor. Satellite number and periodicity were less important as CubeSats are relatively cheap to launch and the effect of periodicity can be offset by having a higher access-coverage ratio.

---

<sup>4</sup>This could practically not be the best means of assigning bias. It was noted that the frequency and number of flights along each path differed. However geographical coverage was considered the most important factor in this case

Table 4.8: Parameters used to evaluate constellation effectiveness

Flight Path	Parameter	Score Calculation Method	Weight
All	Number of Satellites	Simple Linearisation - Down	10
LAX - Heathrow	Fraction of coverage gap to total time analysed	Simple Linearisation - Down	20
LAX - Heathrow	Average Period	Pass-Fail Linearisation	10
LAX - Heathrow	Periodicity Deviation	Pass-Fail Linearisation	5
LAX - Heathrow	Maximum coverage gap time	Simple Linearisation - Down	10
LAX - Heathrow	Minimum Received RX Power	Simple Linearisation - Up	15
LAX - Narita	Fraction of coverage gap to total time analysed	Simple Linearisation - Down	20
LAX - Narita	Average Period	Pass-Fail Linearisation	10
LAX - Narita	Periodicity Deviation	Pass-Fail Linearisation	5
LAX - Narita	Maximum coverage gap time	Simple Linearisation - Down	10
LAX - Narita	Minimum Received RX Power	Simple Linearisation - Up	15
LAX - Sydney	Fraction of coverage gap to total time analysed	Simple Linearisation - Down	20
LAX - Sydney	Average Period	Pass-Fail Linearisation	10
LAX - Sydney	Periodicity Deviation	Pass-Fail Linearisation	5
LAX - Sydney	Maximum coverage gap time	Simple Linearisation - Down	10
LAX - Sydney	Minimum Received RX Power	Simple Linearisation - Up	15

## 4.5.2 Score Calculation

### 4.5.2.1 Simple Linearisation

In order to simplify numerical analysis, the numerical results (other than periodicity) from each of experiments conducted in Part 4 were linearised between minimum and maximum values. The direction of linearisation was adjusted such that a higher score meant a more favourable result. In the case of maximum, average and fraction of coverage gap times and number of satellites, this meant that a lower value was more favourable, resulting in the formula

$$\text{Linearised score} = 10 \times \left[ 1 - \frac{\text{result} + \text{minimum}}{\text{maximum} - \text{minimum}} \right]. \quad (4.1)$$

For the minimum received RX power a higher the value was more favourable, resulting in the calculation

$$\text{Linearised score} = 10 \times \left[ \frac{\text{result} + \text{minimum}}{\text{maximum} - \text{minimum}} \right]. \quad (4.2)$$

No further normalisation was applied. This allowed for a very basic comparison of a parameter for a set of constellations.

### 4.5.2.2 Pass - Fail Linearisation

The score for coverage-gap periodicity was calculated using a pass - fail criteria. It was determined that a minimum, a second harmonic deviation away from the ideal straight-line flight path would need to be detected and mapped. As illustrated in Figure 4.20, this required three discrete sample points in addition to the data from the source and destination. This meant that the maximum allowable period was one quarter of the total flight time. The score was

## CHAPTER 4. RESULTS AND ANALYSIS

---

then calculated with the adjusted maximum using Equation (4.1), meaning that any period greater than the maximum would be a ‘0’ or a ‘fail’.

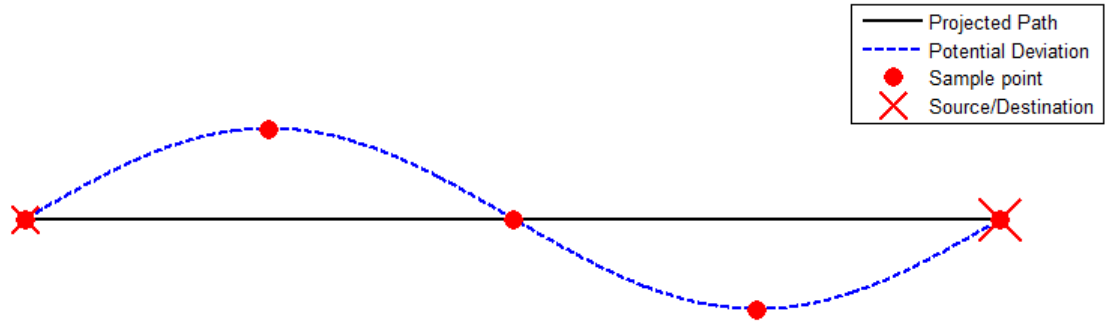


Figure 4.20: The second harmonic deviation from a straight line path, showing required sample points

The regularity of the period was also of concern to the ‘sampling’ ability of a given constellation. A more regular period represented a more ‘reliable’ sampling rate and therefore a lower standard deviation of period was desired. As discussed in Section 4.4, the distribution of periods which fitted a student’s t distribution with an undefined standard deviation represented the greatest confidence for regularity. These cases were automatically assigned a full 10/10 score, whilst other situations with non-singular standard deviations were calculated using Equation 4.2 with the minimum set to ‘0’.

### 4.5.3 Results

The three highest scoring constellations, with their relative scores, are shown in Table 4.9. The decision matrix heavily favoured the constellations with more satellites and lower altitudes. A higher number of satellites had a positive impact on the access-coverage characteristics, whilst lower altitude satellites had much more favourable potential signal strengths. A different set of results could be produced if the decision matrix were weighted according to a different set of

## CHAPTER 4. RESULTS AND ANALYSIS

---

design principles. The distribution of scores showed that most scores fell within a tight band around 70 %, as seen in Figure 4.21

Table 4.9: The three highest scoring constellations after applying the weighted decision matrix

Case Number	Satellite Parameters	Score (%)
22	Altitude (km above mean radius of Earth)	700
	Inclination (deg)	60
	Number of Planes	3
	Number of Satellites per plane	6
	Number of Satellites (Total)	18
21	Altitude (km above mean radius of Earth)	700
	Inclination (deg)	60
	Number of Planes	3
	Number of Satellites per plane	5
	Number of Satellites (Total)	15
1	Altitude (km above mean radius of Earth)	400
	Inclination (deg)	60
	Number of Planes	3
	Number of Satellites per plane	4
	Number of Satellites (Total)	12

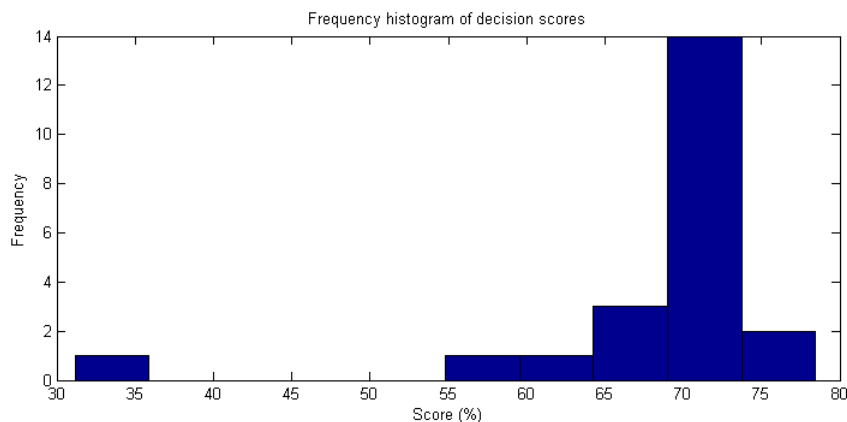


Figure 4.21: Distribution of scores from decision matrix

## 4.6 Special Case Study - MH370

The Malaysia Airlines Flight MH370 disappeared on the evening of March the 7th, GMT after losing contact with air traffic control at approximately 5:20pm GMT [48]. Publicly available data of the flight after 5:21pm GMT was unavailable, at which point the flight was approximately 6.92°N and 101.70°E [49]. Military radar information suggests that the flight visited a series of known way points west of the planned flight path before being completely lost [50]. Data from satellite pings and international search efforts suggested that the aircraft may have crashed in the Indian Ocean, as illustrated in Figure 4.22 [51–53]. As of April 16th 2014, there is an ongoing international effort to attempt to locate the possible crash site and location of the debris from the MH370.

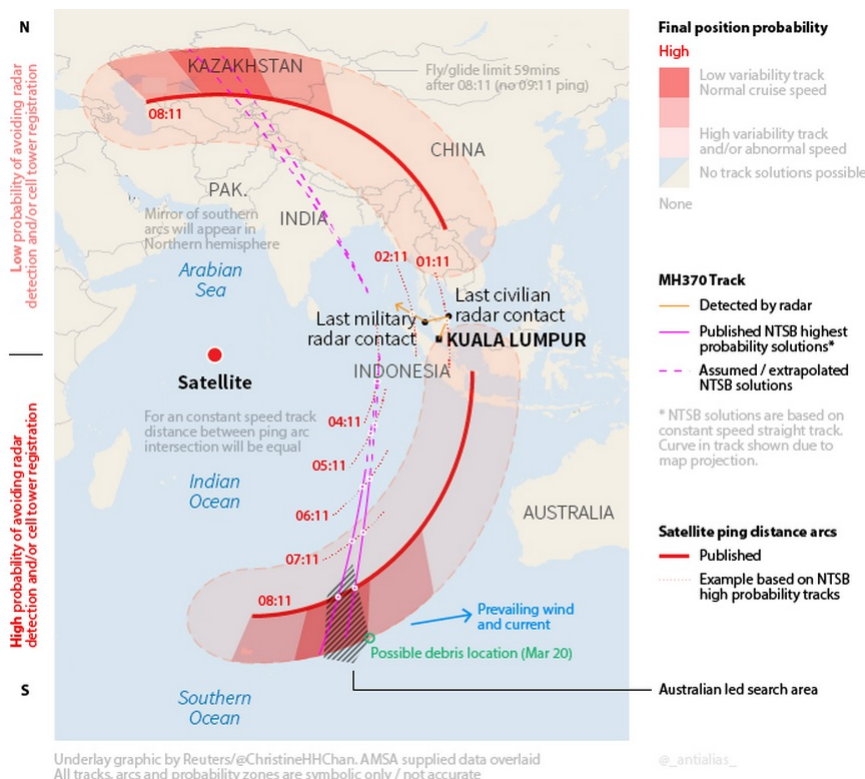


Figure 4.22: Probability map of possible crash locations of the MH370, reproduced from [51]

### 4.6.1 Simulation

As seen in Figure 4.22, it is most likely that the majority of the flight time after lost radar coverage would be spent over oceanic regions where an ADS-B constellation could provide coverage. The best performing constellation (18 satellites at 700km altitude) was tested against an estimated flight path for the MH370 alongside its standard path. This estimated path assumed that the flight terminated over the Indian Ocean, as shown in Figure 4.23. For the sake of coverage analysis it was assumed that the ADS-B transponder remained operational for the duration of the flight.



Figure 4.23: Simulated MH370 flight path with 18 satellite constellation

### 4.6.2 Results

The coverage results are summarised in Table 4.10. Results showed that the 18 satellite constellation would have allowed for near constant coverage, with the flight only being out of sight for 10% of the flight. The high number of discrete accesses for the one flight would have also allowed for deviations in the flight path to be detected early and accurately mapped with many sample points.

Table 4.10: Results from MH370 simulation using 18 satellites

Parameter	Value
Coverage Gap Fraction	0.10%
Discrete Accesses	20.00
Maximum Gap	309.72 seconds
Minimum RX Power	-139.95 dBW

### 4.6.3 Discussion

The results from this simulation show that the 18 satellite constellation would have provided coverage to almost continually track the MH370 during its flight. If the ADS-B transponder remained operational during the flight, the probable crash and debris locations could be much smaller providing for a much more feasible search area.

The exact status of the ADS-B transponder during the flight is currently unknown. No ADS-B data exists beyond of that reported by [49]. ADS-B receivers in the vicinity of this disappearance suggest that the ADS-B transponder was inoperable after this period. In this case the constellation would have not been able to track the entirety of the deviated flight path. However, the high effective ADS-B sample rate of the 18 satellite constellation would have provided a more accurate estimation as to the exact time and location when the ADS-B signal would have been lost. This could have aided in search efforts and generated potential flight paths with greater confidence.

# Chapter 5

## Conclusions and Future Work

With further development and refinement of small satellite based ADS-B technology, near constant global coverage can be achieved with a constellation of CubeSats in LEO. The experiments conducted showed that all chosen constellations provide the geographic coverage for the major transoceanic flight corridors. Varying degrees of coverage time and update rate effectiveness was achieved by varying constellation parameters, with the best result achieved by an 18 satellite constellation at an altitude of 700km. Future work needs to be conducted in order to create more realistic models for full system analysis and further design.

## 5.1 Conclusions

The suite of simulations showed that constellations with higher altitude or a higher number of satellites provided more raw coverage time. A higher altitude allowed for a greater sensor footprint, meaning that a trans-oceanic flight would stay in-view for longer. Having more satellites increased the probability of a satellite being above a trans-oceanic flight at any one point in time. The effect of this was significant enough such that the penalty of the increased constellation cost was offset by the net benefit to the coverage opportunities.

Despite the improved geographic coverage performance of high altitude constellations, low altitude constellations showed a marked improvement in signal performance. Less distance was required to travel by any one ADS-B transmission at lower altitudes, resulting in lower signal loss. This effect was dramatic enough such that the lowest altitude constellation performed better than most other constellations as seen in Table 4.9.

The inclination trend analysis suggested that a constellation with all satellites inclined at 90 degrees may represent the best coverage trade-off between the three flights. This inclination represented the best possible geometric configuration for full global coverage. However, the nature of one-dimensional parameter variance in the tests conducted and the weighted decision matrix meant that the 90 degree inclination configuration did not feature in the ‘best choices’, with system coverage overriding the potential cost of the system as a performance metric.

### 5.1.1 Chosen Constellation

The results from the weighted decision matrix show that a satellite constellation with parameters as defined in Table 5.1 is the best performing space based ADS-B system of those tested. This particular constellation performed strongly in being able to provide a high level of coverage

## CHAPTER 5. CONCLUSIONS AND FUTURE WORK

---

for the three trans-oceanic flights studied in this thesis. A 3D model of this constellation is shown in Figure 5.1 and the ground tracks in Figure 5.2

Table 5.1: 18 satellite configuration with the best score

Parameter	Value
Altitude (km above mean radius of Earth)	700
Inclination (deg)	60
Number of Planes	3
Plane Separation (deg RAAN)	120
Number of Satellites per plane	6
True Anomaly Separation (deg)	60
Number of Satellites (Total)	18

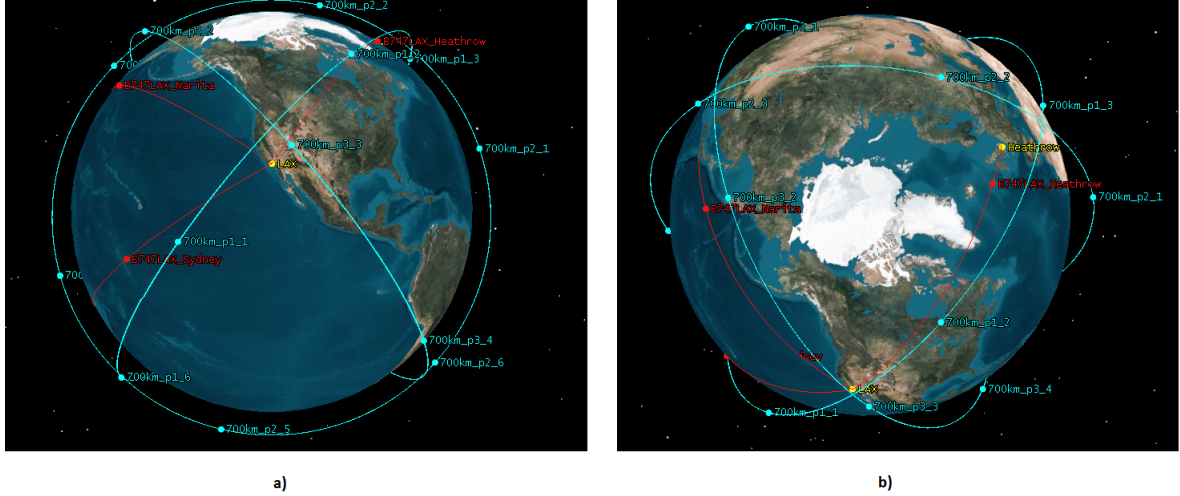


Figure 5.1: 18 satellite configuration rendered in STK showing a) the view above North America and b) the view above the Arctic

This particular result shows that a higher-number of satellites performs more favourably when considering ADS-B coverage requirements. Interestingly, a fewer satellites in a lower orbit performed almost as well due to dramatically increased communication link quality. In this case, the benefit of having more effective coverage outweighed the benefit of having less satellites.

## CHAPTER 5. CONCLUSIONS AND FUTURE WORK

---

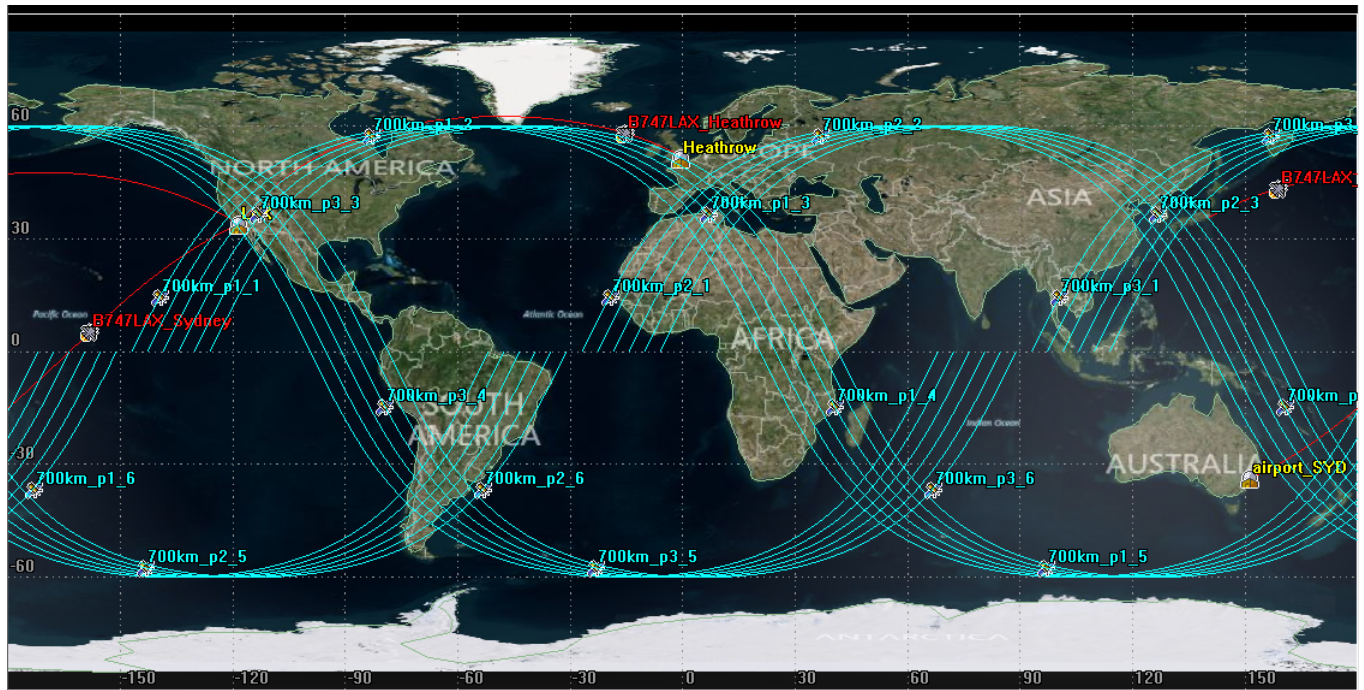


Figure 5.2: Ground track of the 18 satellite configuration, rendered in STK

This may not be the case if the decision matrix was weighted more heavily to budgetary considerations. The tests conducted only examined variation of one parameter at a time and can not provide a conclusion on whether a combination of two or more parameters would result in better performance.

## 5.2 Future Work

The following work should be conducted in order to fully develop a set of mission and system specifications for a CubeSat based ADS-B system.

### 5.2.1 Full Parametric Study

The findings of this thesis are as a result of one-dimensional parameter studies. As such they are indicative of general trends observed when varying only one constellation parameter at a time. This only gives an indication of what the best possible satellite configuration could be. In order to determine the global best performer, a full n-dimensional parametric study should be carried out, simulating all possible variations of all the orbital parameters. In particular, given the results of the weighted decision matrix in Section 4.5, it is expected that a lower altitude (approximately 400km) with a higher number of satellites could produce a more optimal result than any constellation tested in this thesis. The simulations created for this thesis form a good basis from which a full parametric set of simulations can be generated.

### 5.2.2 Transmitter Receiver Model Improvements

As noted in Section 3.2.1, the simple transmitter and receiver models used produced an unrealistic link-budget characterisation for ADS-B communication links. Although received isotropic power is a good metric to compare constellation performance, the link budget results in this thesis do not represent realistic system behaviour. Incorporating a more sophisticated antenna design and better radio-frequency front-end into the communication models would more accurately characterise ADS-B signal performance. This would be necessary in further systems analysis and design.

### **5.2.3 Ground Link**

Further study needs to be performed into how to establish a regular downlink between the satellites in the constellation and a ground station. The regularity of this downlink would determine the ‘total system update rate’ or the speed with which data on all detected flights can be disseminated to ANSPs and therefore general use. Potential methods could be to

- Use network of community-run amateur radio ground stations
- Transmit downlink packets to currently in-orbit communication constellations, such as Iridium or Globalstar
- Relay raw ADS-B data to airports and terrestrial ADS-B receivers.

The benefits and potential performance of each option needs to be further explored before a full space-based ADS-B solution can be designed.

# References

- [1] Department of Transportation and Federal Aviation Administration, “Automatic Dependent Surveillance-Broadcast (ADS-B) Out Performance Requirements to Support Air Traffic Control (ATC) Service,” in *Federal Register*, May 2010, vol. 75, Final Rule.
- [2] Civil Aviation Safety Authority, Australia, “Automatic Dependent Surveillance-Broadcast,” November 2012.
- [3] Radio Technical Comission for Aeronautics, *Minimum Operational Performance Standards for 1090 MHz Extended Squitter Automatic Dependent Surveillance - Broadcast (ADS-B) and Traffic Information Services - Broadcast (TIS-B)* RTCA/DO-260B, 2009.
- [4] International Civil Aviation Organisation, *ADS-B Implementation and Operations Guidance Document*, 4th ed., September 2011.
- [5] Civil Aviation Safty Authority, Australia, *Airworthiness Approval of Airborne Automatic Dependant Surveillance Broadcast Equipment (Advisory Circular AC 21-45(1))*, February 2012.
- [6] Radio Technical Comission for Aeronautics, *Minimum Operational Performance Standards for Universal Access Transceiver (UAT) Automatic Dependent Surveillance-Broadcast(ADS-B)* RTCA/DO-282B, 2009.

## REFERENCES

---

- [7] H. Blomenhofer, P. Rosenthal, A. Pawlitzki, and L. Escudero, “Space-based Automatic Dependent Surveillance Broadcast (ADS-B) payload for In-Orbit Demonstration,” in *2012 6th Advanced Satellite Multimedia Systems Conference (ASMS) and 12th Signal Processing for Space Communications Workshop (SPSC)*. IEEE, Sep. 2012, pp. 160–165. [Online]. Available: <http://ieeexplore.ieee.org/lpdocs/epic03/wrapper.htm?arnumber=6333069>
- [8] Federal Aviatian Administration. (2013) NextGen Technologies Interactive Map. Accessed 2013-07-29. [Online]. Available: <http://www.faa.gov/nextgen/flashMap/index.cfm>
- [9] Aireon, “Global Aviation Surveillance System,” Brochure, 2012. [Online]. Available: <http://www.iridium.com/about/industryleadership/Aireon.aspx>
- [10] S. Nelson, A. J. Navarr, and M. Melum, “Real Space-Based ADS-B for NextGen,” *Avoinics Magazine*, Jun. 2013, webinar.
- [11] S. Lee, A. Hutputanasin, A. Toorian, W. Lan, and R. Munakata, “CubeSat design specification,” *The CubeSat Program*, 2011. [Online]. Available: <http://brownncubesat.org/wp-content/uploads/2013/01/Cubesat-Reqs.pdf>
- [12] GOMspace. (2013) QB50-Platform. Accessed 2013-08-13. [Online]. Available: <http://gomspace.com/index.php?p=products-qb50>
- [13] I. Nason, J. Puig-Suari, and R. Twiggs, “Development of a family of picosatellite deployers based on the CubeSat standard,” *Proceedings, IEEE Aerospace Conference*, vol. 1, pp. 1–457–1–464, 2002. [Online]. Available: <http://ieeexplore.ieee.org/lpdocs/epic03/wrapper.htm?arnumber=1036865>
- [14] CubeSat Kit. (2013) 3D Models of the CubeSat Kit. Accessed 2013-08-13. [Online]. Available: <http://www.cubesatkit.com/content/design.html>

## REFERENCES

---

- [15] University of Toronto Institute for Aerospace Studies. (2011) CanX-1: Canada's First Nanosatellite. Accessed 2013-08-22. [Online]. Available: <http://www.utias-sfl.net/nanosatellites/CanX1/>
- [16] University of Tokyo. (2005) XI-V Missions. Accessed 2013-08-22. [Online]. Available: <http://www.space.t.u-tokyo.ac.jp/cubesat/mission/V/index-e.html>
- [17] J. Wertz and W. Larson, *Space Mission Analysis and Design*, ser. Space Technology Library. Springer Netherlands, 1999.
- [18] Iridium. (2011, September) Iridium Suprasses 500,000 Subscribers Worldwide. Accessed 2013-08-31. [Online]. Available: <http://investor.iridium.com/releasedetail.cfm?ReleaseID=604474>
- [19] International Civil Aviation Organisation, *Manual for ICAO Aeronautical Mobile Satellite (Route) Service, Part 2 - IRIDIUM*, May 2007.
- [20] C. E. Fossa, R. A. Raines, G. H. Gunsch, and M. A. Temple, "An overview of the iridium (r) low earth orbit (leo) satellite system," in *Aerospace and Electronics Conference, 1998. NAECON 1998. Proceedings of the IEEE 1998 National*. IEEE, 1998, pp. 152–159.
- [21] S. Pratt and R. Raines, "An operational and performance overview of the IRIDIUM low earth orbit satellite system," ... *Surveys & Tutorials*, ..., pp. 2–10, 1999. [Online]. Available: [http://ieeexplore.ieee.org/xpls/abs\\_all.jsp?arnumber=5340513](http://ieeexplore.ieee.org/xpls/abs_all.jsp?arnumber=5340513)
- [22] F. Dietrich, P. Metzen, and P. Monte, "The Globalstar cellular satellite system," *Antennas and Propagation*, ..., vol. 46, no. 6, pp. 935–942, 1998. [Online]. Available: [http://ieeexplore.ieee.org/xpls/abs\\_all.jsp?arnumber=686783](http://ieeexplore.ieee.org/xpls/abs_all.jsp?arnumber=686783)

## REFERENCES

---

- [23] D. Smith, “Operations innovations for the 48-satellite globalstar constellation,” *Proceedings of the 16th AIAA International ...*, pp. 537–542, 1996. [Online]. Available: <http://arc.aiaa.org/doi/pdf/10.2514/6.1996-1051>
- [24] Aireon, “Aireon Coverage Comparison,” Brochure, 2012. [Online]. Available: <http://www.aireon.com/Solutions/TheGlobalAdvantage>
- [25] J. Dawson, “ADS-B via Low Earth Orbiting Satellites Benefits Assessment,” pp. 1–25, 2013. [Online]. Available: <http://www.mexico.icao.int/Meetings/ANIWG/ANIWG1/ANIWG01P04.pdf>
- [26] S. Finkelstein and S. Sanford, “Learning from corporate mistakes:: The rise and fall of Iridium,” *Organizational Dynamics*, vol. 29, no. 2, pp. 138–148, 2000. [Online]. Available: <http://www.rentcell.com/manuals/Iridium.pdf>
- [27] V. A. Orlando, “Automatic Dependent Surveillance Broadcast ( ADS-B ) Mode S Extended Squitter,” Federal Aviation Administration, Tech. Rep., 2001. [Online]. Available: [http://adsb.tc.faa.gov/WG3\\_Meetings/Meeting8/](http://adsb.tc.faa.gov/WG3_Meetings/Meeting8/)
- [28] DLR, “ADS-B over satellite – first aircraft tracking from space,” *DLR Press Portal*, 2013. [Online]. Available: [http://www.dlr.de/dlr/presse/en/desktopdefault.aspx/tabcid-10308/471\\_read-7318/year-all/#gallery/11231](http://www.dlr.de/dlr/presse/en/desktopdefault.aspx/tabcid-10308/471_read-7318/year-all/#gallery/11231)
- [29] The European Space Agency, “Proba Missions.” [Online]. Available: [http://www.esa.int/Our\\_Activities/Technology/Proba\\_Missions/Overview2](http://www.esa.int/Our_Activities/Technology/Proba_Missions/Overview2)
- [30] ——, “Tracking aircraft from orbit / Proba Missions,” 2013. [Online]. Available: [http://www.esa.int/Our\\_Activities/Technology/Proba\\_Missions/Tracking\\_aircraft\\_from\\_orbit](http://www.esa.int/Our_Activities/Technology/Proba_Missions/Tracking_aircraft_from_orbit)

## REFERENCES

---

- [31] Insero Software, “DSE Airport Solutions changes its name to Insero Software,” 2014. [Online]. Available: <http://inserosoftware.dk/dse-airport-solutions-changes-name-insero-software/>
- [32] GomSpace, “GomSpace GOMX-1,” 2014. [Online]. Available: <http://www.gomspace.com/index.php?p=gomx1>
- [33] L. Alminde and J. Christiansen, “GomX-1: A Nano-satellite Mission to Demonstrate Improved Situational Awareness for Air Traffic Control,” pp. 1–7, 2012. [Online]. Available: <http://digitalcommons.usu.edu/smallsat/2012/all2012/13/>
- [34] EoPortal, “GATOSS - Satellite Missions - eoPortal Directory,” 2014. [Online]. Available: <https://directory.eoportal.org/web/eoportal/satellite-missions/g/gatoss>
- [35] T. Nguyen. (2014) 2014Thesis. GitHub repository. [Online]. Available: <https://github.com/tnguyenbluesat/2014Thesis>
- [36] OpenFlights, “Airport and airline data.” [Online]. Available: <http://openflights.org/data.html>
- [37] AGI. (2013) STK 10.1 Online Help. Accessed 2014-04-04. [Online]. Available: <http://www.agi.com/resources/help/online/stk/10.1/>
- [38] Garmin, “GTX 330/330D Mode-S transponders,” 2007.
- [39] Avidyne Corporation, “AXP340 Mode S Transponder with ADS-B Out,” 2011.
- [40] Trig Avionics, “THE TT31 1090ES ADS-B OUT TRANSPONDER,” pp. 5–6, 2013.
- [41] BendixKing, “KT 74 ADS-B Ready Mode S Transponder that’s ahead of its time,” 2013.

## REFERENCES

---

- [42] RTCA, “Minimum Operational Performance Standards for 1090 MHz Extended Squitter Automatic Dependent Surveillance – Broadcast ( ADS-B ) and Traffic Information Services – Broadcast ( TIS-B ),” 2013.
- [43] Boeing. (2014) 747 Family - Techincal Information. Accessed 2014-04-04. [Online]. Available: <http://www.boeing.com/boeing/commercial/747family/specs.page>
- [44] ——. (2014) 777 Family - Techincal Information. Accessed 2014-04-04. [Online]. Available: [http://www.boeing.com/boeing/commercial/777family/pf/pf\\_200product.page](http://www.boeing.com/boeing/commercial/777family/pf/pf_200product.page)
- [45] ——. (2014) 757 Family - Techincal Information. Accessed 2014-04-04. [Online]. Available: [http://www.boeing.com/boeing/commercial/757family/pf/pf\\_200tech.page](http://www.boeing.com/boeing/commercial/757family/pf/pf_200tech.page)
- [46] G. Frawley, *The International Directory of Civil Aircraft*. Aeorspace Publications, September 2013.
- [47] M. Sheppard, “ALLFITDISTfit all valid parametric probability distributions to data,” <http://www.mathworks.com.au/matlabcentral/fileexchange/34943-fit-all-valid-parametric-probability-distributions-to-data/content/allfitdist.m>, 2012.
- [48] A. A. Rahman, “PRESS CONFERENCE: MH370,” 2014. [Online]. Available: [http://www.mot.gov.my/my/Newsroom/PressRelease/Tahun2014/MH370PressStatementbyDato%27AzharuddinAbdulRahmanon10March2014\(12.00PM\).pdf](http://www.mot.gov.my/my/Newsroom/PressRelease/Tahun2014/MH370PressStatementbyDato%27AzharuddinAbdulRahmanon10March2014(12.00PM).pdf)
- [49] FlightRadar24, “MH370 - Malaysia Airlines - Flight history,” 2014. [Online]. Available: <http://www.flightradar24.com/data/pinned/mh370-2d81a27/#2d81a27>
- [50] N. Koswanage and S. Gobvindasamy, “Exclusive: Radar data suggests missing Malaysia plane deliberately flown way off course

## REFERENCES

---

- sources.” [Online]. Available: <http://www.reuters.com/article/2014/03/14/us-malaysia-airlines-radar-exclusive-idUSBREA2D0DG20140314>
- [51] P. Colgan, “MAP: The Possible MH370 Debris Sighting Fits The Former Pilot’s Theory Of A Fire Or Smoke In The Cockpit,” 2014. [Online]. Available: <http://www.businessinsider.com.au/map-the-possible-mh370-debris-sighting-fits-the-theory-of-a-fire-or-smoke-in-the-cockpit-2014-3>
- [52] S. Pandey and J. Ruwitch, “Australian PM says searchers confident of position of MH370’s black boxes,” 2014. [Online]. Available: <http://www.reuters.com/article/2014/04/11/us-malaysia-airlines-idUSBREA3A06W20140411>
- [53] ABC News, “MH370 search area now larger than Australia,” Mar. 2014. [Online]. Available: <http://www.abc.net.au/news/2014-03-18/malaysia-search-area-larger-than-australia/5329748>
- [54] R. Hogg, J. McKean, and A. Craig, *Introduction to mathematical statistics*, ser. Pearson education international. Pearson Education, 2005.

## **Appendix A**

**2013 AIAA Region VII-AU Student  
Conference**

**Full Text of Accepted Paper**

# Tracking Aircraft via a Low-Earth-Orbit CubeSat Constellation

Thien H. Nguyen\*

*The University of New South Wales, Kensington, New South Wales, 2052, Australia*

**Automatic Dependant Surveillance-Broadcast (ADS-B)** is quickly becoming the primary method that Air Navigation Service Providers (ANSPs) and Air Traffic Control (ATC) systems use to track aircraft during flight. ADS-B coverage can be supplemented by space based receiving stations in order to track aircraft over regions where ground-based stations cannot be installed, for example, over oceans and poles. Commercial interest for ADS-B coverage from space is strong and two low risk but high-cost solutions have been proposed as secondary payloads on the Globalstar and Iridium NEXT constellations of commercial telecommunication satellites. Hosting the service in a constellation of low-cost CubeSats will provide a more economical solution, with lower production and launch costs. The key challenge in the design of the system is balancing coverage area, revisit times and link-budgets against cost and CubeSat technological limitations.

## Nomenclature

ADS-B	Automatic Dependant Surveillance-Broadcast
AIS	Automatic Identification System
ALAS	ADS-B Link Augmentation System
ANSP	Air Navigation Service Provider
ATC	Air Traffic Control
ATCRBS	Air Traffic Control Radar Beacon System
DLR	German Aerospace Centre
ESA	European Space Agency
LEO	Low Earth Orbit
PolyCal	California Polytechnic University
PSTN	Public Switched Telephone Network
RAAN	Right Angle of Ascending Node
SAPID	Space-Based ADS-B In-Orbit Demonstration Payload Developoment for Air Traffic Surveillance Project
SNOC	Satellite Network Operations Center
SSR	Secondary Surveillance Radar
TCAS	Traffic Collision Avoidance System

## I. Introduction

AUTOMATIC Dependant Surveillance Broadcast (ADS-B) is an aircraft tracking system based upon digital aircraft-to-ground and aircraft-to-aircraft transmissions. It is intended to support and eventually replace the existing Air Traffic Control Radar Beacon System (ATCRBS) which uses a radar call-and-response protocol in order to track aircraft within range of ATC stations. ADS-B is now being adopted as a primary Air Traffic Control (ATC) management system in the United States of America,<sup>1</sup> the European Union and Australia.<sup>2</sup>

---

\*Undergraduate Student, Australian Centre for Space Engineering Research (ACSER), UNSW Kensington Campus, AIAA Student Member.

ADS-B specifies that aircraft continuously broadcast data packets containing their identification, position and aircraft health using information generated by on-board avionics. Data packets are transmitted with an average update rate of once per second with broadcast periods ranging between 0.5 seconds and 5 seconds.<sup>3,4</sup> Transmissions occur over the L-band 1090 MHz Mode S Extended Squitter frequency shared by Aircraft Secondary Surveillance Radar (SSR) and Traffic Collision Avoidance System (TCAS). ADS-B is broadcast on a random access basis with particular aircraft identified by information in their data packets.<sup>4</sup>

Tracking via ADS-B requires aircraft to be within the line-of-sight of a ground station. ADS-B coverage areas vary with altitude and the existence of obstructing features in the terrain surrounding a ground station. Out of the range of these ground stations, aircraft tracking via ADS-B is not possible. Although comprehensive coverage is already in place in Australia,<sup>2</sup> the Asia-Pacific region<sup>5</sup> and much of North America,<sup>1</sup> there still exists areas, particularly over oceanic and polar regions where the service is not available. These areas are illustrated in Figure 1. Some solutions exist for ADS-B coverage in remote and marine areas. Ground stations installed on oil platforms currently provide coverage over the Gulf of Mexico<sup>1</sup> - a solution which could be extended to other bodies of water. However, relying on terrestrial systems to provide global ADS-B coverage is not cost effective.

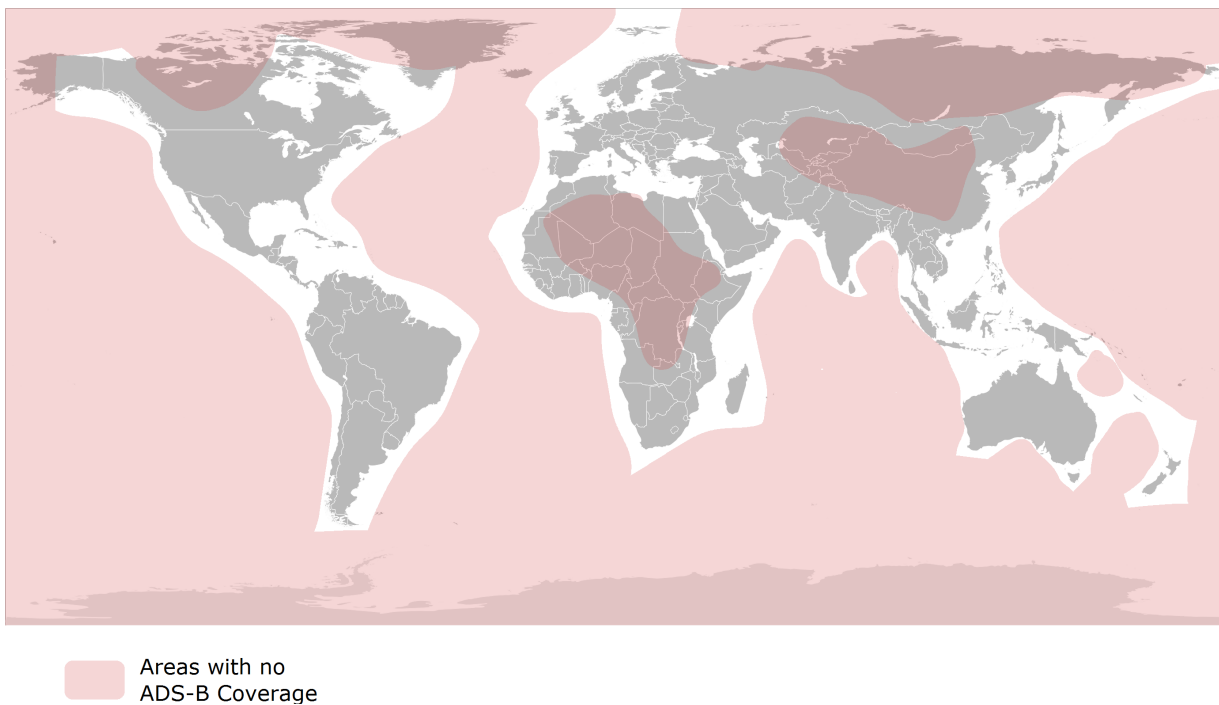


**Figure 1. Approximate areas with a lack of adequate terrestrial ADS-B coverage.**

This paper presents a background study on satellite constellations and space ADS-B technology. Design concepts from existing communications satellite constellations and space ADS-B receiving technologies will be used in order to determine the mission parameters of the required space-based ADS-B tracking system. This will lay down the foundation for future work in the development of a constellation of CubeSats which can be used to augment terrestrial ATC systems.

Strong interest is being shown by American, European and Australian Aviation authorities in implementing a satellite-based ADS-B system in order to address this coverage gap. The European Space Agency has commissioned a series of studies into the feasibility of receiving ADS-B from Low Earth Orbit (LEO).<sup>4</sup> The German Aerospace Agency (DLR),<sup>6</sup> and private companies such as Aireon<sup>7</sup> and ADS-B Technologies<sup>8</sup> have already invested heavily into implementing space-based ADS-B.

## II. Mission Overview

The root requirement of a satellite-based ADS-B system is the provision of ADS-B coverage over regions where terrestrial systems do not currently provide coverage (in particular, oceans and poles). Within this requirement are a number of variable mission parameters that effect the design and economic cost of resulting satellite systems. Varying the parameters and analysing the performance of resulting designs will allow for more effective mission trade-off analysis.

### A. System Users

A spaced based ADS-B system would have two key user groups

- Air Navigation Service Providers
- Airlines and air transportation service providers

Although Australia, America and Europe are able to implement terrestrial ADS-B stations, rolling out terrestrial stations to cover all interest areas is not necessarily cost effective. This is particularly true in regions such as South East Asia. In such regions, the technology and economic base does not exist to make terrestrial deployment viable.<sup>4</sup> In these situations a satellite-based system can more effectively augment existing ADS-B coverage for use by ANSPs.

Another key user would be airlines and other air transportation services. Greater position and telemetry coverage of aircraft over oceanic and polar regions allows for more optimal flight path co-ordination. ADS-B assisted flight routing will allow for narrower longitudinal and latitudinal track separation, allowing for more flights to travel on desired fuel-saving paths. A flight simulation analysis presented by Aireon suggests that increased density of planes in jet streams can result in fuel savings of up to 450 litres per oceanic flight.<sup>9</sup>

### B. System Update Rate

The update rate of a space-based ADS-B system defines timeliness with which aircraft data can be updated and disseminated terrestrially. Having a high-effective update rate is crucial in range of Airports with ATC towers having to co-ordinate a large density of aircraft traffic. With ADS-B, terrestrial ATC towers typically achieve an update rate of less than 10 seconds depending on airport capacity.<sup>10, 11</sup> For the purposes of live tracking and safety control, an update rate in the order of 10 to 30 seconds will be required [11, B.5.2]. An update rate in the order of 5 to 10 minutes would enable satisfactory tracking by airlines and air transport services at less cost. A lowest cost system with an update rate of 1-2 hours could be useful for occasional tracking of aircraft making oceanic flights. This, however, would be inadequate for safety applications or any short-range terrestrial flights.

In order to determine the update rate, all communication delays must be considered, encompassing all communication links between the aircraft and end users. The desired update rate will define the down-link requirements for the system. This will then affect the communication architecture of the resulting satellite system. Higher downlink requirements will necessitate that the space-segment have more downlink opportunities. This will require either a higher number of ground stations or inter-satellite data-linking.

### C. Revisit Time

Due to the random access nature of Mode S Extended Squitter, the number of aircraft surveyed by an ADS-B receiver is limited. With current technology, a terrestrial omni-directional Mode S antenna with a 100 nautical mile operational range can cover a maximum of 120 aircraft with a 99.5 % detect probability over 5 seconds.<sup>10</sup> Regulations for civil aviation equipment in Europe specify a detect probability of at least 95% over an update interval of 10 seconds [11, B.5.2]. Scanning for a shorter period, or scanning an area with more aircraft will result in more ADS-B collisions and a drastically reduced detect rate. ‘Missing’ aircraft in this manner is unacceptable from a safety perspective. Suggested solutions for high density areas include more sophisticated antenna design with spot beams,<sup>4</sup> or variable-periodicity of ADS-B signals.<sup>10</sup>

For ADS-B reception via satellite, a populated area can be either scanned for a longer period, or ‘re-scanned’ over multiple revisits. This would mediate the need for a larger or more sophisticated and costly antenna array. A longer scanning period can be achieved slowing the ground-track of the space segment over key areas. Such behaviour can be achieved using Molniya orbits. Slowing the ground-track will require

a higher-altitude, which then requires a higher gain antennae to effectively service. This is particularly a problem on CubeSats where technology implementation is limited. The revisit time will therefore be defined by limitations of the antennae array and on-board processing technology for ADS-B signal reception. Satellite ADS-B receivers are currently being tested by the German Aerospace Centre (DLR) in conjunction with the European Space Agency (ESA)<sup>6</sup> and Thales Alenia Space.<sup>4</sup>

#### D. Geographical Coverage

Full global coverage would be achieved by a series of polar or near polar orbits, such as the Iridium Satellite constellation.<sup>12,13</sup> Achieving full coverage would be the most costly solution, requiring the largest number of satellites and ground stations. At the very least, the ADS-B system should cover the poles, the North Atlantic, North Pacific and Indian Oceans and South East Asia in order to meet the root system requirement. These areas have the highest amount of air traffic not covered by terrestrial ADS-B systems. Monitoring these regions with specific orbits can reduce the number of spacecraft required in order to provide the coverage gap required by the system.

#### E. Mission Parameter Summary

- The ADS-B system should at least provide coverage gaps over the North and South Poles, The North Atlantic, North Pacific and Indian Oceans and South East Asia.
- The system will be used to service both ANSPs and commercial Airlines
- The system should have an update rate of less than 30 seconds for safety tracking applications,<sup>11</sup> 5-10 minutes for low-fidelity tracking applications<sup>9</sup> and 1 to 2 hours for basic flight path studying.
- Revisit times will be affected by the effectiveness of antenna technology available for ADS-B reception on a CubeSat scale
- Constellation configurations, including satellite orbits and ground station placement will then affect revisit times and system update rates.

### III. Space Based ADS-B

A number of existing technologies are being investigated to evaluate the effectiveness space-based ADS-B technology. At the moment, none of these systems would comply with the size and power-requirements of a CubeSat systems. However the general design principles can be adopted for development of a CubeSat ready implementation.

#### A. ADS-B Link Augmentation System (ALAS)

ADS-B Technologies have developed the ALAS as a space-based ADS-B coverage solution. The ALAS will be flown as hosted payloads on the Globalstar's second generation constellation of satellites. The system is expected to provide global coverage with a one-second update rate.<sup>14,8</sup> The system is intended to operate by relaying ADS-B data received L band transmissions to ground based gateways through the C band. These gateways then relate that data to Air Traffic Management (ATM) systems as necessary. The system is full duplex and is designed to transparently augment the existing ADS-B ground coverage network.

The system will require both ANSPs and Aircraft to purchase additional L and S band transceivers to communicate with the space segment. ALAS will not be compatible with standard ADS-B hardware implementation.

The second Globalstar constellation will have limited coverage due to its orbit configuration and communication infrastructure. The inclination of the Globalstar orbits will not provide ADS-B coverage over the poles, and reliance on a permanent link with ground stations restricts the predicted coverage to continental areas. The predicted ADS-B coverage is much the same as the first constellation, shown in Figure 2,<sup>14</sup> missing key oceanic and polar areas.

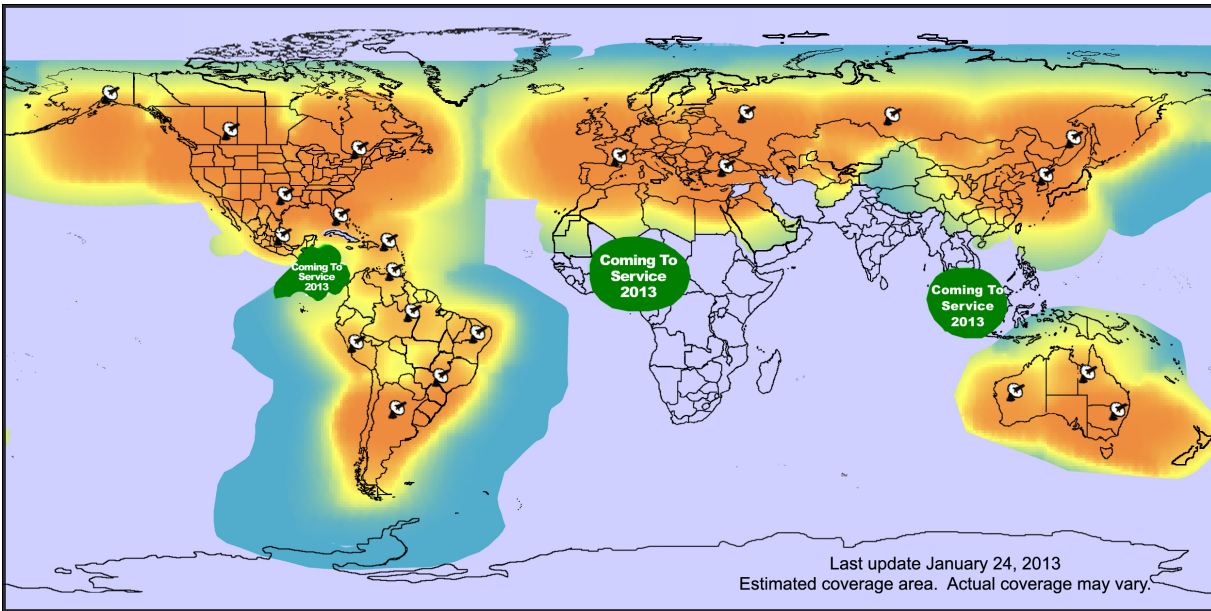


**Figure 2.** Globalstar System Coverage, from<sup>15</sup>

## B. Aireon

Aireon LLC are currently developing an space-based, ADS-B reliant ‘global aviation surveillance system’<sup>7</sup> to be flown on the Iridium NEXT constellation of Low-Earth Orbit satellites. The constellation is expected to provide complete global coverage, including over polar regions.<sup>16</sup>

This system is presented as flight path solutions for both ANSPs and Aircraft Carriers. Marketing material claims that intelligent flight path planning will save Airlines money in fuel with more optimised routes.<sup>16</sup> The Aireon Payload and Iridium NEXT satellites are being developed by Thales Alenia Space. The service is expected to be available by 2017.

The concept presented for the system suggest that unlike the Globalstar hosted ALAS, Aireon will use the standard Mode S Extended Squitter carrier signal in order to receive ADS-B signals.<sup>9</sup> This has a distinct advantage in that no additional hardware is required in order to implement the system.

### *Space-Based ADS-B In-Orbit Demonstration (SAPID)*

Thales Alenia Space has been involved in the development of the Space-Based ADS-B In-Orbit Demonstration Payload Development for Air Traffic Surveillance Project (SAPID) transceiver. The involvement of Thales suggests that similar technology will be used for the Aireon system. The SAPID attempts to address key issue of signal collision on the 1090Mhz RF link over an area densely populated by aircraft. The proposed solutions focuses the receiving system into multiple spot beams to increase the ‘hit rate’ of aircraft detection.<sup>4</sup>

## C. Proba V

In early 2013, the European Space Agency (ESA) launched their fifth experimental Proba satellite, Proba V, with a guest ADS-B Payload. Like SAPID, the ADS-B payload is designed to receive signals via the native Mode S 1090Mhz carrier. The receiver, designed by the German Aerospace Center (DLR) is designed to receive ADS-B from LEO in Proba V’s 820km orbit.<sup>6,17,18</sup> Proba V is travelling in a Sun-Synchronous polar orbit at an altitude of 820km.<sup>17</sup>

The satellite is currently tracking Aircraft over Northern Europe.<sup>6</sup> Tests to determine how sensitive the receiver is to problems caused by signal density (as put forward by<sup>4</sup>) are ongoing. No results beyond the initial proof of concept have been published.

## IV. Satellite Constellation Survey

A number of LEO satellite constellations with similar coverage requirements were studied and their performance requirements compared against those needed by an ADS-B satellite constellation

### A. Iridium

The Iridium Satellite Constellation is a network of 66 LEO satellites which provide mobile communication services over a truly global coverage network. The system provides voice and data coverage for subscribers equipped with Iridium hardware, including mobile handsets and data modems. The intention is that the system will work in remote areas of the Earth where reliable mobile and wireless data over conventional means (i.e. 3G and emerging 4G technologies) is not available.

#### 1. Communication

The Iridium network relies inter-satellite and satellite-to-ground communication in order to complete data and voice links between Iridium subscribers and other service providers. User end-devices, such as mobile handsets, data receivers and in-vehicle radio units link with satellites using L-band transmissions. A connection with a data source or other L-Band transceiver is routed between satellites and ground based gateways over K-Band transmissions.<sup>12, 19</sup> A second K band ‘control’ link is used by ground operators to monitor the space segment through the Iridium Satellite Network Operations Center (SNOC).

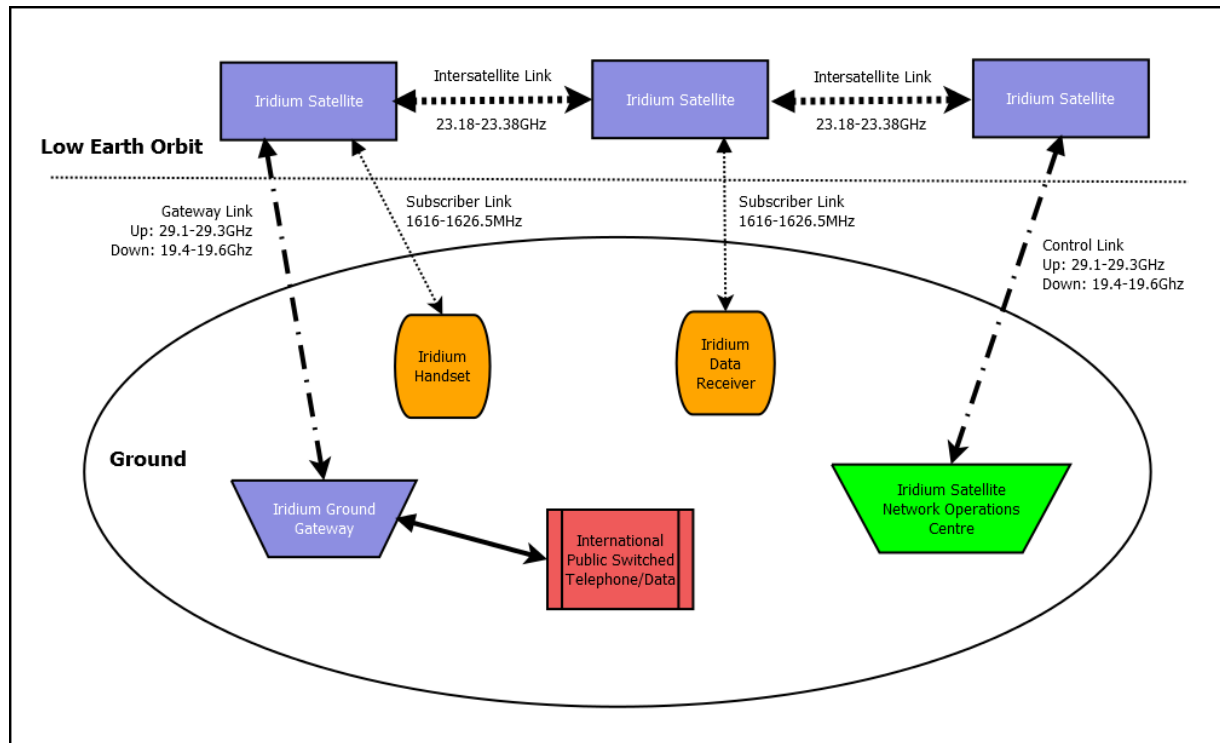


**Figure 3. Overview of the Iridium Satellite Network, after<sup>12, 20, 13</sup>**

An ADS-B system would benefit from employing a similar communications architecture. Employing inter-satellite communication links would increase the system-update rate and potential coverage without increasing the number of satellites or ground stations required. Alternatively, the Iridium payload data link itself could be employed to relay information from an ADS-B constellation to the ground.

## 2. Space Segment

The space segment of the system consists of 66 satellites in Low Earth Orbit at an altitude of approximately 780km. The satellites are evenly distributed amongst six polar co-rotating planes each spaced 31.6° apart in longitude, with the first and sixth planes counter-rotating and spaced 22 degrees apart.<sup>12,13</sup> The planes have a near circular orbit<sup>21</sup>. Each orbital plane has 11 satellites evenly distributed across the orbit. This configuration is shown in Figure 4. High inclination polar orbits such as this would be ideal for providing coverage over the north and south poles.

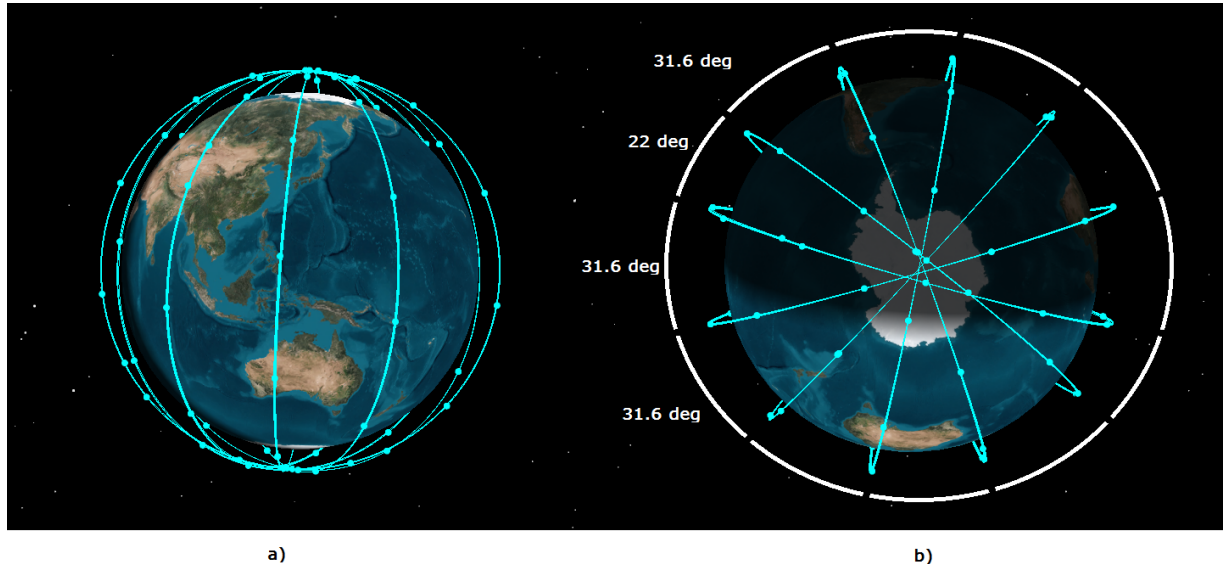


Figure 4. Iridium Satellite constellation showing a) a view over Australia and South East Asia and b) the view from above the south pole. Data taken from STK

## B. Globalstar

The Globalstar Constellation consists of 48 LEO satellites that provide mobile communication services that, as far as end-users are concerned, are much the same as those offered by Iridium. Globalstar Inc. provide voice and data coverage over service areas where traditional PSTN data links are not available. Unlike Iridium, Globalstar does not provide 100% global coverage, with swaths only cover areas between 70° north and south latitudes.<sup>22</sup>

### 1. Communication and Coverage

The Globalstar provides a simple ‘bent-pipe’ architecture for completion of communication links. Globalstar user terminals (for example, handsets or modems) connect directly with an overhead satellite via L and S band radios. The voice or data path is then routed through a ground gateway to international Public Switch Telephone Networks (PSTNs)<sup>22,23</sup>. The ability for a satellite to complete this link relies on the satellite being within the line of site of a ground-gateway. Globalstar provides no inter-satellite linking and as such the system coverage is limited by gateway locations. This limitation can be seen in Figure 2.

The restriction of coverage to terrestrial areas does not provide an ideal solution for space-based ADS-B coverage. A space ADS-B system would be in operation to address coverage issues over areas where terrestrial systems cannot be installed. A Globalstar like system would not provide an ideal solution to this problem.

## 2. Space Segment

The space segment of the Globalstar system consists of 48 satellites equally distributed in eight orbital planes. Each orbital plane contains 6 satellites has a 52° inclination.<sup>23,22</sup> Data from STK indicates that the

orbits have equally spaced right ascensions of ascending node (RAANs) between  $0^\circ$  and  $360^\circ$ , offset  $45^\circ$  from each other. Each satellite is in a roughly circular orbit, with an altitude of 1414 kilometres<sup>23</sup> and a period of approximately 115 minutes. Although this configuration does not provide coverage over polar regions, satellites and launch operate at lower cost - a potential mission trade-off for ADS-B.

### C. Automatic Identification System (AIS)

The Automatic Identification System (AIS) is the maritime analogue to ADS-B. The system consists of VHF transponders which relay ship telemetry (identity, heading, destination etc.) between ships and between ships and shore stations. The viability of augmenting AIS with a LEO space-segment has been in investigation since 2003.<sup>24</sup> The primary goal of the proposed Satellite AIS systems is to provide route monitoring, allowing for longer update periods and data-lag.

The key challenge with Satellite-based AIS, is the detection of signals in high density areas where signal collision is prominent. Like ADS-B, AIS operates on a random-access basis on a single RF channel. Low density areas with less than 2000 ships will yield a detection rate of 99% from conventional AIS receivers.<sup>24, 25</sup> This number drops off significantly as more ships enter the antenna footprint, dropping as low as 50% with 2500 ships for an observation time of 15 minutes.<sup>24</sup>

The performance parameters for each of the Satellite AIS systems investigated<sup>26, 24, 27</sup> do not meet the immediacy requirements of ADS-B. The proposed AIS constellation designs can be mimicked in order to provide basic route monitoring for aircraft, but not live tracking data. However, the technologies investigated and basic system design provide a good base model from which a more immediate system can be designed. In particular, having more satellites and implementing inter-satellite links as per Iridium can drastically improve the update time performance of the proposed system.

## V. CubeSat Capabilities

The CubeSat picosatellite standard maintained by California Polytechnic University (PolyCal) has eased space access for non-military and non-commercial space interest groups, including Academic and Hobbyist groups. The launch interface design is such that multiple CubeSats can be launched on the same vehicle at reduced cost.<sup>28</sup> The proliferation of open-source CubeSat designs has allowed the academic and hobbyist community to collaborate and refine CubeSat design concepts. The resulting reduction in design and launch makes developing space-bound payloads more accessible with less design risk. CubeSats come in a range of sizes, from the 1 Unit (1U)  $10\text{cm} \times 10\text{cm} \times 10\text{cm}$  cube to the 3-unit (3U)  $30\text{cm} \times 10\text{cm} \times 10\text{cm}$  square prism.

Launching a constellation of CubeSats to provide a global ADS-B service could potentially be more cost effective than launching large telecommunications satellites for the same purpose. However, due to size and the lack of maturity for key CubeSat technologies, the capability for CubeSats to carry out long term or large scale missions is severely limited. In particular propulsion, attitude control and power systems limit the capability of CubeSat payloads.

### A. Propulsion

In LEO, satellites are subject to an atmospheric drag, resulting in orbital decay. LEO orbits are maintained using on-board propulsion systems which perform station keeping manoeuvres to correct the effects of atmospheric drag.

Research conducted in<sup>29</sup> shows that some Electric Propulsion Systems may be suitable for attitude control and station keeping on a 2U or 3U CubeSat. The Ionic Liquid Field Emission Electric Propulsion (IL-FEEP) thruster presented in<sup>30</sup> and the Hydrazine Propulsion module presented in<sup>31</sup> are promising candidates for long-term station keeping. However both require a significant portion of the mass, volume and power budget available on a CubeSat, and neither have had extensive flight heritage.

The lack of a clear thruster system complicates the design of the proposed ADS-B CubeSat Constellation. The inability to perform station keeping manoeuvres could significantly limit the lifespan of a CubeSat, without the ability to manage orbital perturbations and orbital decay.

## B. Attitude Control

Attitude determination and control on CubeSats is an area of on-going study. The pointing accuracy possible on CubeSat missions will affect telecommunications-like payloads, such as an ADS-B receiver. [32, Chapter 3.1.2] summarises the determination and control capability reported by on-going CubeSat missions and claimed by commercial off-the-shelf CubeSat Part suppliers.

The CubeSat Kit offers an attitude determination and control system that has 1° pointing accuracy. The system uses 3-axis reaction wheels, torque coils and magnetometers and sun-sensors in order to determine and control attitude. The system's mass and volume is non-trivial, taking up 1 whole unit of a CubeSat.<sup>33</sup>

Research summarised in [32, Chapter 3.1.2] suggests that pointing accuracies of less than 5° be reliably achieved with existing, flight proven systems. Improvements to pointing systems seem to chiefly rely in the software and control space, without any significant changes to available hardware. This existing capability will be taken into account during the CubeSat mission design.

Attitude control will be important in order to maintain a desired coverage area and for inter-satellite communication. To address signal density issues, the on-board ADS-B receiver must have a limited Earth-footprint. Maintaining accurate knowledge and control of this footprint will be necessary in order to achieve the desired coverage from the satellite.

## C. Electrical Power

The small size and limited bus capability of CubeSats restrict the areas on which solar-panels can be mounted. This restricts the power budget for a CubeSat mission, which then have design ramifications for the design of on-board electrical systems, such as sensors, communication arrays and electric thrusters.

A survey conducted in<sup>32</sup> yielded that theoretically, 1U CubeSats can only generate less than 2W, given the limited surface area and available solar panel technologies. 3U CubeSats identified by the study claim between 5.5W and 6W in peak power generation capabilities.

## D. Typical Mission Life

CubeSat mission life varies and is typically limited by catastrophic systems failures. One of the first CubeSats launched, the Japanese CUTE I operated for 4 years between launch in 2003 and 2007.<sup>34</sup> Other than CubeSats who have failed during launch, the lifespan of CubeSats range between 2 months (CUTE II) to 3 years (QuakeSat, XI-V and others). The majority of these failures have occurred due to unexpected component or systems failures during satellite operation. In some cases failures occurred well beyond the design life of the mission.<sup>35</sup>

# VI. Summary and Future Work

The work conducted so far has identified the key user group for a satellite-based ADS-B system. Varying mission parameters, particularly revisit times and system update rates will have significant effects on the design and cost of the subsequent system. There are some technologies in development that are able to track Aircraft from space using ADS-B. However, these have not been implemented to the scale and performance required for true global ADS-B integration. Implementing a CubeSat constellation in either a global coverage or oceanic and polar coverage configuration will require the balance of system requirements of similar constellations (seen in Iridium and Globalstar) with the technological limitations of CubeSats.

The following work needs to be carried out in future.

- Simulation of different system configurations with varying mission parameters.
- Performance of each simulation will be evaluated against functional requirements and cost (both launch and maintenance).
- In order to address CubeSat limitations, simulations will be run with ‘ideal’ cases where technology is not limited by CubeSats. The configurations will then be scaled down to what is achievable by CubeSats and re-evaluated.

The final result of the above work will result in another study quantitatively comparing the performance of all the above configurations.

## References

- <sup>1</sup>Department of Transportation and Federal Aviation Administration, "Automatic Dependent Surveillance-Broadcast (ADS-B) Out Performance Requirements to Support Air Traffic Control (ATC) Service," *Federal Register*, Vol. 75, May 2010, Final Rule.
- <sup>2</sup>Civil Aviation Safety Authority, Australia, "Automatic Dependent Surveillance-Broadcast," 2012.
- <sup>3</sup>Civil Aviation Safety Authority, Australia, *Airworthiness Approval of Airborne Automatic Dependant Surveillance Broadcast Equipment (Advisory Circular AC 21-45(1))*, February 2012.
- <sup>4</sup>Blomenhofer, H., Rosenthal, P., Pawlitzki, A., and Escudero, L., "Space-based Automatic Dependent Surveillance Broadcast (ADS-B) payload for In-Orbit Demonstration," *2012 6th Advanced Satellite Multimedia Systems Conference (ASMS) and 12th Signal Processing for Space Communications Workshop (SPSC)*, IEEE, Sept. 2012, pp. 160–165.
- <sup>5</sup>International Civil Aviation Organisation, *ADS-B Implementation and Operations Guidance Document*, 4th ed., September 2011.
- <sup>6</sup>DLR, "ADS-B over satellite first aircraft tracking from space," *DLR Press Portal*, 2013.
- <sup>7</sup>Aireon, "Global Aviation Surveillance System," Brochure, 2012.
- <sup>8</sup>ADS-B Technologies, "What is Space-Based ADS-B?" 2011, Accessed 2013-07-22.
- <sup>9</sup>Dawson, J., "ADS-B via Low Earth Orbiting Satellites Benefits Assessment," 2013.
- <sup>10</sup>Orlando, V. A., "Automatic Dependent Surveillance Broadcast (ADS-B) Mode S Extended Squitter," Tech. rep., Federal Aviation Administration, 2001.
- <sup>11</sup>The European Organisation for Civil Aviation Equipment, "SAFETY, PERFORMANCE AND INTEROPERABILITY REQUIREMENTS DOCUMENT FOR ADS-B-NRA APPLICATION," 2005.
- <sup>12</sup>International Civil Aviation Organisation, *Manual for ICAO Aeronautical Mobile Satellite (Route) Service, Part 2 - IRIDIUM*, May 2007.
- <sup>13</sup>Fossa, C. E., Raines, R. A., Gunsch, G. H., and Temple, M. A., "An overview of the IRIDIUM (R) low Earth orbit (LEO) satellite system," *Aerospace and Electronics Conference, 1998. NAECON 1998. Proceedings of the IEEE 1998 National*, IEEE, 1998, pp. 152–159.
- <sup>14</sup>Nelson, S., Navarr, A. J., and Melum, M., "Real Space-Based ADS-B for NextGen," *Avionics Magazine*, June 2013, Webinar.
- <sup>15</sup>Globalstar, "Coverage Map," Aug. 2013.
- <sup>16</sup>Aireon, "Aireon Coverage Comparison," Brochure, 2012.
- <sup>17</sup>The European Space Agency, "Proba Missions," .
- <sup>18</sup>The European Space Agency, "Tracking aircraft from orbit / Proba Missions," 2013.
- <sup>19</sup>Maine, K., Devieux, C., and Swan, P., "Overview of IRIDIUM satellite network," *WESCON/'95. Conference . . .*, 1995.
- <sup>20</sup>Lemme, P., Glenister, S., and Miller, A., "Iridium(R) aeronautical satellite communications," *IEEE Aerospace and Electronic Systems Magazine*, Vol. 14, No. 11, 1999, pp. 11–16.
- <sup>21</sup>Pratt, S. and Raines, R., "An operational and performance overview of the IRIDIUM low earth orbit satellite system," *Surveys & Tutorials, . . .*, 1999, pp. 2–10.
- <sup>22</sup>Dietrich, F., Metzen, P., and Monte, P., "The Globalstar cellular satellite system," *Antennas and Propagation, . . .*, Vol. 46, No. 6, 1998, pp. 935–942.
- <sup>23</sup>Smith, D., "Operations innovations for the 48-satellite globalstar constellation," *Proceedings of the 16th AIAA International . . .*, 1996, pp. 537–542.
- <sup>24</sup>Høye, G. K., Eriksen, T., Meland, B. J., and Narheim, B. r. T., "Space-based AIS for global maritime traffic monitoring," *Acta Astronautica*, Vol. 62, No. 2-3, Jan. 2008, pp. 240–245.
- <sup>25</sup>Carson-Jackson, J., "Satellite AIS Developing Technology or Existing Capability?" *Journal of Navigation*, Vol. 65, No. 02, March 2012, pp. 303–321.
- <sup>26</sup>Cervera, M. a. and Ginesi, A., "On the performance analysis of a satellite-based AIS system," *2008 10th International Workshop on Signal Processing for Space Communications*, Oct. 2008, pp. 1–8.
- <sup>27</sup>Scorzolini, A. and Perini, V. D., "European enhanced space-based AIS system study," *. . . multimedia systems . . .*, 2010, pp. 9–16.
- <sup>28</sup>Nason, I., Puig-Suari, J., and Twiggs, R., "Development of a family of picosatellite deployers based on the CubeSat standard," *Proceedings, IEEE Aerospace Conference*, Vol. 1, 2002, pp. 1–457–1–464.
- <sup>29</sup>Mueller, J., Ziemer, J., and Hofer, R., "A survey of micro-thrust propulsion options for microspacecraft and formation flying missions," *5th Annual CubeSat . . .*, 2008, pp. 1–19.
- <sup>30</sup>Marcuccio, S., Pergola, P., and Giusti, N., "ILFEEP: A SIMPLIFIED, LOW COST ELECTRIC THRUSTER FOR MICROAND NANOSATELLITES," *Journal of Propulsion and Power*, 1998, pp. 1–12.
- <sup>31</sup>Schmuland, D., Masse, R., and Sota, C., "Hydrazine propulsion module for cubesats," 2011.
- <sup>32</sup>Selva, D. and Krejci, D., "A survey and assessment of the capabilities of Cubesats for Earth observation," *Acta Astronautica*, Vol. 74, May 2012, pp. 50–68.
- <sup>33</sup>Pumpkin Inc., "Miniature 3-Axis Reaction Wheel and Attitude Determination and Control System for CubeSat Kit Nanosatellites," April 2011, Accessed 2013-09-06.
- <sup>34</sup>Tokyo Institute of Technology, "CUTE-1 Status," June 2007, Accessed 2013-07-28.
- <sup>35</sup>denMike, "Michael's List of Cubesat Satellite Missions," Aug. 2009, Accessed 2013-07-28.

## **Appendix B**

# **65th International Astronautical Congress**

## **Abstract and Acceptance Letter**

65th International Astronautical Congress 2014

21st IAA SYMPOSIUM ON SMALL SATELLITE MISSIONS (B4)  
Small Earth Observation Missions (4)

Author: Mr. Thien Nguyen  
University of New South Wales, Australia, thien.nguyen@unsw.edu.au

Dr. Ediz Cetin  
University of New South Wales, Australia, e.cetin@unsw.edu.au  
Dr. Barnaby Osborne  
University of New South Wales, Australia, barnaby.osborne@gmail.com  
Dr. Naomi Tsafnat  
University of New South Wales, Australia, n.tsafnat@unsw.edu.au

SPACE BASED ADS-B VIA A LOW-EARTH ORBIT CUBESAT CONSTELLATION

**Abstract**

Automatic Dependent Surveillance-Broadcast (ADS-B) is currently being adopted by aviation authorities around the world as the standard method for tracking aircraft during flight. ADS-B coverage is available on most of the landmass in Europe, North America, Australia and South East Asia. However, gaps in coverage exist over regions where installing ADS-B receiver stations is not economically viable or feasible, such as over oceans and poles. To close these gaps, ADS-B signals can be received and retransmitted from satellites in Low Earth Orbit (LEO). There is an increased commercial interest in implementing ADS-B re-transmitting satellite constellations. The Iridium NEXT and second Globalstar constellations of LEO satellites that are currently under development will provide a space based ADS-B service. Using a constellation of CubeSats provides a more economical solution, with lower production, launch and satellite replacement costs. The key challenge in the design of such system entails balancing coverage area and revisit times against cost and CubeSat technological limitations.

In this paper we provide analysis of these trade-offs and provide an insight into requirements of such a system. We have modelled popular flights over the North Pole and Pacific and Atlantic Oceans (where ADS-B coverage is not available) in Systems Tool Kit (STK) with standard commercial ADS-B transmitters. These flight paths were analysed to determine the coverage requirements of a space based ADS-B system. Aviation safety requirements from various global authorities were researched to determine the system update rates necessary to provide a safety critical service. These requirements lay the groundwork for the systems development necessary to launch and operate an ADS-B constellation.



# INTERNATIONAL ASTRONAUTICAL FEDERATION

9 May 2014

Thien Nguyen  
Student  
University of New South Wales  
Australia

65<sup>th</sup> International Astronautical Congress  
Toronto, Canada  
29 September – 3 October 2014

**Subject:** IAC 2014 – Notification to Authors

Dear Mr. Nguyen,

As Co-Chairs of the International Programme Committee for the 65<sup>th</sup> International Astronautical Congress, we are pleased to inform you that your abstract “**Space Based ADS-B via a Low-Earth Orbit CubeSat Constellation**” has been accepted for a **15'-minute** oral presentation (Q&A time included). Please find the details hereunder.

Symposium	B4. 21st IAA SYMPOSIUM ON SMALL SATELLITE MISSIONS		
Session	4. Small Earth Observation Missions		
Order of presentation	8	Paper ID Nr.:	IAC-14,B4,4.8x25309

*-Please always indicate this paper ID in your correspondence with IAF Secretariat for faster identification and answer-*

Please note that the exact date of your presentation will be communicated to you by **mid-June** with the contact details of your session chairs, instructions on how to upload your final paper and Congress presentation. Note also that the duration of your oral presentation may be modified by your session chairs.

We would like to ask you to confirm your attendance and presentation to the IAF Secretariat ([support@iafastro.org](mailto:support@iafastro.org)) and session Chairs by **15 June 2014**, and to inform your co-author(s) that the above mentioned abstract has been accepted.

Session Chairs	Larry Paxton	Email	<a href="mailto:larry.paxton@jhuapl.edu">larry.paxton@jhuapl.edu</a>
	Amnon Ginati	Email	<a href="mailto:amnon.ginati@esa.int">amnon.ginati@esa.int</a>

Online registration will be available shortly ([www.iac2014.org](http://www.iac2014.org)) and Early bird fees will be valid **until 30 June 2014**. Please note that the publication of the papers in the Congress proceedings will only be possible if the registration fee is paid by at least one the authors and if the paper is uploaded on the IAF website before 10 September 2014.

Do not hesitate to contact the IAF Secretariat ([support@iafastro.org](mailto:support@iafastro.org)) should you have any questions on the technical programme.

We look forward to seeing you in Toronto!



## INTERNATIONAL ASTRONAUTICAL FEDERATION

Yours Sincerely,

**Virendra Jha**  
IPC Co-Chair

**Igal Patel**  
IPC Co-Chair

**Michel Arnaud**  
Advisor to the IPC Co-Chairs

# Appendix C

## Experimental Parameters

Table C.1: Orbital parameters of all experimental cases studied

Case Number	Section	Altitude (km)	Semi-major axis (km)	Inclination (deg)	Satellites (Total)	Satellites per plane	Planes	Plane separation (deg RAAN)	True Anomaly Separation
1	4.3.2	400	6778.14	60	12	4	3	120	90
2	4.3.2	450	6828.14	60	12	4	3	120	90
3	4.3.2	500	6878.14	60	12	4	3	120	90
4	4.3.2	550	6928.14	60	12	4	3	120	90
5	4.3.2	600	6978.14	60	12	4	3	120	90
6	4.3.2	650	7028.14	60	12	4	3	120	90
7	4.3.2	700	7078.14	60	12	4	3	120	90
8	4.3.2	750	7128.14	60	12	4	3	120	90
9	4.3.2	800	7178.14	60	12	4	3	120	90
10	4.3.3	700	7078.14	30	12	4	3	120	90
11	4.3.3	700	7078.14	40	12	4	3	120	90
12	4.3.3	700	7078.14	50	12	4	3	120	90
13	4.3.3	700	7078.14	60	12	4	3	120	90
14	4.3.3	700	7078.14	70	12	4	3	120	90
15	4.3.3	700	7078.14	80	12	4	3	120	90
16	4.3.3	700	7078.14	90	12	4	3	120	90
17	4.3.4	700	7078.14	60	3	1	3	120	360
18	4.3.4	700	7078.14	60	6	2	3	120	180
19	4.3.4	700	7078.14	60	9	3	3	120	120
20	4.3.4	700	7078.14	60	12	4	3	120	90
21	4.3.4	700	7078.14	60	15	5	3	120	72
22	4.3.4	700	7078.14	60	18	6	3	120	60

# Appendix D

## Student's t Distribution

The majority of data analysed statistically in this thesis found that a Students t distribution with a location-scale transformation provided the best fit statistical model. The periodicity analysis of satellite-revisit time showed slight bimodal behaviour, resulting in heavy tails, typical of a ‘t Location-Scale Distribution’ [54].

The Student’s t distribution probability density function (PDF) is given by

$$f_X(x) = \frac{\Gamma\left(\frac{\nu+1}{2}\right)}{\sqrt{\nu\pi}\Gamma\left(\frac{\nu}{2}\right)} \left(1 + \frac{x^2}{\nu}\right)^{-\frac{\nu+1}{2}} \quad (\text{D.1})$$

where  $\nu$  is the parameter defined as the ‘degrees of freedom’ and  $\Gamma$  is the standard gamma function [54]. To shift and scale the data, we need to apply the location scale transformation to the random variable  $X$

$$Y = \sigma X + \mu \quad (\text{D.2})$$

the probability density function then becomes

$$f_Y(y) = \frac{\Gamma\left(\frac{\nu+1}{2}\right)}{\sigma\sqrt{v\pi}\Gamma\left(\frac{\nu}{2}\right)} \left(1 + \frac{1}{\nu} \left(\frac{x-\mu}{\sigma}\right)^2\right)^{-\frac{\nu+1}{2}} \quad (\text{D.3})$$

In Section 4.2.1, Equation (D.3) is shown to be distribution of best fit for most sets of data of interest. The errors observed between the fitted distribution and the observed frequencies were within acceptable ranges for the purposes described later in Section 4.2.1.

The parameters analysed in Section 4.2.1 required a measure of the variance of the data. For the Student's t distribution described by Equation (D.1), this is given by

$$\text{Variance} = \frac{\nu}{\nu - 2}. \quad (\text{D.4})$$

With the location-scale transformation (D.2), the variance is described in terms of the three parameters  $\nu, \mu$  and  $\sigma$  by

$$\text{Variance} = \frac{\nu}{\nu - 2}. \quad (\text{D.5})$$

This value is not defined for  $\nu \leq 2$  [54]. In cases where the variance was undefined, the processed data was analysed manually to determine the 'variance score' used in the weighted decision matrix.